Progetto S3 – Scenari di scuotimento in aree di interesse prioritario e/o strategico

Responsabili: Francesca Pacor (INGV-MI) e Marco Mucciarelli (Unibas)

TASK 5 – POTENZA - DELIVERABLES D17

BEDROCK SHAKING SCENARIOS

A cura di
UR1 – *F. Pacor, G. Zonno*
UR2 – *G. Cultrera, A. Cirella, A. Herrero, E. Tinti*
UR4 – *D. Albarello, V. D'Amico*
UR10 – *Emolo A., Gallovic F.*
INGV-RM - *R. Basili*

July 2007

INDEX

1. INTRODUCTION

The main goal of this report is the computation of the bedrock seismic scenarios in the Potenza city (Southern Italy) to be used for evaluating damage scenarios (described in *PS3-Deliverables D18-D19-D24*). This area represents one of the prediction case studies, planned in the framework of Project S3 which aim is the production of ground shaking scenarios for high and moderate magnitude earthquakes. The area around Potenza was affected by several destructive earthquakes in historical time (Table 2.1.1) and a number of individual sources representing the causative faults of single seismic events with magnitude up to 7 were identified. Deeper and smaller faults are present very close to the Potenza city, generating events with M up to 5.7 (1990 Potenza earthquake).

Due to the involved source-to-site distances (about 25 km) and to the computation resolution of the simulation techniques, the site is represented by a single point. In total 9 faults were identified and the deterministic shaking scenarios are computed for each of them.
The following strategy is adopted to provide ground motions.
We compute shaking scenarios at level 1, using a simplified simulation technique (DSM, Pacor et al.; 2005) for all the faults. By these simulations we identify the three faults (F3, F7. and F8) producing the maximum expected shaking at the Potenza city, in terms of peak ground acceleration, peak ground velocity and Housner intensity. Based on these results, simulations at level 2, using the broad band technique HIC (Gallovic and Brokeshova, 2007) have been performed at Potenza for F3, F7 and F8 sources.
For the Potenza city, we decided to predict the shaking scenarios at level 2, in order to provide suitable estimates of the low frequency ground motion (e.g. velocity time series) and engineering parameters (e.g. Arias intensity) strictly related to the duration of the signals. For each source, we generated hundreds of rupture models varying slip distribution, nucleation points and rupture velocity, and for each model we simulated the acceleration time series by HIC. Then we computed the probability density functions (PDF) of the ground motion parameters (PGA, PGV, PGD, Arias and Housner intensities) and estimated several statistical quantities in order to select families of accelerograms to be used for damage analysis: mean and associated standard deviation, median, 75% percentile, 84% percentile, mode, minimum and maximum.
Finally we provided to the engineering Research Unit 6 of this project three sets of 7 accelerograms, having ground motion parameters equal to the statistical requirements computed by the synthetic distributions.
The first set includes 7 accelerograms (three components), each of them having PGA equal to the mean, median, mode, 75-percentile, 84-percentile, minimum and maximum values of the PGA distribution. The second set and third sets include 7 accelerograms (horizontal components only), having PGA and Housener Intensity in the neighborhood of the median values of the corresponding distributions. A further comparison of adopted procedure for the predicted ground motion at Potenza was performed with respect to stochastic ground motions generated with EXSIM method (Motazedian and Atkinson; 2005). Even if the scenarios modelling was carried out varying different kinematic parameters, the statistical parameter were quite similar.
Finally to provide shaking scenarios in term of macroseismic intensity, we applied a probabilistic empirical approach, developed in Progetto DPC-INGV S1.

2. DEFINITION OF REFERENCE EARTHQUAKES

2.1 TECTONIC SETTING AND SEISMICITY

The southern Apennines are part of a Late-Cenozoic accretionary wedge resulting from westward subduction of the Apulian lithosphere (Doglioni et al. 1996). Potenza is located between the Apennines axial zone and the Apulia foreland, both corresponding to well-identified seismogenic zones (Fig. 2.1.1).

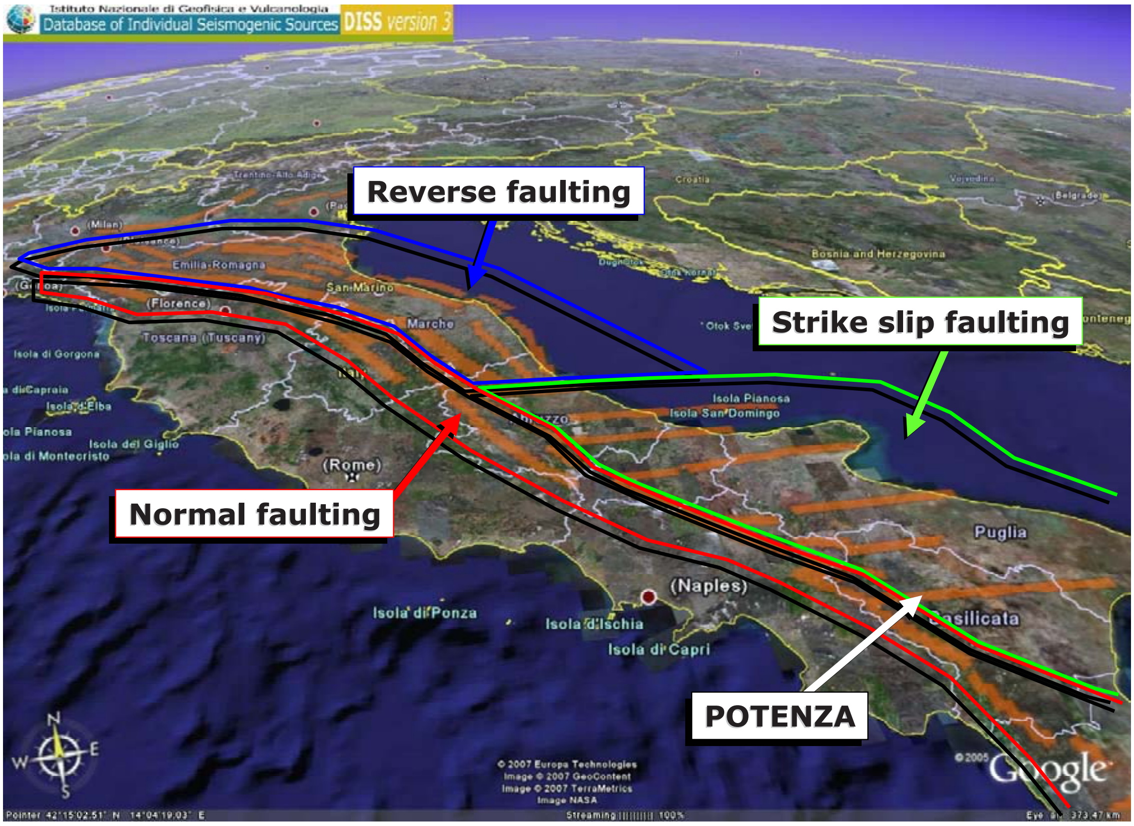

Figura 2.1.1 – Oblique view of peninsular Italy showing the main faulting types in wide regions and the Seismogenic Areas (composite faults) that appear in DISS v. 3.0.2.

The Apulia Platform underlies the southern Apennines edifice and is the locus of the largest NW-SE striking, NW dipping normal faulting earthquakes (e.g. 1857 Val d'Agri, 1980 Irpinia) that take place in this major seismogenic district (Improta et al. 2003). The depth of the 1990-91 Potenza and 2002 Molise earthquakes (>15 km), however, suggests that they nucleated well below this unit (Azzara et al., 1993; Chiarabba et al., 2005). Tectonic studies on these events and other historical earthquakes in the area revealed a rather systematic pattern of EW striking right-lateral strike-slip faulting (Valensise et al., 2004; Di Bucci et al., 2006; Fracassi and Valensise, 2007).
The area around Potenza was affected by several destructive earthquakes in historical time. Table 2.1.1 shows a selection from the CPTI04 catalog (CPTI Working Group, 2004) of historical earthquakes within 50 km from Potenza.

Table 2.1.1 – Selection from the CPTI04 catalog of the largest earthquakes within 50 km from Potenza.

#	Yyyy/mm/dd	Area	Io	Lat	Lon	Mw
58	1273	POTENZA	VIII-IX	40.630	15.800	5.84
157	1461/06/	CASTELCIVITA	VII	40.500	15.250	5.16
256	1561/08/19	VALLO DI DIANO	IX-X	40.520	15.480	6.36
414	1694/09/08	IRPINIA-BASILICATA	X-IX	40.880	15.350	6.87
555	1759/05/20	GRUMENTO	VI	40.333	15.833	4.83
709	1807/11/11	TRAMUTOLA	VII	40.297	15.845	5.16
759	1826/02/01	BASILICATA	VIII	40.520	15.730	5.67
854	1846/08/08	CAMPOMAGGIORE	VI-VII	40.530	16.113	5.32
878	1851/08/14	BASILICATA	IX-X	40.950	15.670	6.33
880	1852/04/02	MELFI	VI	41.000	15.667	4.83
912	1857/12/16	BASILICATA	X-XI	40.350	15.850	6.96
915	1858/08/06	RICIGLIANO	VII	40.750	15.550	5.16
919	1859/02/04	VIETRI	VI-VII	40.650	15.517	5.03
930	1861/11/19	POTENZA	VI-VII	40.633	15.800	5.03
1201	1893/01/25	AULETTA	VII	40.583	15.417	5.16
1234	1895/07/19	BRIENZA	VI	40.417	15.700	4.83
1323	1899/10/02	POLLA	V-VI	40.555	15.654	4.63
1415	1905/06/29	BRIENZA	VI	40.525	15.599	4.83
1441	1906/07/02	MONTEMURRO	VI	40.300	16.000	4.83
1520	1909/12/03	CASTELGRANDE	VI	40.833	15.400	4.83
1533	1910/06/07	IRPINIA-BASILICATA	VIII-IX	40.900	15.420	5.86
1538	1910/10/03	MONTEMURRO	VI-VII	40.283	15.983	5.03
1658	1917/10/13	CASTELSARACENO	VI	40.231	16.009	4.83
1701	1920/03/07	SANT'ILARIO	VI	40.800	15.700	4.83
1744	1923/11/08	MURO LUCANO	VI	40.677	15.449	5.00
1848	1930/11/06	S. NICOLA	VI-VII	41.067	15.700	5.03
1855	1931/05/10	S. NICOLA	VI	41.067	15.700	4.88
1866	1931/11/10	MELFI	V-VI	41.000	15.700	4.63
1877	1932/12/03	MARSICO VETERE	V-VI	40.400	15.800	4.63
1907	1935/12/03	CALVELLO	VI	40.467	15.867	4.83
2078	1954/08/06	PIETRAGALLA	VI	40.667	15.883	5.28
2092	1956/01/09	GRASSANO	VI-VII	40.570	16.366	5.03
2109	1957/05/03	SANT'ILARIO	V-VI	40.800	15.700	4.63
2113	1957/10/19	BRIENZA	VI	40.500	15.700	4.83
2187	1963/02/13	TITO	VII	40.658	15.782	5.26
2206	1964/06/04	BRIENZA	VI	40.500	15.667	4.83
2224	1966/07/06	LUCANIA	IV	40.956	16.194	4.61
2225	1966/10/04	PICERNO	VI	40.600	15.700	4.83
2249	1968/03/22	MONTEMURRO	V-VI	40.300	16.000	4.60
2274	1969/11/14	POLLA	V	40.583	15.567	4.61
2307	1971/11/29	MARSICO	VI	40.500	15.800	4.83
2325	1973/08/08	VIETRI	V	40.650	15.517	4.97
2413	1980/11/23	IRPINIA-BASILICATA	X	40.850	15.280	6.89
2415	1980/12/03	POTENZA	-	40.650	15.750	4.89
2944	1983/07/27	MONTE VULTURE	-	40.734	15.245	4.45
3114	1986/07/23	POTENTINO	VI	40.625	15.671	4.63
3260	1990/05/05	BASILICATA	VII	40.711	15.299	5.83
3261	1990/05/05	POTENTINO	-	40.659	15.880	4.72
3295	1991/05/26	BASILICATA	VII	40.668	15.803	5.21
3454	1996/04/03	IRPINIA	VI	40.854	15.293	4.92

2.2 SEISMOGENIC SOURCES

The faults illustrated in this section are those that appear in DISS v. 3.0.2, a database of seismogenic sources for Italy and some surrounding countries (DISS Working Group, 2006; Basili et al., 2007).

In the Potenza area, DISS shows a number of individual sources (ITGG008, ITGG010, ITGG084, ITGG077, ITGG078, ITGG079, ITGG007), that were identified and characterized by the DISS' compilers mainly by surface and subsurface geological investigations. These sources represent the causative faults of single seismic events. In this area, DISS also shows several Seismogenic Areas (ITSA005, ITSA063), composite faults that may contain an unspecified number of individual sources (see Basili et al., 2007 for more details). Figure 2.2.1 shows an excerpt of the DISS seismogenic sources in the area around Potenza.

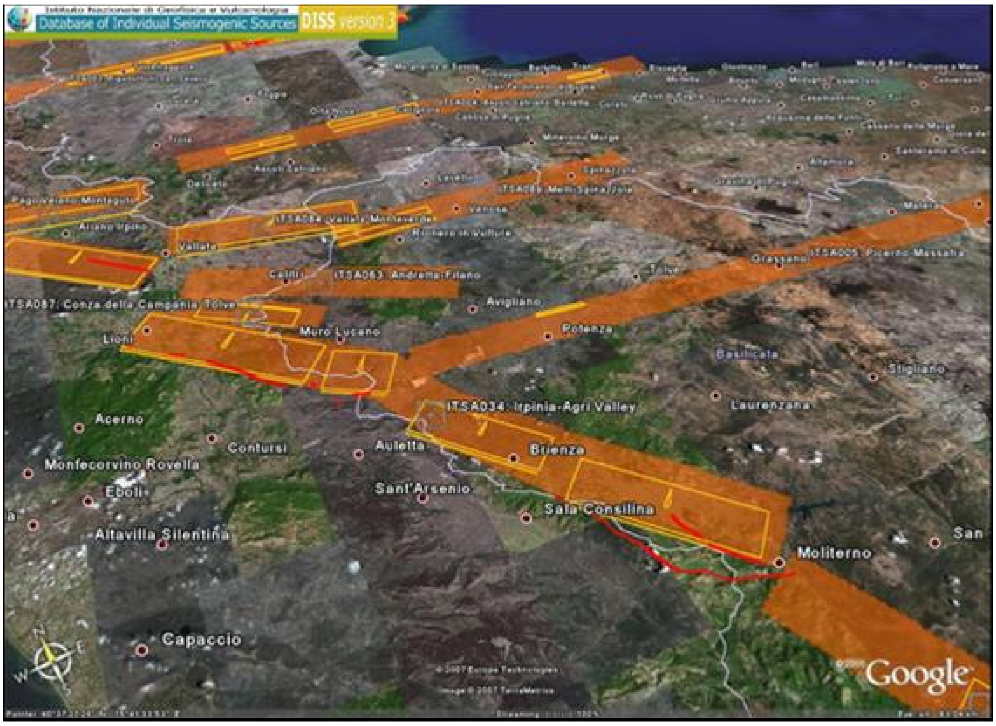

Fig. 2.2.1 – Oblique view showing the seismogenic sources around Potenza as they appear in DISS v. 3.0.2.

Figure 2.2.2 and Tables 2.2.1 and 2.2.2 show a map of the seismogenic sources and their parameters, respectively. The uncertainties associated to these parameters are based on geological wisdom, taking into account the accuracy of investigation methods and techniques.

In more detail, the fault identified as ITGG077, ITGG078, and ITGG079 are respectively the sources of the three main shocks of the 1980 Irpinia earthquake, generally referred to as 0 sec, 20 sec and 40 sec events. The fault identified as ITGG007, instead, was conceived for the purpose of this study and accounts for the 0 sec and 20 sec events put together by summing seismic moment and averaging the geometry of the ITGG077 and ITGG078 faults. Similarly, the faults identified as ITGG008 and ITGG010 are respectively the sources of the two main shocks of the 1857 Basilicata earthquake, as hypothesized by Burrato and Valensise (2007).

The fault identified as ITSA063 does not appear in this form in DISS because geological/geophysical knowledge of this fault is not yet accurate enough to fully characterize an individual fault segment. This individual source is thus proposed only for the purpose of this study as the source of the 1694 Irpinia earthquake. The geometric and kinematic parameters were determined by averaging those of its parent Seismogenic Area and its size adjusted to the moment magnitude of the 1694 earthquake. Its location is taken at the southern edge of the parent structure. The uncertainties shown in Table 2.2.1 do not apply to this case.

Table 2.2.1 – Fault parameters of the 1980 earthquake.

ID	ITGG077	ITGG078	ITGG079	ITGG007*	Uncertainty
Lon Centroid	15.2944	15.4826	15.3509	15.3358	±0.01
Lat Centroid	40.8021	40.6842	40.8524	40.7690	±0.01
Strike (deg)	310	300	124	310	±10
Dip (deg)	60	60	70	60	±5
Rake (deg)	270	270	270	270	±10
Length (km)	28.0	9.0	15.0	38.0	±2
Width (km)	15.0	15.0	10.0	15.0	±2
Min Depth (km)	1.0	1.0	1.0	1.0	±1
Max Depth (km)	14.0	14.0	10.4	14.0	±2
Slip (m)	1.65	0.7	0.5	1.4	±0.1
M_0 (Nm)	2.29E+19	3.12E+18	2.48E+18	2.63E+19	
Mw	6.8	6.3	6.2	6.9	

* See text for the peculiarities of this seismogenic source.

Table 2.2.2 – Fault parameters of the 1694, 1857, and 1990 earthquakes.

ID	ITGG008	ITGG010	ITSA063*	ITGG084	Uncertainty
Lon Centroid	15.7828	15.6026	15.5359	15.8517	±0.01
Lat Centroid	40.3483	40.5260	40.8577	40.6785	±0.01
Strike (deg)	316	317	296	95	±10
Dip (deg)	60	60	70	88	±5
Rake (deg)	270	270	230	175	±10
Length (km)	23.0	17.9	35.0	7.9	±2
Width (km)	13.5	11.3	18.0	6.2	±2
Min Depth (km)	1.0	1.0	1.0	14.8	±1
Max Depth (km)	12.7	10.8	17.9	21.0	±2
Slip (m)	0.74	0.57	1.3	0.26	±0.1
M_0 (Nm)	7.58E+18	3.80E+18	2.46E+19	4.20E+17	
Mw	6.5	6.3	6.9	5.7	

* See text for the peculiarities of this seismogenic source.

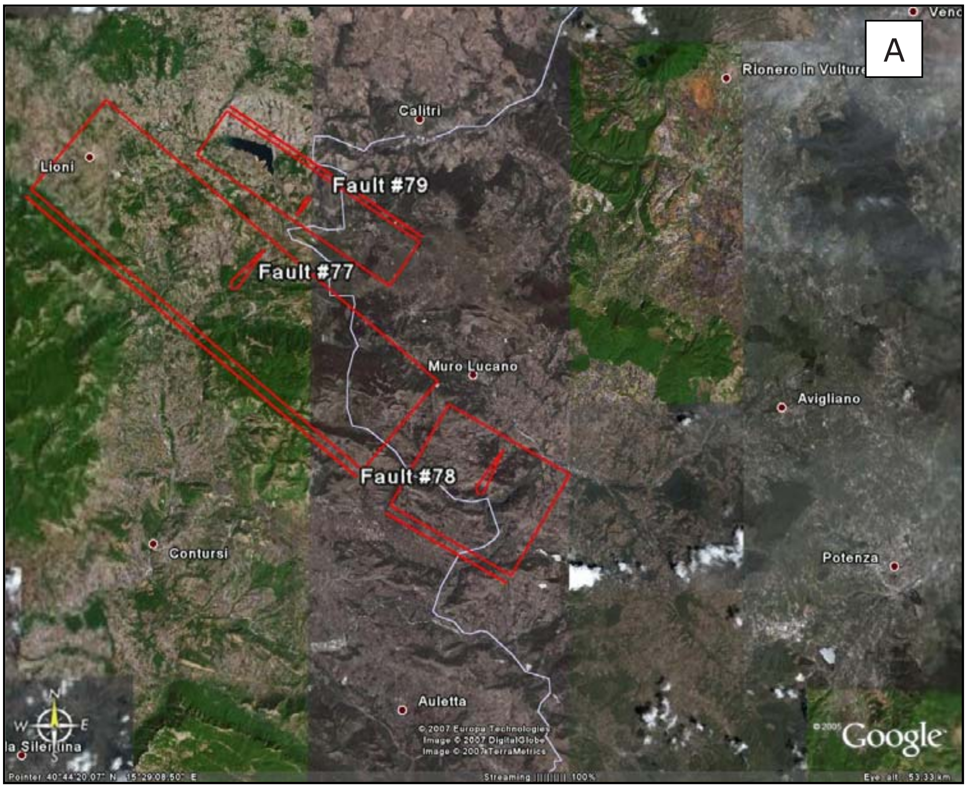

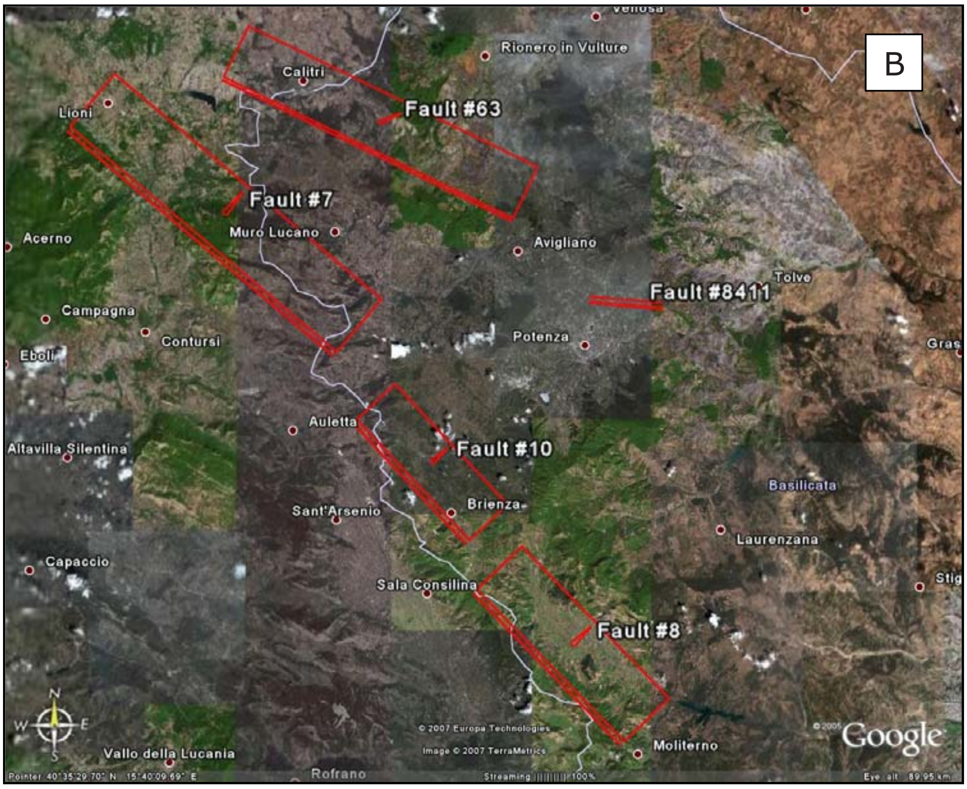

Fig. 2.2.2 – (A) Map showing the seismogenic sources of the 1980 Irpinia earthquake listed in Table 2.2.1 except for the ITGG007. (B) Map showing the seismogenic sources the 1694, 1857, and 1990 earthquakes listed in Table 2.2.2 and including the ITGG007 listed in Table 2.2.1.

The fault identified as ITGG084 is the source of the May 5, 1990, Potenza earthquake. This source is part of a much bigger fault system (identified as ITSA005 in DISS) stretching in the E-W direction across the Basilicata Region (Fig. 2.2.4 and Fig. 2.2.5).
For the purpose of this study, we let the ITGG084 assume various positions within its parent structure (ITSA005). Table 2.2.3 lists the fault centroid coordinate pairs that are needed to make the source span across strike the entire width of its parent structure in the vicinity of Potenza and Table 2.2.4 lists those to make it span along strike a number of positions at one fault length distance from one another.

Table 2.2.3 – Coordinate pairs of the ITGG084 source centroid to make the fault span across strike.

Code	Lon Centroid	Lat Centroid
84-11	15.8517	40.6785
84-12	15.7462	40.6846
84-13	15.7463	40.6305
84-14	15.8515	40.6245

Table 2.2.4 – Coordinate pairs of the ITGG084 source centroid to make the fault span along strike.

Code	Lon Centroid	Lat Centroid
84-21	15.6096	40.6668
84-22	15.6565	40.6636
84-23	15.7034	40.6606
84-24	15.7503	40.6577
84-25	15.7972	40.6548
84-26	15.8441	40.6519
84-27	15.8910	40.6486
84-28	15.9379	40.6456
84-29	15.9848	40.6424

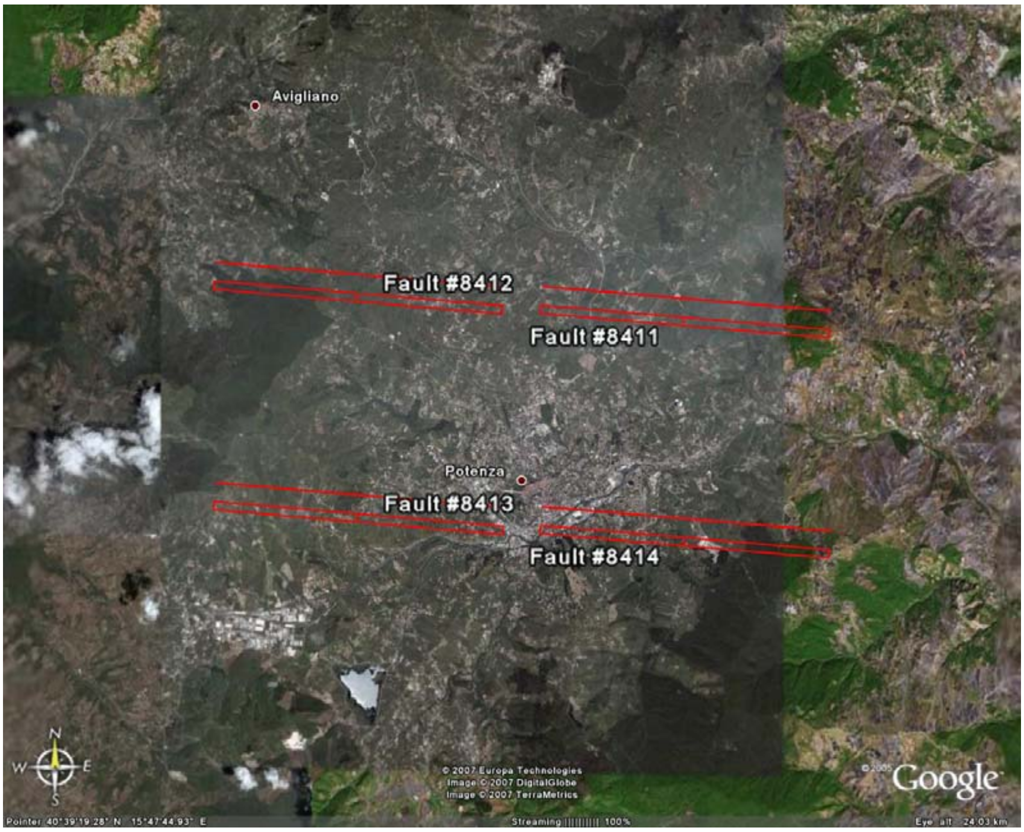

Fig. 2.2.3 – Map showing the seismogenic source of the 1990 Potenza earthquake and its hypothetical positions for the purpose of this study listed in Table 2.2.3.

Fig. 2.2.4 – Map showing the seismogenic source of the 1990 Potenza earthquake and its hypothetical positions for the purpose of this study listed in Table 2.2.4.

2.3 THE SCORCIABUOI FAULT

Following detailed morphotectonic and geological investigations, several electrical resistivity tomographies and a palaeoseismological trench, the Late Quaternary tectonic activity of the Scorciabuoi Fault and its seismogenic potential have been documented for the first time.

In map view, the trace of the Scorciabuoi Fault is quite rectilinear with a mean N115°-120° trend (Fig. 2.3.1). Only the southeastern sector has a NW-SE trend, likely because the structure progressively merged with the blind thrust associated with the Valsinni anticline. In the two wing sectors, the fault mainly affects deposits belonging to the Sicilide units and the Miocene flysch (Gorgoglione Fm), while in the central sector the above described Pliocene-Middle Pleistocene deposits of the Sant'Arcangelo Basin are extensively involved.

In the latter sector, the fault affects the pelitic portion of the Sauro deposits forming a narrow zone of intense shear deformation and confirming a sinistral kinematics. This sense of motion is geodynamically associated with the late orogenic compressional phase (Late Pliocene-Middle Pleistocene) and it is superimposed by a normal dip-slip kinematics, therefore supporting the recent (Middle *p.p.*-Late Quaternary) extensional behaviour of the Scorciabuoi Fault. Although Pieri *et al.* (1997) suggest that the change in stress field possibly occurred at 0.7-0.5 Ma, our mesostructural analysis indicates it is likely younger.

Remote sensing techniques and dedicated field-work allowed to recognise and map four fill terraces along the Sauro valley showing differential cumulative displacements across the fault. These terraces have been genetically and chronologically associated with as many high-stand sea-level periods likely between 80-100 ka and Present. The fault was active throughout the investigated period (Late Quaternary) up to very recently, while quantitative estimates suggest slip-rates values broadly ranging between 0.5 and 1.0 mm/a that in any case represent a not negligible amount of tectonic activity.

Due to the linear geometry of the Scorciabuoi Fault trace and its apparent lack of segmentation, it is possible that a future earthquake will re-activate the entire fault length. If this will be the case, the associated seismic event could reach a magnitude of about 6.8 and, assuming a linear morphogenic earthquake, it will generate *ca.* 1 m of maximum vertical displacement (equations [1] and [4] of Pavlides and Caputo, 2004). Such a seismic event would be of comparable size (and damaging effects) with the 'Great Neapolitan earthquake' that affected and devastated a large sector of Southern Italy in 1857 (Mallet, 1862).

Source Name	Scorciabuoi	
Strike_deg	110	
Dip_deg	75	
Rake_deg	270	
Length_km	30	
Width_km	16	
MinDepth_km	1	
MaxDepth_km	16.6	
Slip_m (*)	0.87	(*) Hanks & Kanamori (1979)
Mw_KA	6.7	
M0_Nm	1.26E+19(*)	
LonA-LonB	16.030-16.363	**A,B=** fault trace (surface intersection of the fault)
LatA-LatB	40.400-40.308	

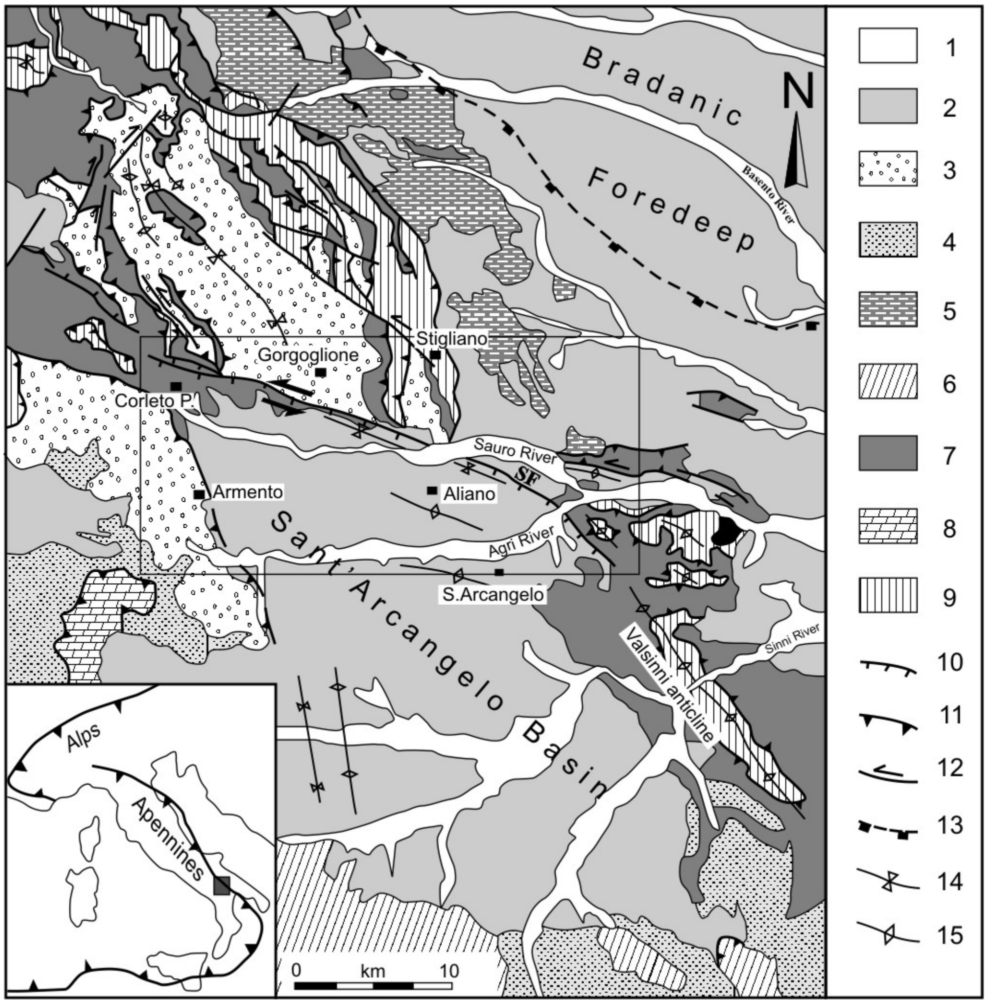

a)

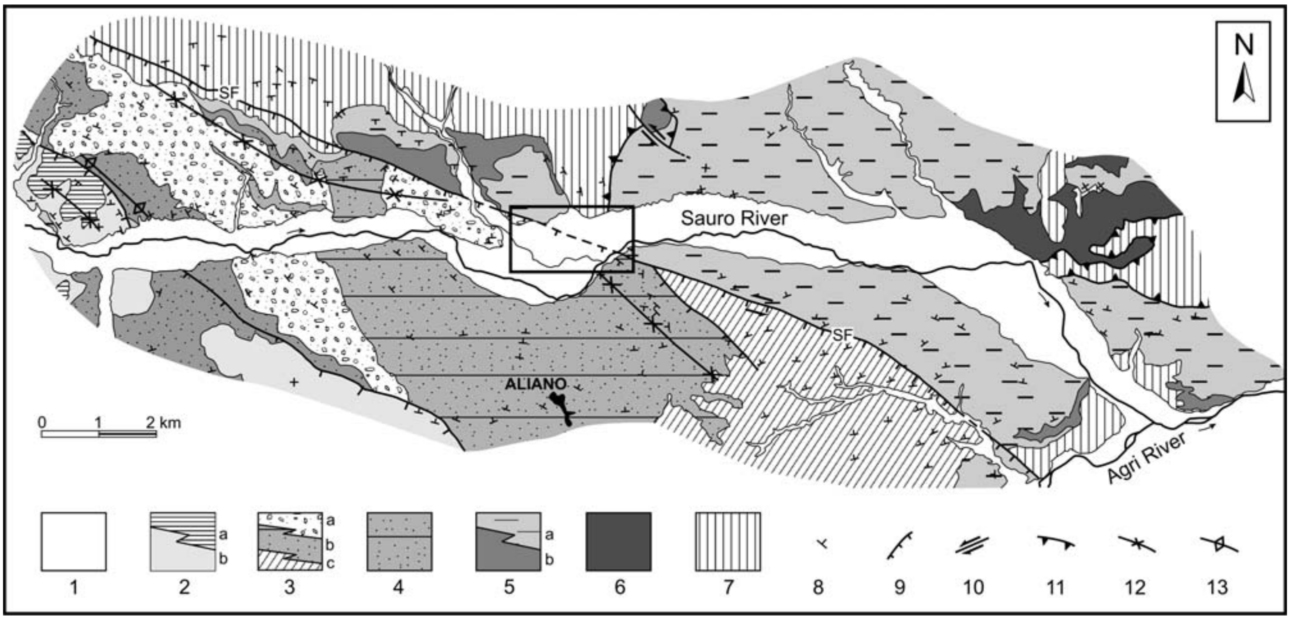

b)

Figure 2.3.1. Scorciabuoi fault

3. BEDROCK SCENARIOS AT LEVEL 1 AND LEVEL 2

The ground motion simulations at Potenza were computed with the two hybrid techniques described in *PS3-Deliverable D0 (2006)*: deterministic-stochastic method, DSM (Pacor et al., 2005), and hybrid *k*-squared source modeling technique, HIC (Gallovic and Brokeshova, 2007). DSM technique was used to simulate the ground motion on the faults selected in Chapter 1 adopting different rupture models (shaking scenarios at level 1). The results in terms of PGA, PGV and Housner Intensity allowed us to select fewer faults producing the maximum shaking scenario at Potenza (shaking scenarios at level 2). For this subset of faults, the HIC technique was used to simulate the broad-band time series.

3.1 FAULTS MODELS

We performed the ground motion simulations at Potenza using the 9 faults described in Chapter 2 (see ***Table 3.1*** and ***Figure 3.1***).

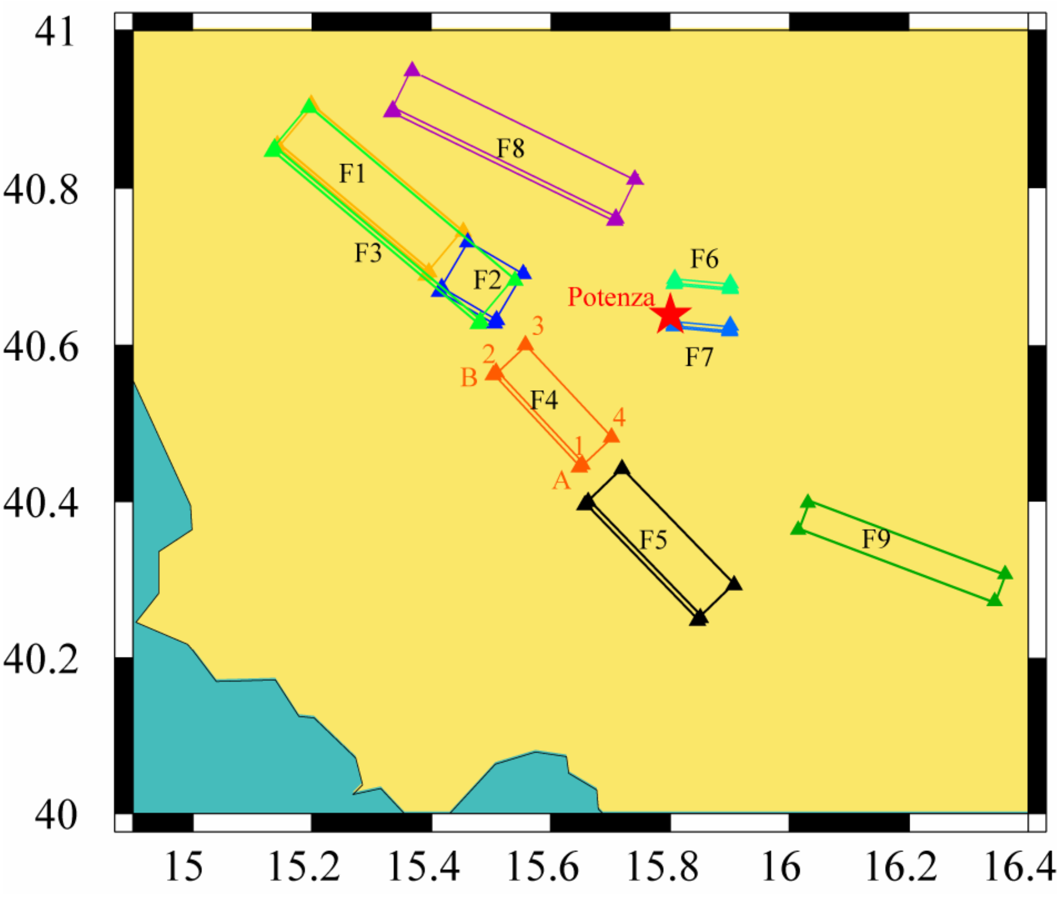

Figure 3.1 Map of the faults location with respect to Potenza.

We simulated with DSM 15/30 rupture models for each fault, depending on the earthquake magnitude: 15 models for M < 6.5 (5 rupture velocities x 1 slip models x 3 nucleation points) and 30 models for M>=6.5 (5 rupture velocities x 2 slip models x 3 nucleation points). For the selected subset of faults, we simulated with HIC 96 to 432 rupture models depending on the number of nucleation points which can vary on the fault: 360 models for F3 (2 rupture velocities x 6 slip models x 30 nucleation points), 96 models for F7 (2 rupture velocities x 6 slip models x 8 nucleation points), 432 models for F8

(2 rupture velocities x 6 slip models x 36 nucleation points).

Table 3.1 Faults' geometries

	F1	F3	F4	F5	F6	F7	F8	F9
Source Name	ITGG077: Colliano	ITGG007: Irpinia	ITGG010: Melandro-Pergola	ITGG008: Agri Valley	ITGG084: Potenza	ITGG084: Potenza	ITSA063: Andretta-Filano	Scorciabuoi
Nucleation points: DSM down-dip (km) along strike (km)	10 7-14-21	10 9.5-19-28.5	8 4.5-9-13.5	8.5 6-11.5-17	6 2-4-6	6 2-4-6	13 8-17.5-27	11 7.5-15-22.5
HIC down-dip (km) along strike (km)		4-8-12 1-5-9-13-17-21-25-29-33-37				2-4 1-3-5-7	3-6-9-12 2-6-10-14-18-22-26-30-34	

Propagation model

We used the same propagation model adopted for the simulation of the 1980 Irpinia earthquake in the first year of the project (***Table 3.2***; *PS3-Deliverable D0*, 2006). The model has been proposed by Improta (personal communication, 2005) and it has based on the Amato and Selvaggi (1993) work. It is worthy to note that the depth of the Apula platform in the 1D model is only a rough approximation of its strong variability in the area (Improta et al., 2003).

Table 3.2 crustal velocity model

h (km)	Vp (km/s)	Vs=Vp/1.81	Qs	Rho (g/cm3)	comments
0	3.5	1.93	100	2.3	
2	4.5	2.49	100	2.5	
4	5.7	3.15	100	2.6	Apula platform
10	6.5	3.59	100	2.7	
25	7.5	4.14	100	2.9	
35	8.1	4.48	100	3.2	Moho

Site

The selected site is indicated in ***Figure 3.1*** and it is representative for the city of Potenza (Lon 15.800-Lat 40.639). The site parameter k is set equal to 0.03 s-1, to account for damping in shallow layers.

Slip distribution

The final slip distributions on the faults were computed with the k-squared slip model (Herrero and Bernard, 1994; Gallovic and Brokešová, 2004), and it decreases to zero on the most superficial part of the faults to avoid super shear effects (even if DSM is not sensitive to it). In the DSM simulations, 2 slip distributions were considered for each fault with magnitude M >= 6.5 (F1, F3, F5, F8, F9): one with a random slip distribution and one with 1 asperity close to Potenza; for the faults with M<6.5 (F4, F6, F7) only a random slip distribution was considered. As an example, ***Figure 3.2*** shows the two slip distributions for F3 fault.

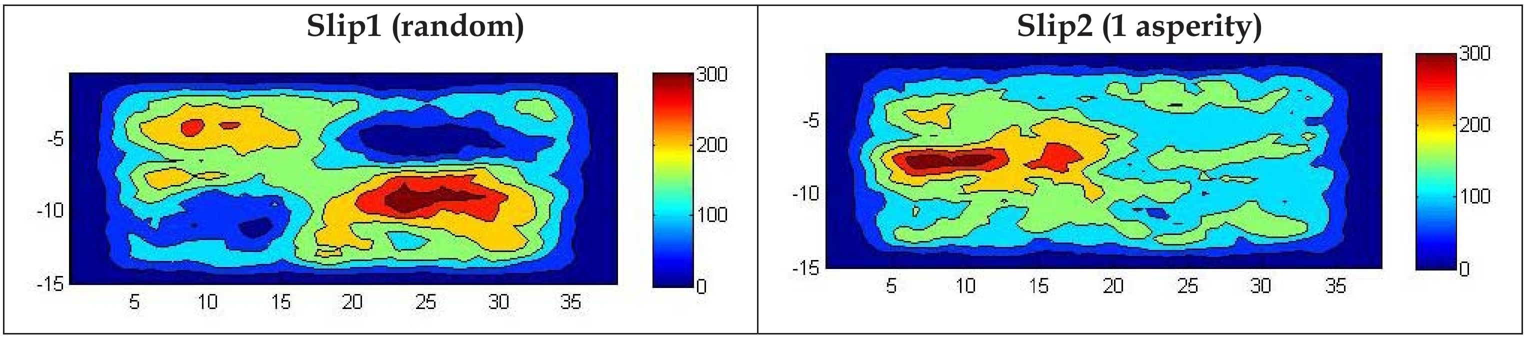

Figure 3.2. Slip distributions for F3 fault (DSM simulations).

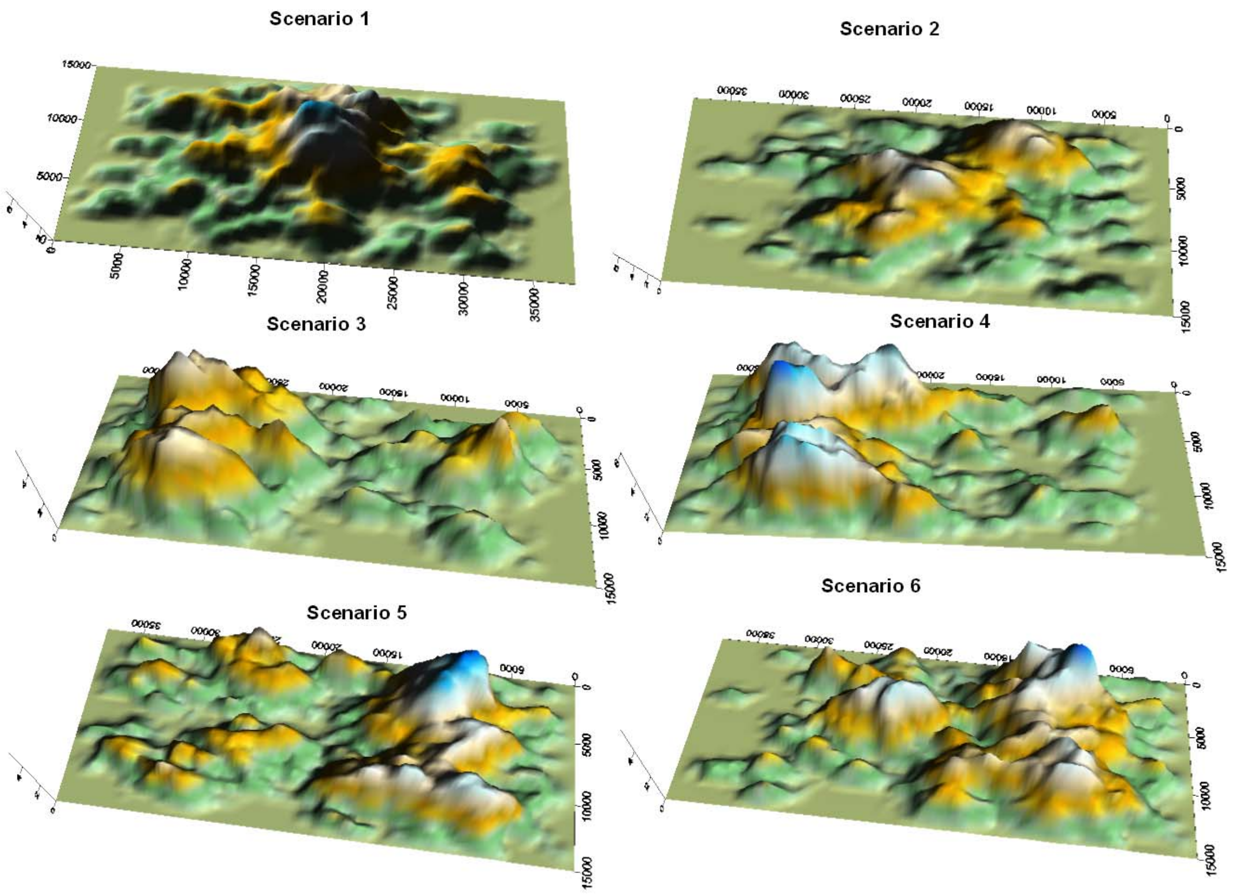

Figure 3.3. Slip distributions for F3 fault (HIC simulations).

For HIC simulations, only two rupture velocities were assumed: Vr2 (=0.8Vs= 2.4 km/s) and Vr3 (=0.9Vs= 2.7 km/s). Moreover, the rupture velocity and subsource corner frequency is affected by the decrease of velocity between 4 and 2km depth: the rupture velocity decreases in order to keep Vs/Vr constant. The corner frequency decreases according to the amount of subsource area that lies in the low-velocity zone.

Nucleation points

In the DSM rupture scenarios 3 nucleation points were used, laying in the lower half of the fault (close to the left and right edges and at the centre). For HIC simulations, 8-to-36 hypocenters were considered, shifted in both strike and dip directions (***Table 3.1***).

3.2 SHAKING SCENARIOS AT LEVEL 1 (DSM RESULTS)

The DSM simulations are summarized in terms of

- PGA, PGV ($PGX_{HOR} = \sqrt{[X_{NS}(t)]^2 + [X_{WE}(t)]^2}$) and
- Housner Intensity ($I_H = \int_{0.1s}^{2.5s} PSV(\xi;T)\,dT$, with 5% damping ξ)

experienced at Potenza and produced by different rupture scenarios on each fault.

Figure 3.4 shows both the single peak values (upper panels) and a representation of their average and associated distribution (bottom panels). The computed values are compared also with the Sabetta and Pugliese (1996) results at fault distances of 5-30km, where most of the faults lie (***Table 3.3***): empirical PGV are within the 25th and 75th percentile of the synthetics (***Figure 3.4***), whereas the PGA overestimate our results. This is probably because of the chosen distance metric (closest distance from the fault) which is computed for faults geometry not clearly defined; the fit increases with Ambraseys et al. (2005), where lower PGA values are estimated at the same fault distances.

Table 3.3 Magnitude and Fault distance (Rjb) from Potenza for each fault.

	F1	F3	F4	F5	F6	F7	F8	F9
R	32	23	19	23	5	1	16	33
M	6.8	6.9	6.3	6.5	5.7	5.7	6.9	6.7

These results are also shown in terms of their probability distribution (PDF), that is the histograms of PGV and Housner Intensity (0.1-2.5 s) values produced by different rupture models (***Figure 3.5*** and ***Figure 3.6***). The Figures distinguish the contribution of nucleation point positions and rupture velocities: the ground motion parameters are clearly dependent on the position of the hypocenter, due to the directivity effect at this site (farther is the nucleation point from Potenza, larger is the ground motion). The variability on the displayed ground motion due to different slip distributions is not significant, therefore it is not shown in the figures. From the previous figures it is possible to infer that the maximum shaking scenario at Potenza is produced by F3, F6 (or F7) and F8 faults. An example of simulated time series and related amplitude Fourier spectra for F3 rupture model is shown in ***Figure 3.7.***

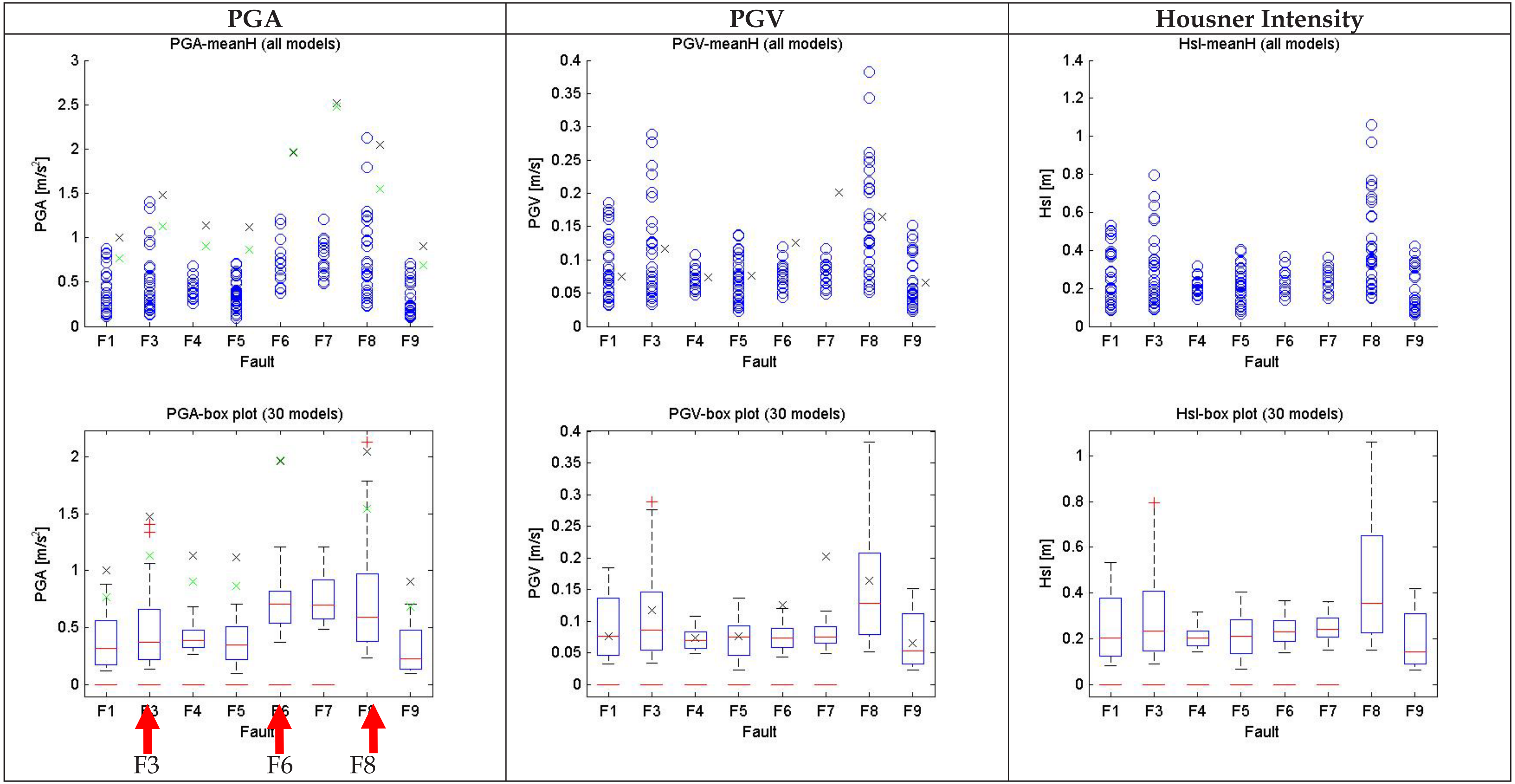

Figure 3.4. PGA, PGV, and Housner Intensity for the simulated faults. The tops and bottoms of each "box" are the 25th and 75th percentiles of the samples (i.e. interquartile ranges). The line in the middle of each box is the sample median. The "whiskers" are lines extending above and below each box to show the extent of the rest of the data. Observations beyond the whisker length are marked as outlier (by default, an outlier is a value that is more than 1.5 times the interquartile range away from the top or bottom of the box. Outliers are displayed with a red + sign). Crosses are the values from empirical models at magnitude and fault distance corresponding to each fault (black -Sabetta and Pugliese, 1996; green - Ambraseys et al., 2005).

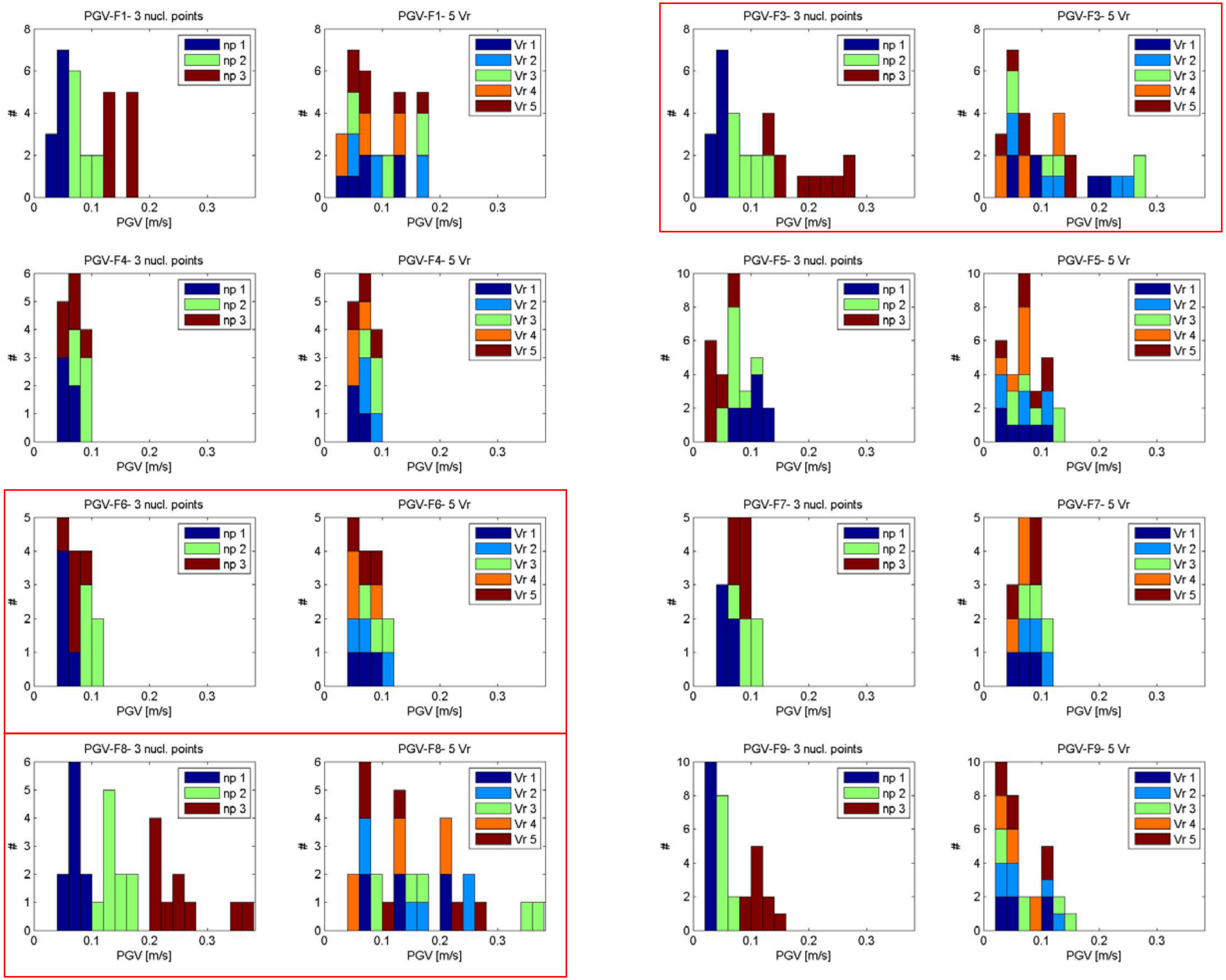

Figure 3.5. PGV variability (nucleation points – Rupture velocity). Red boxes indicate the faults which produce the maximum shaking scenario at Potenza.

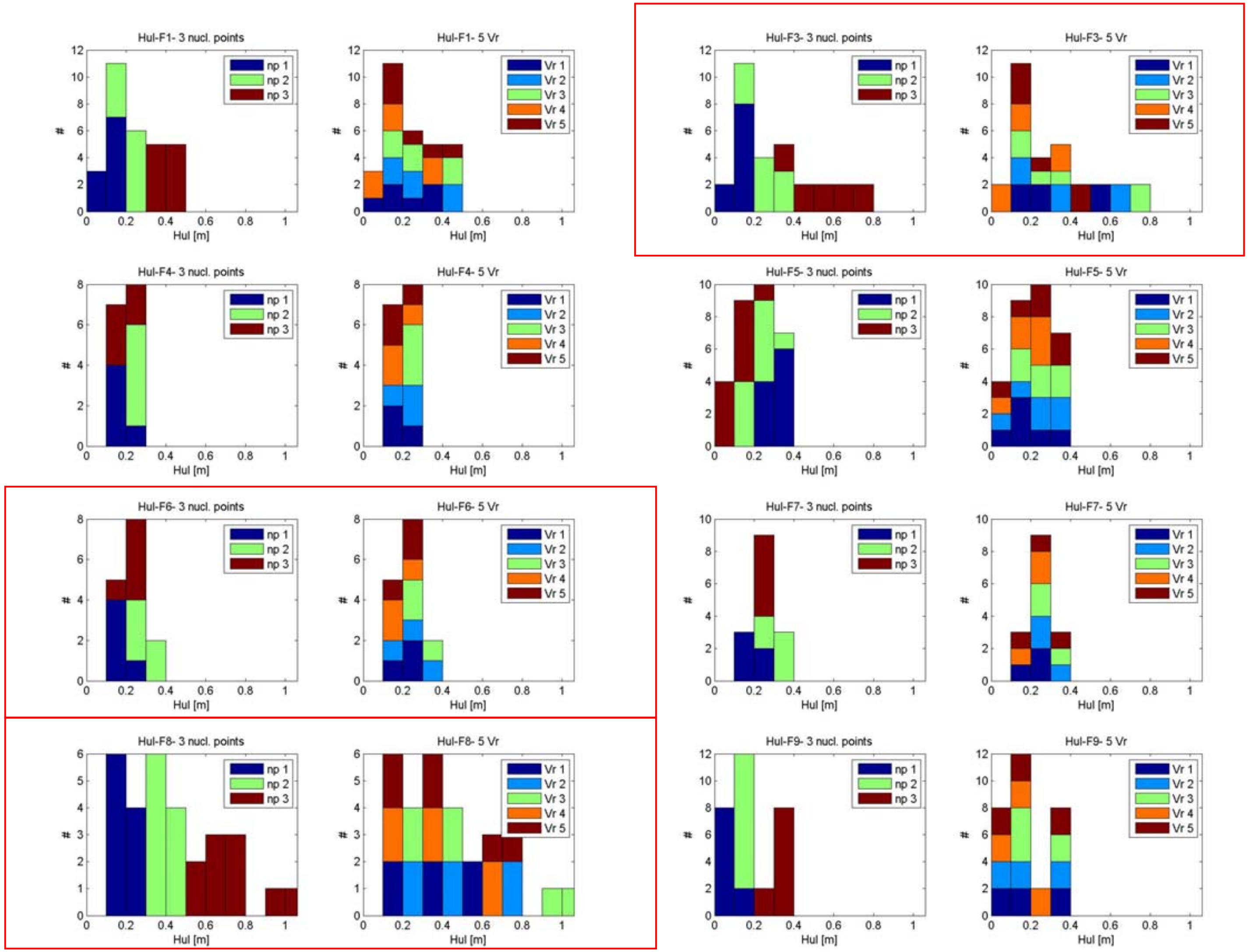

Figure 3.6. Housner Intensity computed between 0.1 and 2.5 seconds: variability due to nucleation point position and rupture velocity. Red boxes indicate the faults which produce the maximum shaking scenario at Potenza.

3.3 SHAKING SCENARIOA AT LEVEL 2 (HIC)

Based on the results obtained with DMS technique, HIC simulations have been performed at Potenza for F3, F7 and F8 models (***Figure 3.1*** and ***Table 3.1***).
First of all, we compared the time series and Fourier amplitude computed with HIC (***Figure 3.8***) and DSM (***Figure 3.7***) for similar rupture model on F3. The large difference in the NS and EW amplitudes is due to the radiation pattern: the low-frequency part (modeled only with HIC) is affected by the radiation pattern while the high-frequency part (modeled with both techniques) is due to artificial random mechanisms of the subsources.

NS

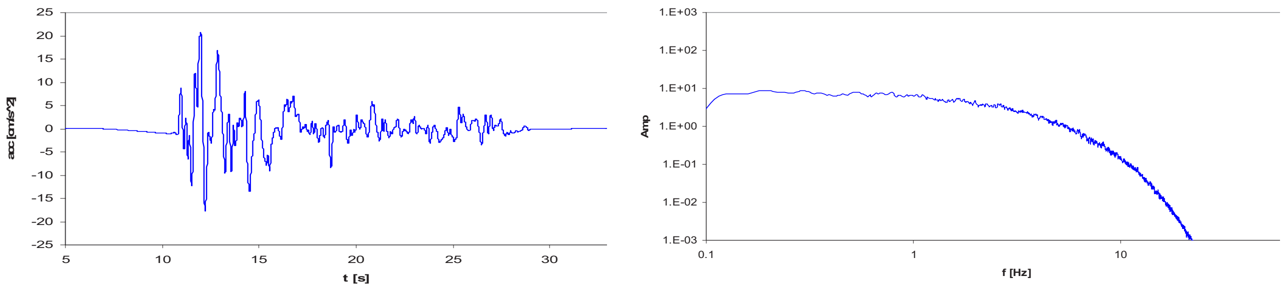

EW

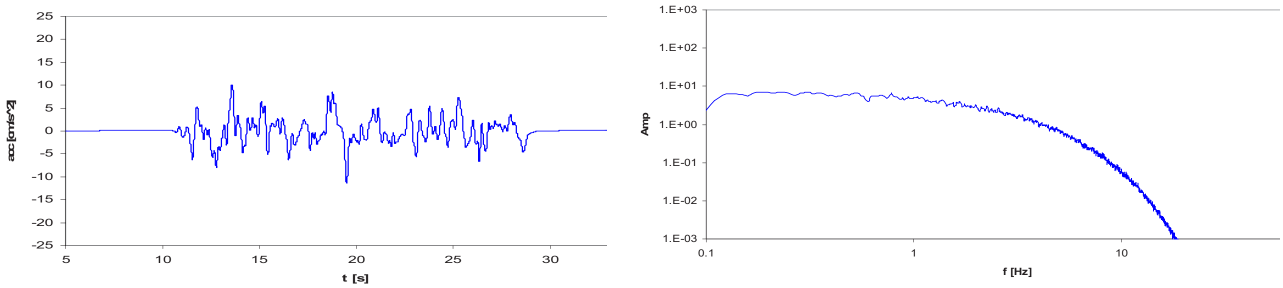

Figure 3.7. DSM Acceleration (NS and EW components) simulated at Potenza from F3 fault scenario (slip2 -1 asperity close to Potenza, Vr=2.7 km/s, nucleation point at 9.5km along strike): time series (left) and Fourier spectral amplitudes (right).

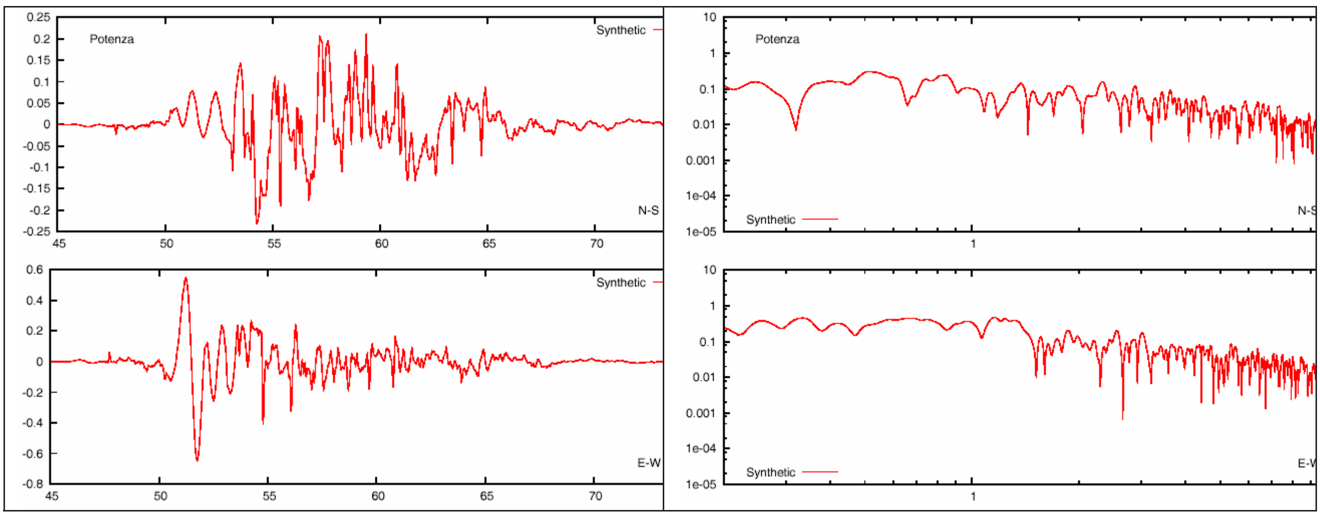

Figure 3.8. HIC Acceleration (NS and EW components in m/s^2) simulated at Potenza from F3 fault scenario (slip model 6, Vr=2.7 km/s, nucleation point at 9 km along strike and 8km along dip): time series (left) and Fourier spectral amplitudes (right, in m/s).

The simulation results are summarized in terms of PGA, PGV and Housner intensity (***Figure 3.9*** shows the highest peak between horizontal components). The HIC model seems to give larger values than DSM when comparing **Figures 3.9** and **3.4**. However, this could be mainly due to the larger number of directive scenarios (rupture point very close the the fault border) used in the HIC modeling. Otherwise, the values provided by both of the methods are in agreement with each other.

For each fault we plotted the probability density functions (PDF) of the ground motion parameters (PGA, PGV, PGD, Arias and Housner intensities) to check if the distributions are log-normal (***Figure 3.10***). As expected, the PGA is log normal distributed as this parameter is mainly stochastic and it is controlled by the high frequency part of the simulation techniques. The other parameters follow different probability distributions, such as bi-modal distribution. We can think of two hypotheses for this behaviour:

~~a.~~ the distribution of the other strong motion parameters depends on large scale properties of source and propagation medium.

b. the number of rupture scenarios is not large enough to model all the possible variability of ground motion parameters. However, we increased the number of scenarios for F3 (399 x 6 slip distribution, using a step in nucleation point of 2 km): the distributions of PGV and PGD are still bimodal, while PGA is log-normal (***Figure 3.10a***).

Several statistical quantities of the parameters distribution were computed to select families of accelerograms to be used for damage analysis (***Table 3.4***): mean and its standard deviation, median, 75% percentile, 84% percentile, mode, minimum and maximum.

Because the PDF of PGA fits a log-normal distribution, the mean (<m>) and standard deviation (σ) were inferred from the mean M and standard deviation S of the PGA logarithm:

$$<m>=\exp(M+S^2/2),$$
$$\sigma = \exp(S^2+2M)\,(\exp(S^2)-1).$$

Figures 3.11 to 3.16 show examples from the three families of selected accelerograms which were provided to the engineering Research Units of this project:

1. The first set includes 7 accelerograms (vertical and horizontal components), each of them having PGA equal to the mean, median, mode, 75-percentile, 84-percentile, minimum and maximum of the PGA distribution (*Figure 3.11* for F3, *Figure 3.12* for F7 and *Figure 3.13* for F8).

2. The second set includes 7 accelerograms (horizontal components only), having PGA in the neighborhood of the median value of the PGA distribution (*Figure 3.14* for F3, *Figure 3.15* for F7 and *Figure 3.16* for F8).

3. The third set includes 7 accelerograms (horizontal components only), having Housner Intensity in the neighborhood of the median value of the distribution.

Table 3.4 Mean and standard deviation (std), median, 75% percentile, 84% percentile, mode, minimum and maximum values for PGA, PGV, PGD, Arias and Housner Intensity of F3, F7 and F8 faults.M and S are the mean and standard deviation of the distribution of the logarithmic of thePGA, from which it is possible to evaluate the actual mean and std of the variables itself.

F3	Mean	Std	Median	75% perc.	84% perc.	Mode	Min	Max
PGA [m/s2]	0.68 (M=-0.56)	0.439 (S=0.59)	0.585	0.369	0.304	0.403	0.162	3.302
PGV [m/s]	0.244	0.179	0.226	0.085	0.044	0.061	0.014	0.795
PGD [m]	0.166	0.104	0.159	0.063	0.045	0.069	0.022	0.383
Arias [m/s]	3.120	3.892	1.712	0.419	0.219	0.187	0.080	27.866
Housner [m]	0.577	0.430	0.521	0.239	0.142	0.167	0.043	2.445
PGA/PGV	6.379	3.151						
F7	**Mean**	**Std**	**Median**	**75% perc.**	**84% perc.**	**Mode**	**Min**	**Max**
PGA [m/s2]	0.430 (M=-0.883)	0.123 (S=0.281)	0.403	0.344	0.320	0.382	0.233	0.918
PGV [m/s]	0.338	0.016	0.028	0.022	0.021	0.025	0.014	0.084
PGD[m]	0.009	0.004	0.008	0.007	0.006	0.008	0.004	0.020
Arias [m/s]	0.193	0.086	0.169	0.138	0.117	0.151	0.089	0.499
Housner [m]	0.102	0.045	0.088	0.070	0.063	0.080	0.048	0.242
PGA/PGV	10.129	2.235						
F8	**Mean**	**Std**	**Median**	**75% perc.**	**84% perc.**	**Mode**	**Min**	**Max**
PGA [m/s2]	0.909 (M=-0.235)	0.515 (S=0.527)	0.772	0.523	0.454	0.599	0.261	2.786
PGV [m/s]	0.224	0.160	0.209	0.073	0.049	0.070	0.022	0.655
PGD [m]	0.136	0.076	0.126	0.062	0.056	0.078	0.033	0.354
Arias [m/s]	3.758	4.350	2.233	0.867	0.678	0.729	0.350	25.120
Housner [m]	0.724	0.532	0.637	0.289	0.170	0.250	0.085	2.499
PGA/PGV	5.890	3.086						

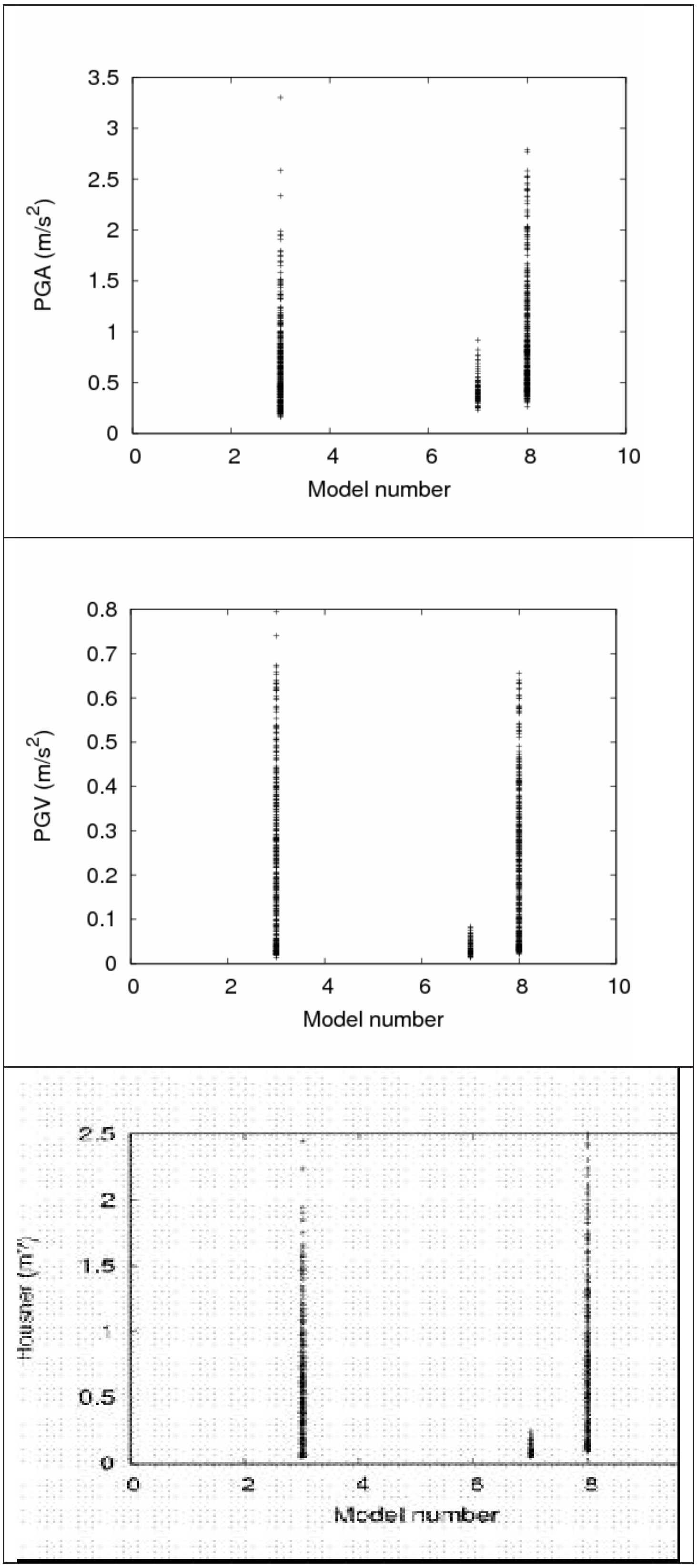

Figure 3.9. PGA, PGV, and Housner Intensity for F3, F7 and F8 faults simulated by HIC.

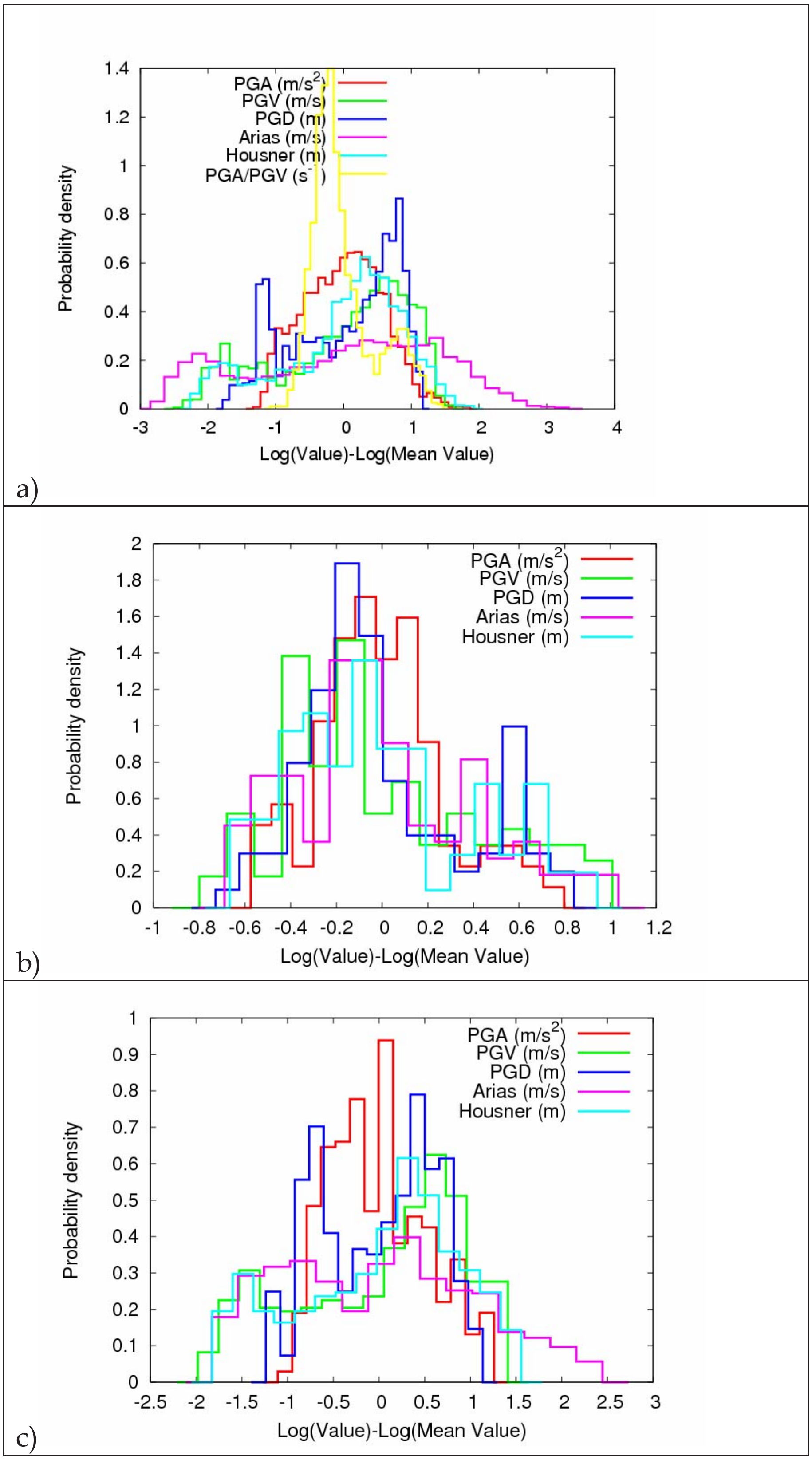

Figure 3.10. Probability density functions of the logarithm of ground motion parameters (PGA, PGV, PGD, Arias and Housner Intensity) from simulations for (a) F3 (including PGA/PGV), (b) F7 and (c) F8 faults. The integral of the density function is normalized to 1.

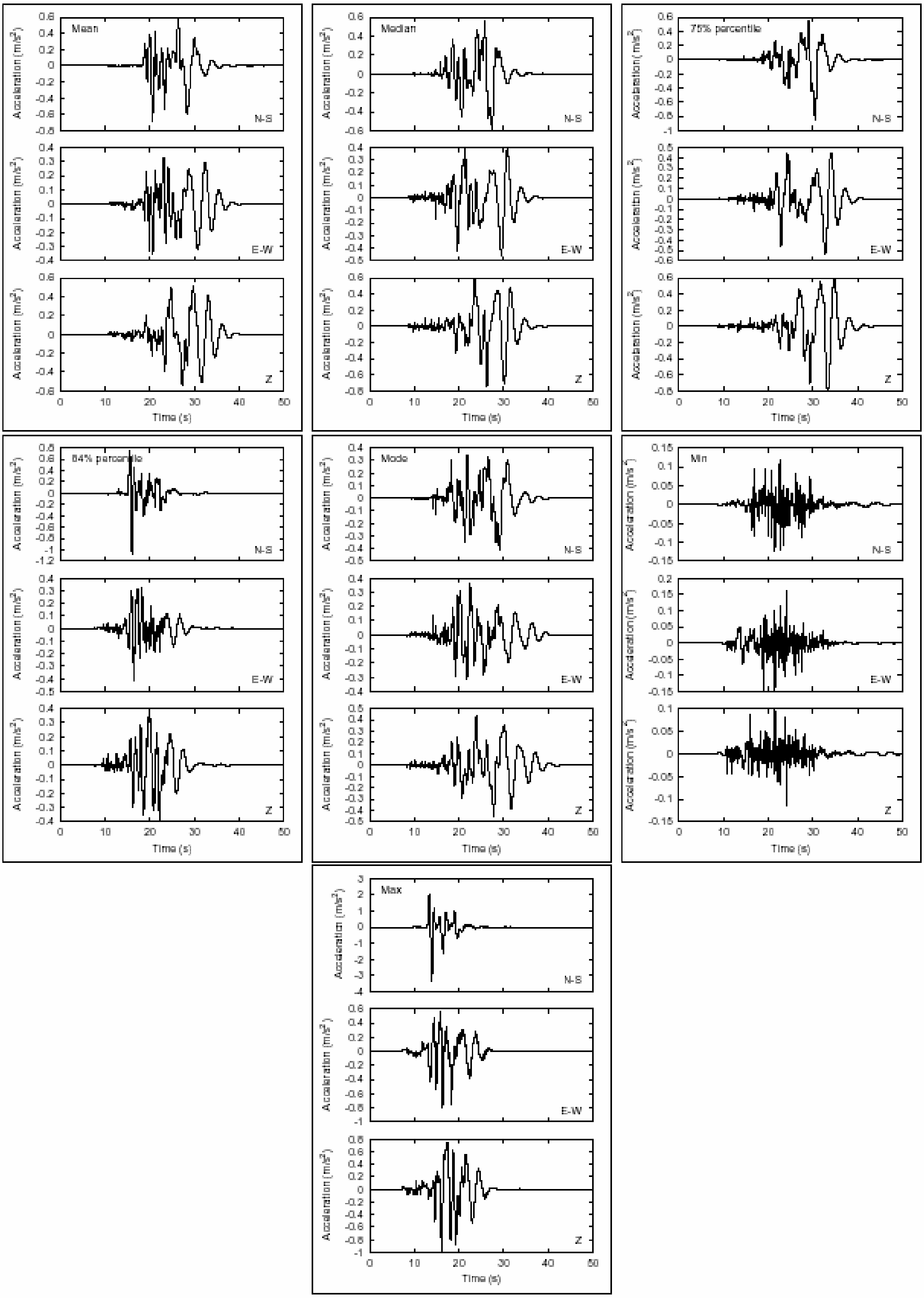

Figure 3.11. Seismograms (NS, EW and vertical components) from F3 fault corresponding to mean, median, 75% percentile, 84% percentile, mode, minimum and maximum PGA.

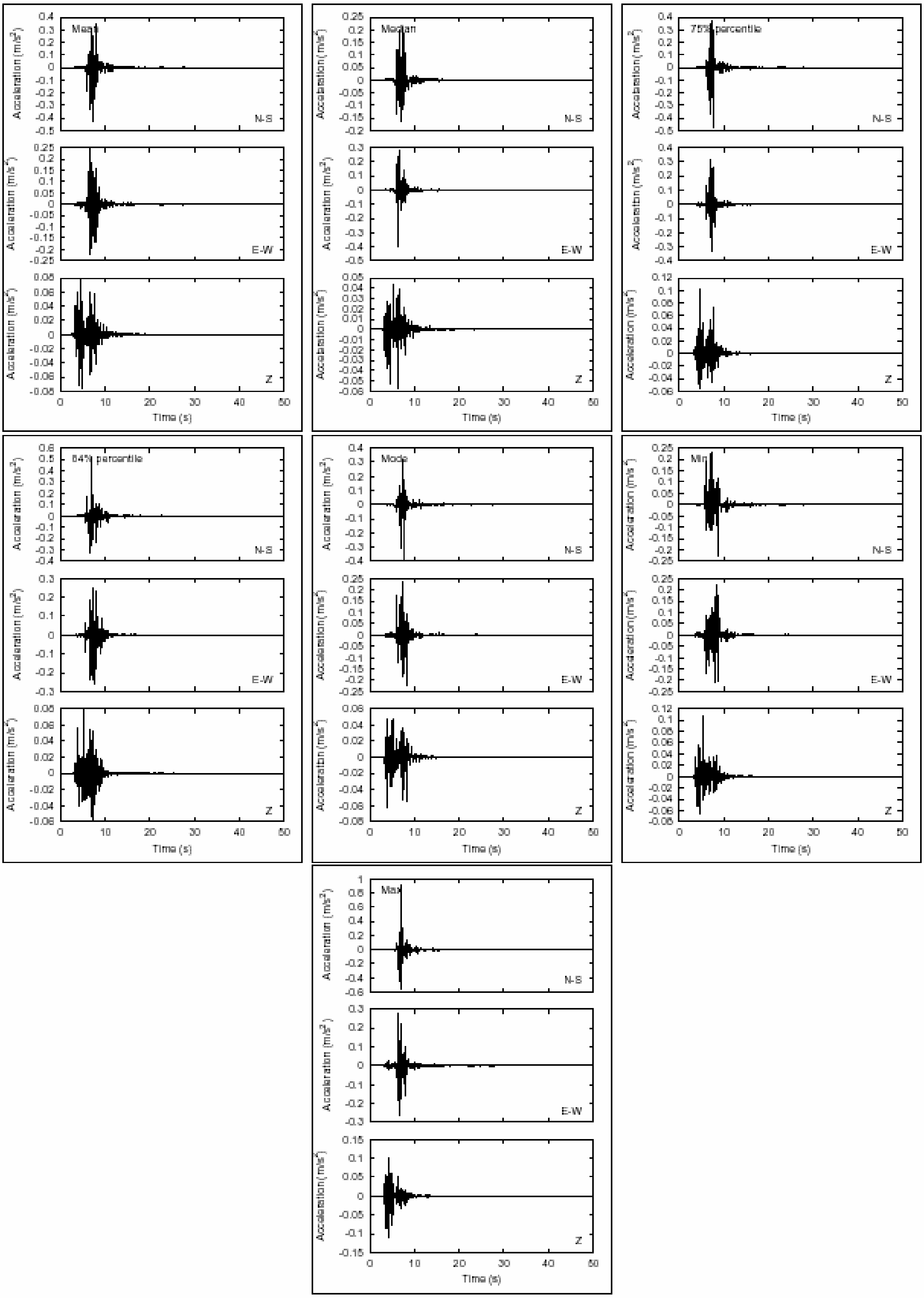

Figure 3.12. Seismograms (NS, EW and vertical components) from F7 fault corresponding to mean, median, 75% percentile, 84% percentile, mode, minimum and maximum PGA.

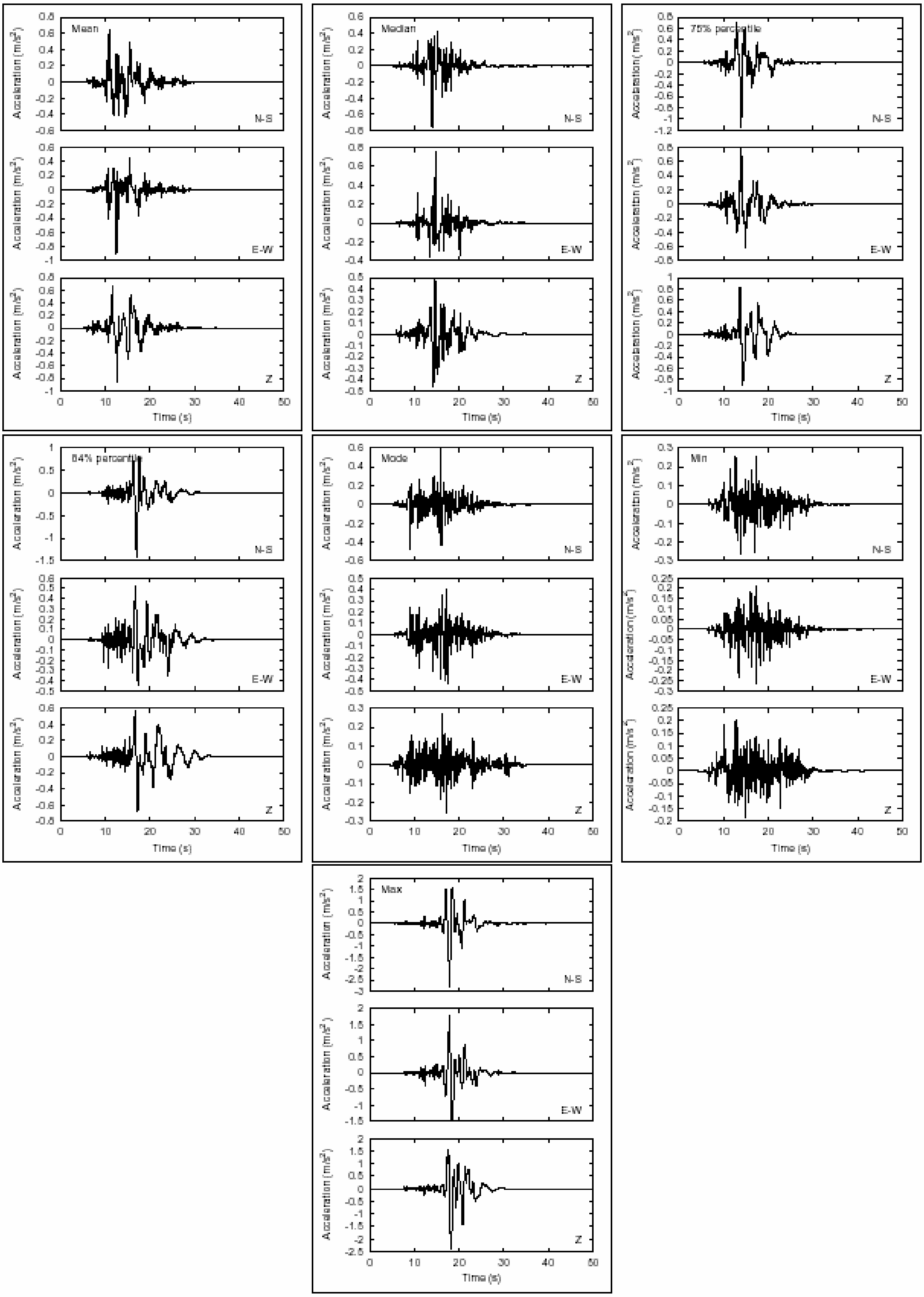

Figure 3.13. Seismograms (NS, EW and vertical components) from F8 fault corresponding to mean, median, 75% percentile, 84% percentile, mode, minimum and maximum PGA.

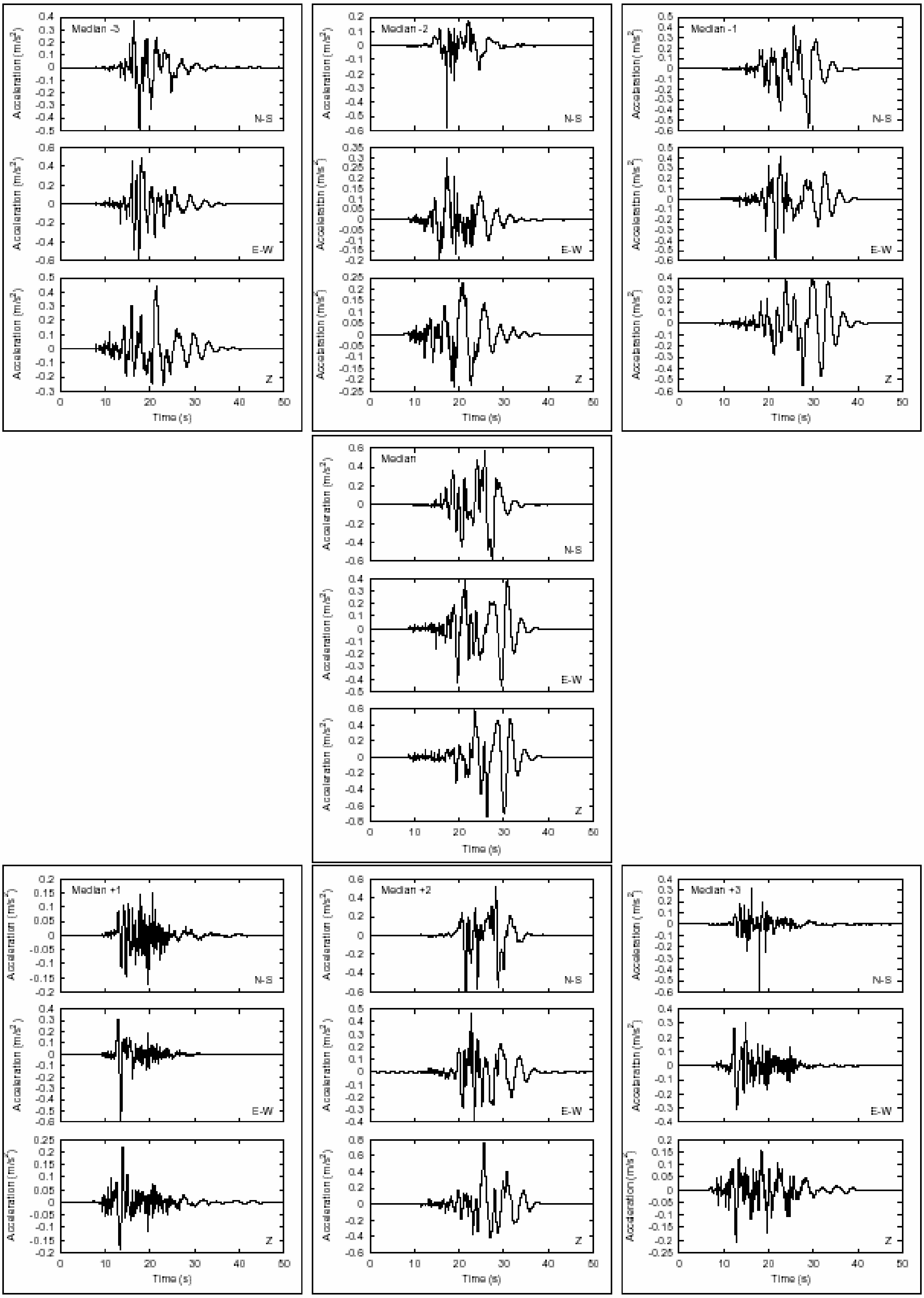

Figure 3.14. Seismograms (EW component) from F3 fault having PGAs in the neighborhood of the median value of the PGA distribution.

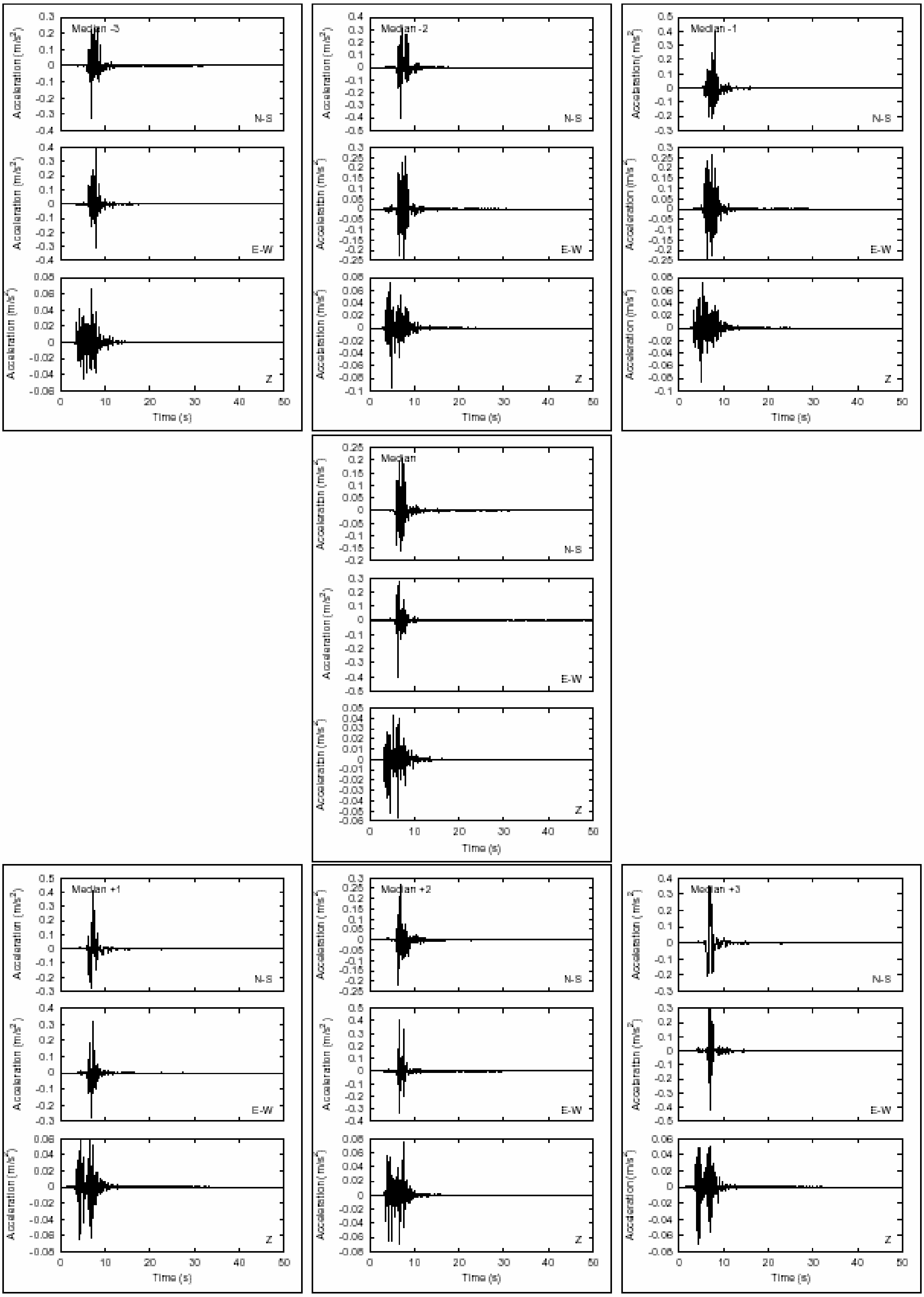

Figure 3.15. Seismograms (EW component) from F7 fault having PGAs in the neighborhood of the median value of the PGA distribution.

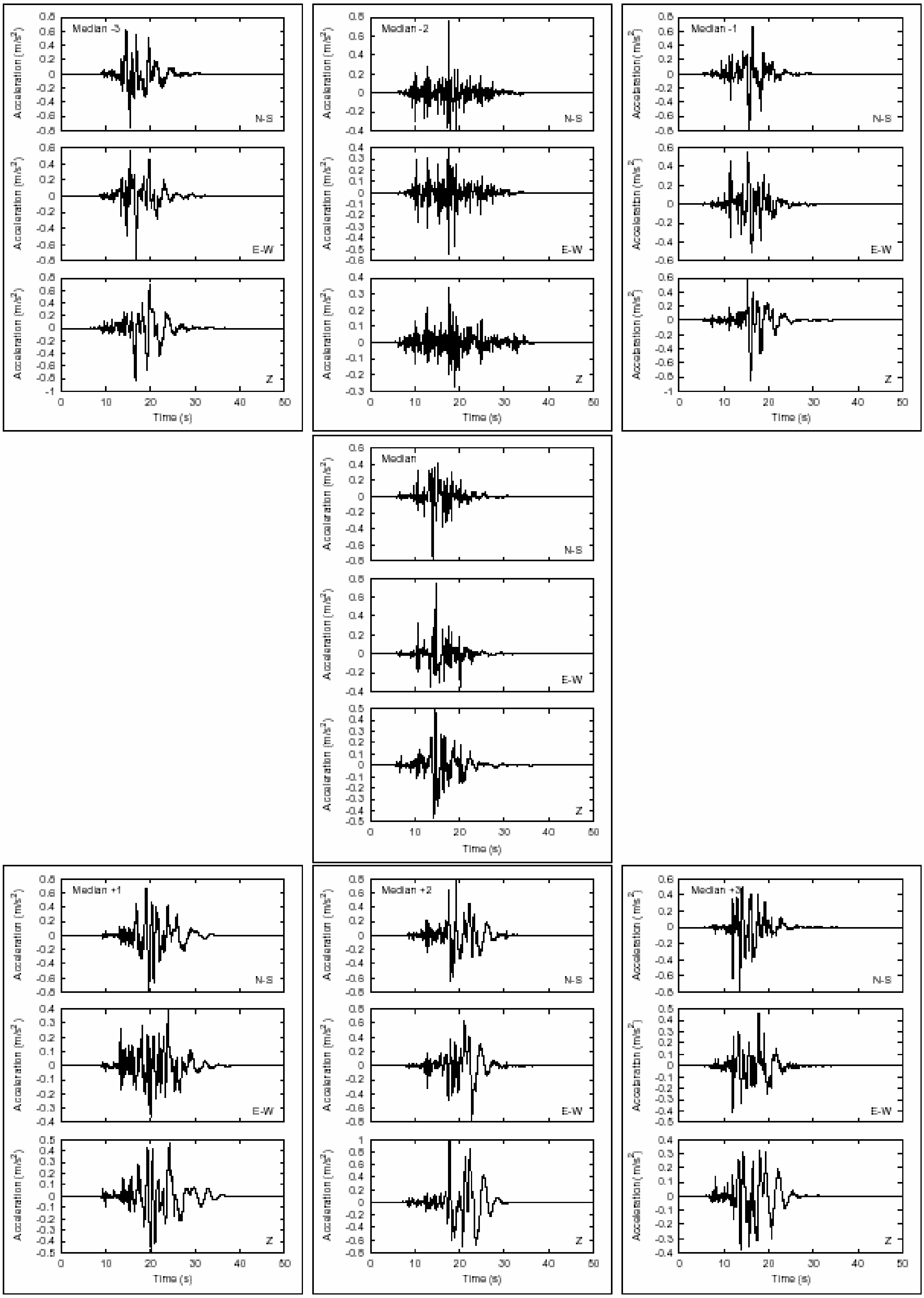

Figure 3.16. Seismograms (EW component) from F8 fault having PGAs in the neighborhood of the median value of the PGA distribution.

3.4 SHAKING SCENARIOS WITH STOCHASTIC METHOD (EXSIM RESULTS)

The prediction of expected strong ground-motions and their natural variability at sites located at a given distance from an earthquake of a given magnitude is one of the most critical elements of any seismic hazard analysis. In recent decades many studies have worked on the stochastic characterization of seismic ground motion by the application of seismological models. The effects of a large finite source, including rupture propagation, directivity and source receiver geometry can profoundly influence the amplitudes, frequency content and duration of ground motion.
The finite-fault simulation method FINSIM (Beresnev and Atkinson, 1997, 1998b), an extension of the stochastic point simulation method of Boore (2003), is an efficient stochastic approach world wide used and known. This method assumes that the fault plane is a rectangle, subdivided into an appropriate number of sub-faults, which are modeled as point sources characterized by a ω^2 spectrum. The sub-fault moment and corner frequency are derived from the size of each sub-fault and the number of triggered sub-faults is adjusted so that the specified target moment is achieved.
In this project we have used a new version of the above mentioned approach that is the code EXSIM (Motazedian and Atkinson, 2005). This program offers several significant advantages over previous stochastic finite-fault models (FINSIM) introducing a new variation based on a "dynamic corner frequency" and implementing the concept of pulsing area.

3.4.1 Simulation parameters

The finite-fault stochastic approach needs model parameters on the fault-plane geometry (length, width, strike, dip, number of sub-faults considered and depth to the upper edge), on the source parameters (seismic moment, slip distribution, stress drop, nucleation point, rupture velocity) and on the crustal properties of the region (geometrical spreading coefficient and anelastic attenuation). For this study we use available published parameters from previous researches in the area. The site-specific soil response information could be specified and inserted as additional input in the used EXSIM program in order to obtain the shaking at the surface but this is not the scope of this part of the study.

Crustal properties of the region

The parameters of the propagation model adopted are those used for the simulation of the 1980 Irpinia earthquake presented in *PS3-Deliverable D0*, 2006 and used in "*Modeling the 1980 Irpinia Earthquake by stochastic simulation. Comparison of seismic scenarios using finite-fault approaches*" (Zonno and Carvalho, 2006). The values of crustal properties parameters used in the simulation are shown in the Table 1. and the parameters have been considered fixed in the analysis done applying the different faults. The attenuation factor, Q(f), is very important but we have decide to have as input variable only the rupture models coming from the different slip distributions and the position of the nucleation point on the fault plane.

Table 3.4.1. Simulation parameters used to evaluate the scenarios with EXSIM

Quality factor, $Q(f)=Q_0 f^{\eta}$	$Q_0 = 100 \quad \eta = 1$
Geometric spreading	1 30. 130. and -1. -0.0 -0.5
Stress drop	100 or 200 bar
Distance-dependent duration (sec)	1. 100. 500. and 0.1 0.1 0.1
Bedrock parameter K	0.03
Shear wave velocity	3.7 km/sec
Rupture velocity	0.8*3.7 km/sec
Crustal density	2.6 gr/cm^3
Trials and damping	30 and 5%
Dynamic Flag with Pulsing Percent	1 and 50
Filter	Saragoni-Hart taper windows

Sources parameters

As described in Chapter 2. the faults that could be generate significative shaking at the site of Potenza nine. They are shown in the Figure 3.1 and 3.4.1. The geometry and the sources parameters of the faults are listed in Table 3.1 and Table 3.4.1.
Table 3.4.2 lists, for each fault, the name, the moment magnitude, the surface rupture length, the fault-orientation parameters (dip and strike) and the depth of the top of the fault. Other information, shown in Table 3.4.2, are the number of sub-faults subdivision and the fault and hypocenter distances in respect to the origin of the fault that are connected to the used simulation procedure.

The nucleation points were located in the half deepest part of the fault generating different rupture directions (i.e. Unilateral NE/SW, Bilateral and Unilateral SW/NE rupture). For each fault is assumed a slip distribution assuming a Gaussian distribution of the slip, centered on the nucleation points 1, 2 and 3 (see Table 3.4.3). The total amount of slip depends from the moment magnitude and we have for each fault a different Gaussian distribution centered on the given nucleation points. We consider also the case of random slip distribution and the case of random nucleation position obtaining a total of 16 rupture models (see Table 3.4.2 and Figure 3.4.5).

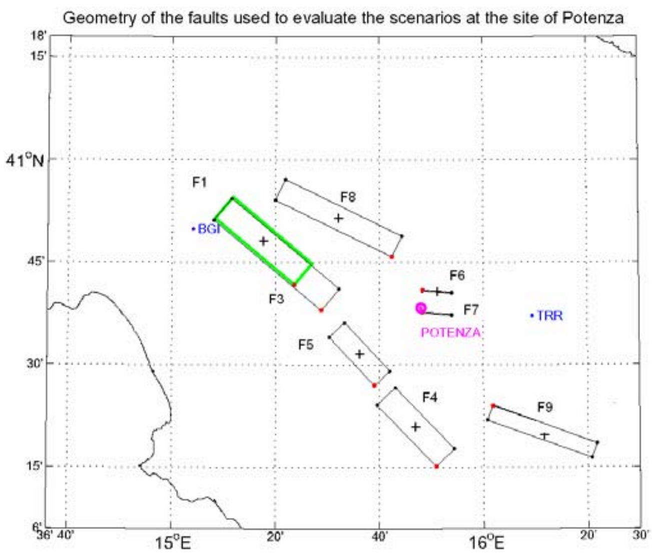

Figure 3.4.1 Geometry of the faults used to compute the scenarios at the site of Potenza.

Table 3.4.2 Sources parameters of the faults used to evaluate the bedrock scenarios at the site of Potenza

Fault code	ITGG077	ITGG007	ITGG010	ITGG008	ITGGa84	ITGGd84	ITGG063	ID XX
Fault name	Colliano	Irpinia (0+20 s)	Melandro Pergola	Agri Valley	Potenza (ID a8411)	Potenza (ID d8411)	Andreatta Filano	Scorcia-buoi
Strike (°)	310	310	317	316	95	95	296	110
Dip (°)	60	60	60	60	88	88	70	75
Length (km)	28.0	38.0	17.9	23.0	7.9	7.9	35.0	30.0
Width (km)	15.0	15.0	11.3	13.5	6.2	6.2	18.0	16.0
Depth (km)	1.0	1.0	1.0	1.0	14.8	14.8	1.0	1.0
# Sub-faults	14 x 7	19 x 7	9 x 6	11 x 7	4 x 3	4 x 3	17 x 9	15 x 8
Ave.Slip (m)	1.2	1.24	0.44	0.57	0.24	0.24	1.12	0.74
Mw (*****)	6.8	6.9	6.3	6.5	5.7	5.7	6.9	6.7
OR-Lon1 (°)	15.3931	15.4799	15.6504	15.8484	15.8052	15.8050	15.7068	16.030
OR-Lat1 (°)	40.6954	40.6333	40.2528	40.2528	40.6826	40.6286	40.7638	40.400
F.-DIST (km)	34.05	25.83	34.95	26.07	15.62 .	14.88	16.04	32.94
H.-NP1 (km)	35.47	27.25	41.04	40.40	20.54 .	20.06	26.26	39.18
H.-NP2 (km)	46.01	40.57	39.04	33.04	18.77 .	18.27	32.48	48.09
H.-NP3 (km)	59.70	59.77	35.29	26.51	21.65 .	21.34	52.26	62.50
H.-NP4 (km)	35.22	32.16	38.89	28.57	18.56	18.00	41.25	60.05

(*****) The relation Moment magnitude = 10.**(1.5*amag+16.05) is used in the EXSIM program

3.4.2 Simulation procedure

The simulation and the analysis of sets of time series at the site of Potenza [POT (40.6387; 15.8000)] is certainly a good way to evaluate how the different faults are be able to generate level of shaking with specific behavior both in amplitude and frequency. The simulation procedure has the general goals to detect the fault able to generate the most severe shaking at the site of Potenza and to validate the simulation results from the assumed models parameters comparing them with some recorded data at given sites. First, we have processed, using the EXSIM program, the 8 selected faults (see Figure 3.4.1 and Table 3.4.2) with the same crustal model parameters (Table 3.4.1) and using two different values of the stress drop. The stress parameter must be chosen carefully because it strongly influences the results. In fact, the amplitude of the source spectrum linearly depends from the square root of this parameter and the have decided to use two values of stress drop (100 and 200 bar). Furthermore, in the case of fault F7 (Potenza), we carried out an additional simulation considering a different value of the depth of the top of the fault (7.8 km).

Another critical factor in the simulation analysis is the slip distribution on the fault plane. In the present study, we evaluated the bedrock shaking scenarios at the Potenza site in terms of PGA and SI (Housner) parameters, considering eight faults. Here, we cannot carry out specific analyses to select the best slip distribution for a good fitting between the simulated and recorded data. We have decided to assume for each fault the same scheme to change the slip distributions and the position of the nucleation point on the fault plane. For each fault we simulated 16 rupture models (4 nucleation points and 4 slip distributions) for a total of 480 scenarios at the

investigated site of Potenza.
Table 3.4.3 list the codes used to identify the rupture models. For example the model **11** means *slip distribution 1* with the *nucleation point 1*.
To validate the simulation results we have considered two stations: Bagnoli Irpino (BGI) and Tricarico (TRR) recording the 1980 Irpinia earthquake (M 6.9). Considering the fault F1 (Colliano) we have compared the simulated and computed response spectra in two extreme cases: BGI very close and TRR very far to the fault F1 (see Figure 3.4.1).

Table 3.4.3 The ID reference code for the 16 rupture models applied to each fault

ID of rupture models	NP 1	NP 2	NP 3	NP 4 (Random)
SLIP 1	**11**	**12**	**13**	**14**
SLIP 2	**21**	**22**	**23**	**24**
SLIP 3	**31**	**32**	**33**	**34**
SLIP 4 (Random)	**41**	**42**	**43**	**44**

When we consider a fault with the above simulation procedure we obtain for 16 rupture models a total of 480 time series at the site. If we consider the maximum value of the PGA for each simulated time series we obtain a set of PGA values of which is possible by statistical analysis to find the values of the median, of the 75%, of the 84%, of the mean, of the mode, of the minimum and of the maximum.
The next step is to associate the time series that matches the 7 statistical values. Table 3.4.4 lists a general summary of the statistical results obtained for different faults and for different sites.
This procedure would be possible with other shaking parameters. In fact, in the simulation procedure, we also used another measure of the shaking, the *Response Spectrum Intensity* (SI, Housner, 1959), which is defined as:

$$SI(\zeta) = \int_{0.1}^{2.5} PSV(\zeta, T)dT$$

for the area under the pseudo velocity response spectrum between the periods of 0.1 s and 2.5 s. The *response spectrum intensity* is calculated for a damping ratio of 5%. This SI parameter captures important aspects of the amplitude and frequency content in a single parameter. In Tables 3.4.4 and 3.4.5, the results from the statistical analyses are shown, using both the SI (Housner) and PGA criteria obtained for different faults and for different sites.

3.4.3 Results

The results of applying the simulation procedure to the eight faults, F1, F3, F4, F5, F6, F7, F8 and F9, can be seen in terms of the number of the frequency versus SI (Housner) classes (Table 3.4.4) or in terms of the number of the frequency versus PGA classes (Table 3.4.5). Figures 3.4.2 and 3.4.3 show, respectively, the number of the frequency in terms of the SI (Housner) and PGA classes. We have a total of 3,840 time series if we consider the contributions from the eight faults at the Potenza site. The comparison of the black bars (all faults) with the yellow bars (single fault) highlights the characteristics of each fault. We can see, for instance, that the yellow bars of faults F3 and F8 indicate a more severe level of shaking in comparison to the other faults. This is confirmed if we use either the PGA or the SI (Housner) criteria.
Figure 3.4.3 gives the different behaviors of the time series associated with the

statistical values of PGA corresponding to the median, 75% percentile, 84 % percentile, mean, mode, minimum and maximum. The results from the different stress drop values show a systematic increase in the values in terms of PGA and SI (Housner) if we consider a higher stress drop value. We note that each time series is identified by a string (for example POT-07-01-19-41.acc) specifying the code of the station, the code of the fault (see Table 3.4.2), the number of the site analyzed, the number of the sequential trial within the total of 30, and the number of the rupture model.

In Table 3.4.5, the details of the results of the statistical analysis of PGA are given, and we note that this fault, F8 (Andreatta Filano), produces more severe levels of shaking than those obtained from fault F3 (Irpinia, 0 + 20 s). In Figures 3.4.2 and 3.4.3, it is possible see how fault F8 has higher values of the number of the frequency *versus* the SI (Housner) and PGA classes. In annex A, the results for each fault for the different source model are reported.

The stochastic finite-fault simulation to evaluate the bedrock scenarios at the Potenza site were performed using the EXSIM program. From the simulation results, we determined that fault F8 (Andreatta Filano) produces the most severe shaking at Potenza. Then, we calculated the 480 time series from the use of 16 rupture models, using a value of 200 bar and the model parameters listed in Tables 3.4.1 and 3.4.2. What makes the differences from the simulated records are the different rupture models, because all of the other parameters are taken as fixed. The rupture models are different both for the slip distribution and for the nucleation points that are at different distances with respect to the Potenza site. The 480 time series were analyzed using the PGA and SI (Housner) criteria, finding for each shaking parameter the corresponding statistical values of the median, 75% percentile, 84% percentile, mean, mode, minimum and maximum. The seven time series associated with the statistical values constitute the seismic input at the bedrock, which is different depending on which selection criteria we consider.

In Figure 3.4.4, the time series selected using the PGA criteria are shown, along with the corresponding response spectra (5% damping). The red line indicates the response spectra with the higher value of PGA, equal to 145. cm/s*s. In the middle, in the grey area, the string-code of the time series associated with the PGA statistical values is listed.

In Figure 3.4.5, the time series selected using the SI (Housner) criteria are shown, along with the corresponding response spectra (5% damping). For the comparison with the case of the PGA criteria, we still present the PSA response spectra, and not PSV response spectra velocity, from which we have computed the SI (Housner) parameter. The red line indicates the response spectra with the higher value of SI, equal to 96. cm. In the middle, in the grey area, the string-code of the time series associated with the SI statistical values is listed.

In the space of the models used for the simulation procedure using the EXSIM program, we are able to select the inputs using different criteria with the same set of time series. We see that the PGA criteria highlight more the PGA range (Figure 3.4.4), while the SI (Housner) criteria highlight more the SI range computed in the range 0.1-2.5 s. This is more evident if we analyze Figures 3.4.6 and 3.4.7, showing the average response spectra (5% and 30 trials) of the corresponding rupture models (see Figures 3.4.4 and 3.4.5).

Table 3.4.4 Summary of the statistical analysis of the shaking SI (Housner) values generated from eight faults: F1, F3, F4, F5, F6, F7, F8 and F9, at the Potenza site (Cases A, B and D), and of the shaking SI (Housner) values generated from fault F1 at the Tricarico and Bagnoli Irpino sites (Cases D and E). The statistical analysis was carried out considering the 480 time series (30 trials x 16 slip models) generated by each single fault. The shaking SI (Housner) values are expressed in cm.

Statistical analysis of the shaking SI (Housner) values at the sites analyzed

Case A --- POTENZA --- Stress drop 100 bar

Fault	median	75%	84%	mean	Mode	Min	Max
F1	26.163	29.689	26.620	31.842	27.500	16.446	45.546
F3	30.654	35.211	31.322	37.717	27.500	18.446	52.821
F4	13.211	14.886	13.419	15.697	12.500	7.925	22.521
F5	20.185	23.446	20.715	25.225	17.500	10.623	33.797
F6	8.267	9.014	8.202	9.423	7.500	5.061	12.098
F7	8.278	9.202	8.406	9.780	7.500	5.163	13.195
F8	36.125	41.780	36.811	44.217	37.500	19.553	63.577
F9	23.230	26.623	23.693	28.284	22.500	11.395	35.207

Case B --- POTENZA --- Stress drop 200 bar

Fault	median	75%	84%	mean	Mode	Min	Max
F1	38.918	43.669	39.285	46.938	37.500	24.579	67.177
F3	45.825	52.125	46.631	56.062	37.500	27.499	78.798
F4	18.376	20.684	18.729	21.884	17.500	11.333	32.016
F5	29.054	33.282	29.583	35.971	27.500	15.553	47.603
F6	10.750	11.736	10.690	12.173	12.500	6.906	15.882
F7	10.761	11.952	10.960	12.694	12.500	6.907	17.196
F8	54.000	62.174	55.016	66.079	52.500	29.795	95.962
F9	32.909	37.154	33.506	40.084	32.500	16.896	51.244

Case C --- POTENZA --- Stress drop 100 bar and depth 7.8 km

Fault	median	75%	84%	mean	Mode	Min	Max
F7	13.535	15.027	13.687	15.762	12.500	9.210	21.097

Case D --- TRICARICO--- BAGNOLI IRPINO Stress drop 100 bar

Fault	median	75%	84%	mean	Mode	Min	Max	
F1	21.508	24.272	21.679	25.615	22.500	12.099	36.243	**TRR**
F1	44.132	52.847	45.923	56.872	42.500	26.476	74.905	**BGI**

Case E --- TRICARICO --- BAGNOLI IRPINO Stress drop 200 bar

Fault	median	75%	84%	mean	Mode	Min	Max	
F1	31.522	35.631	31.768	37.457	32.500	17.815	53.220	**TRR**
F1	78.579	92.329	79.204	98.099	62.500	38.750	147.732	**BGI**

Frequencies of the SI (Housner) classes considering the different faults

Case A --- POTENZA --- Stress drop 100 bar

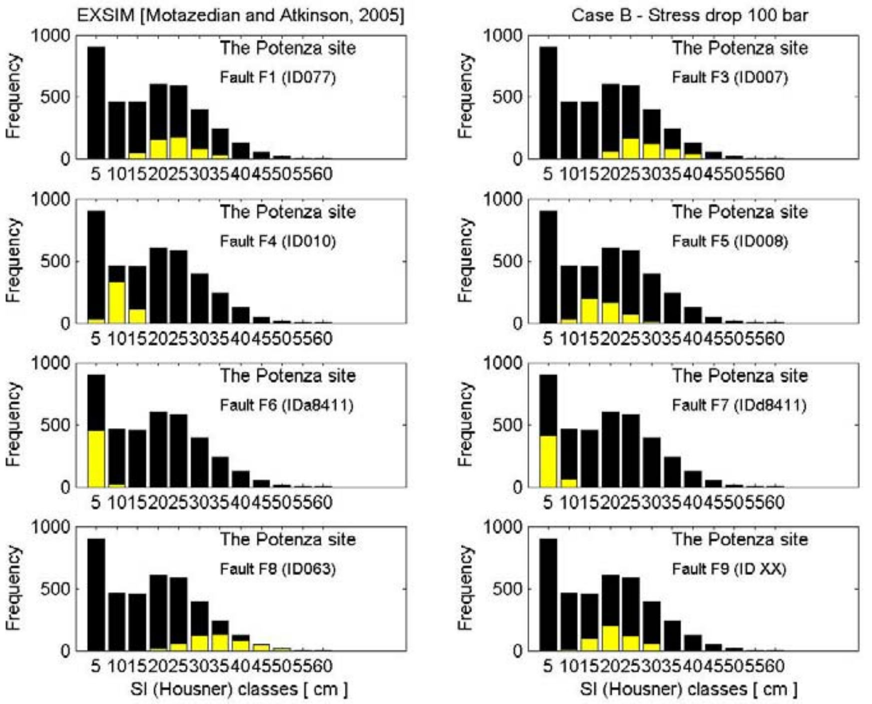

Case B --- POTENZA --- Stress drop 200 bar

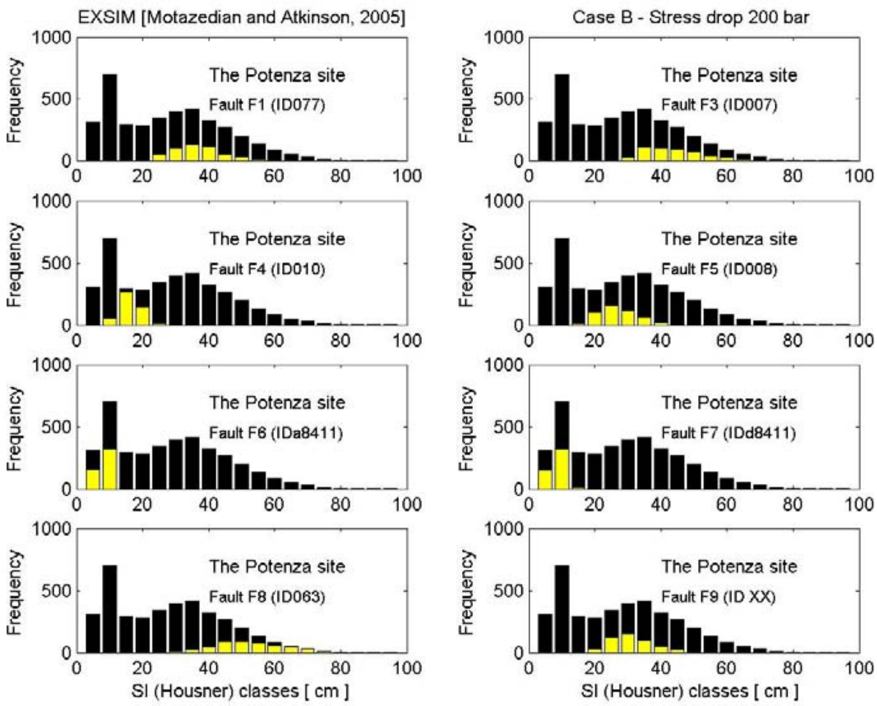

Figure 3.4.2 Comparisons of the frequency *versus* SI (Housner) class graphs considering the 3,840 time series produced from all of the faults (black bars) and considering the 480 time series from each single fault (yellow bars). The results from the different values of stress drop (100 and 200 bar) are shown.

Table 3.4.5 Summary of the statistical analysis on the time series generated from 8 faults: F1, F3, F4, F5, F6, F7, F8 and F9 at the site of Potenza (Cases A, B and D) and on the time series generated from F1 fault at the site of Tricarico and Bagnoli Irpino (Cases D and E). The shaded rows (grey) indicate that the statistical results will discuss analyzing in details the contribution of each different slip distribution. The statistical analysis has been done considering the 480 time series (30 trials x 16 slip models) generated by each single fault. The shaking PGA values are expressed in cm/s*s.

Statistical analysis of the shaking PGA values at the analyzed site

Case A --- POTENZA --- Stress Drop 100 bar

Fault	median	75%	84%	mean	Mode	Min	Max
F1	34.588	39.941	35.567	43.099	32.500	20.541	64.263
F3	40.417	49.707	42.972	55.359	32.500	23.140	84.902
F4	20.658	23.744	21.129	24.964	17.500	12.618	35.624
F5	31.432	36.993	33.192	40.793	27.500	19.272	64.393
F6	22.300	24.692	22.620	26.154	22.500	15.251	36.469
F7	23.059	25.564	23.479	27.118	22.500	14.525	35.102
F8	51.667	63.598	54.015	67.832	47.500	28.956	93.558
F9	29.605	34.817	30.656	37.478	27.500	18.167	57.377

Case B --- POTENZA --- Stress Drop 200 bar

Fault	median	75%	84%	mean	Mode	Min	Max
F1	53.047	60.983	54.437	66.533	47.500	31.133	97.372
F3	62.138	76.630	66.242	84.668	52.500	35.060	128.053
F4	31.069	35.615	31.778	37.686	27.500	18.910	55.230
F5	48.387	56.477	50.599	61.544	42.500	29.592	98.427
F6	33.250	36.890	33.837	39.363	32.500	23.450	54.599
F7	34.502	38.262	35.198	40.842	32.500	22.535	54.203
F8	80.575	98.035	83.535	104.761	72.500	43.426	145.796
F9	45.111	53.169	46.615	57.071	42.500	28.236	88.524

Case C --- POTENZA --- Stress Drop 100 bar & depth 7.8 km

Fault	median	75%	84%	mean	Mode	Min	Max
F7	44.045	48.303	45.075	51.428	42.500	32.361	77.876

Case D --- TRICARICO--- BAGNOLI IRPINO Stress drop 100 bar

Fault	median	75%	84%	mean	Mode	Min	Max	
F1	23.187	26.641	23.735	28.158	22.500	13.382	44.796	**TRR**
F1	97.317	114.761	97.506	122.947	97.500	41.064	182.556	**BGI**

Case E --- TRICARICO --- BAGNOLI IRPINO Stress drop 200 bar

Fault	median	75%	84%	mean	Mode	Min	Max	
F1	35.049	40.090	35.645	42.347	37.500	19.841	67.578	**TRR**
F1	151.193	178.695	151.727	193.091	152.500	64.280	285.293	**BGI**

Frequencies of the PGA classes considering the different faults

Case A --- POTENZA --- Stress drop 100 bar

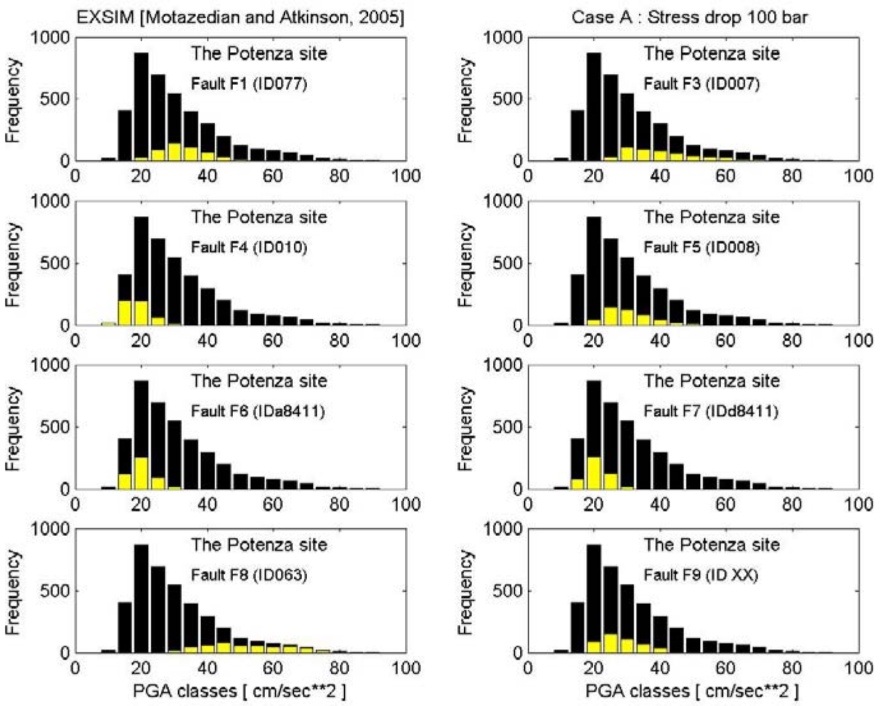

Case B --- POTENZA --- Stress drop 200 bar

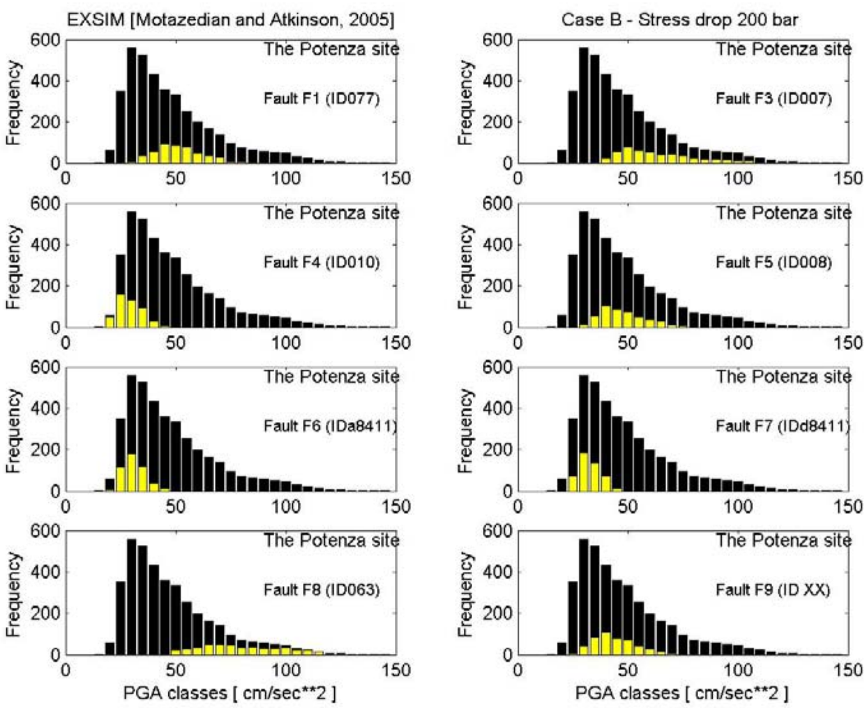

Figure 3.4.3 Comparison of graphs of the frequency versus PGA classes considering the 3840 time series produced from all faults (black bars) and considering the 480 time series from each single faults (yellow bars). The results from a different value of stress drop (100 and 200 bar) are shown.

Case B --- POTENZA --- PGA selection criteria	Stress drop 200 bar

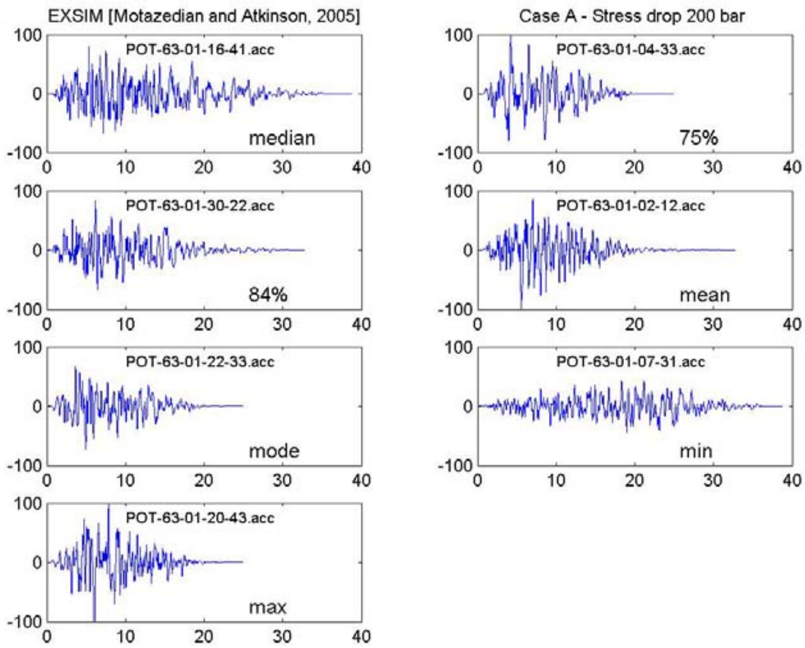

1	**median**	record	381	value	**80.652**	name	**POT-63-01-16-41.acc**
2	**75%**	record	328	value	**98.035**	name	**POT-63-01-04-33.acc**
3	**84%**	record	177	value	**83.542**	name	**POT-63-01-30-22.acc**
4	**mean**	record	53	value	**104.761**	name	**POT-63-01-02-12.acc**
5	**mode**	record	305	value	**72.485**	name	**POT-63-01-22-33.acc**
6	**min**	record	241	value	**43.426**	name	**POT-63-01-07-31.acc**
7	**max**	record	450	value	**145.796**	name	**POT-63-01-20-43.acc**

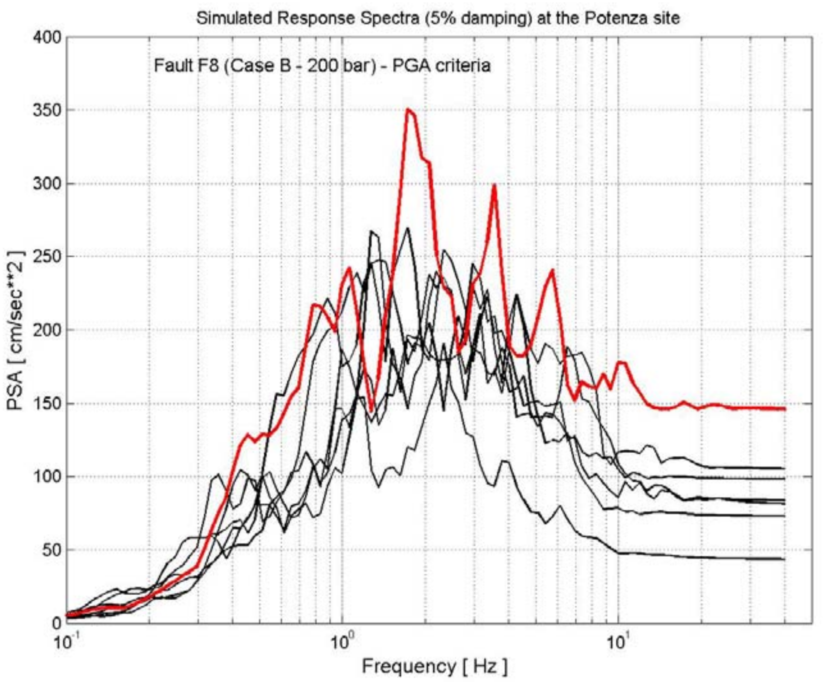

Figure 3. 4.4. The bedrock scenarios at the Potenza site, with input selected from the statistical analysis of the shaking PGA values. The red line shows the response spectra that corresponds to a value of PGA equal to 145.796 (cm/s*s). The string-codes of the time series are listed on the shaded grey area.

Case B --- POTENZA --- SI (Housner) selection criteria Stress drop 200 bar

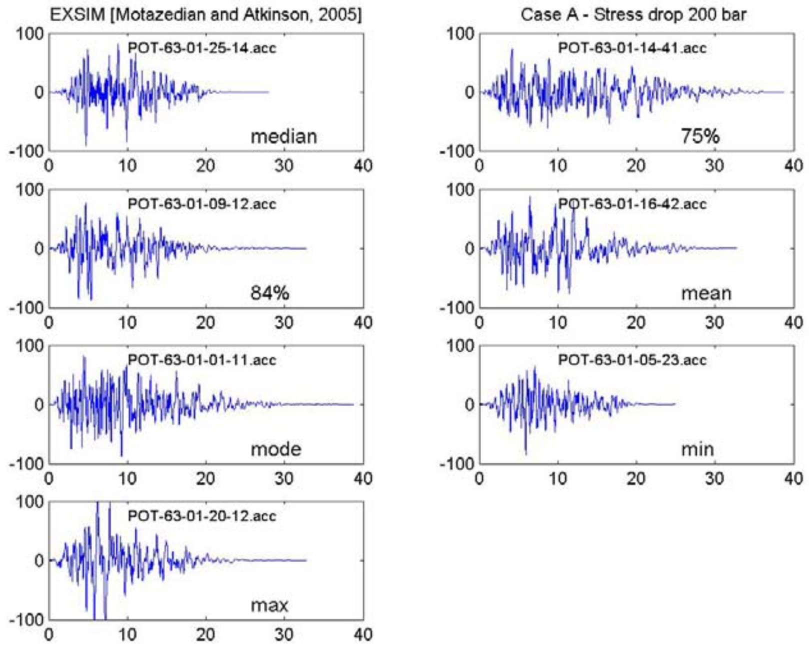

1	**median**	record	94	value	**54.053**	name	**POT-63-01-25-14.psv**
2	**75**%	record	389	value	**62.174**	name	**POT-63-01-14-41.psv**
3	**84**%	record	37	value	**55.088**	name	**POT-63-01-09-12.psv**
4	**mean**	record	418	value	**66.079**	name	**POT-63-01-16-42.psv**
5	**mode**	record	3	value	**52.475**	name	**POT-63-01-01-11.psv**
6	**min**	record	181	value	**29.79**5	name	**POT-63-01-05-23.psv**
7	**max**	record	60	value	**95.962**	name	**POT-63-01-20-12.psv**

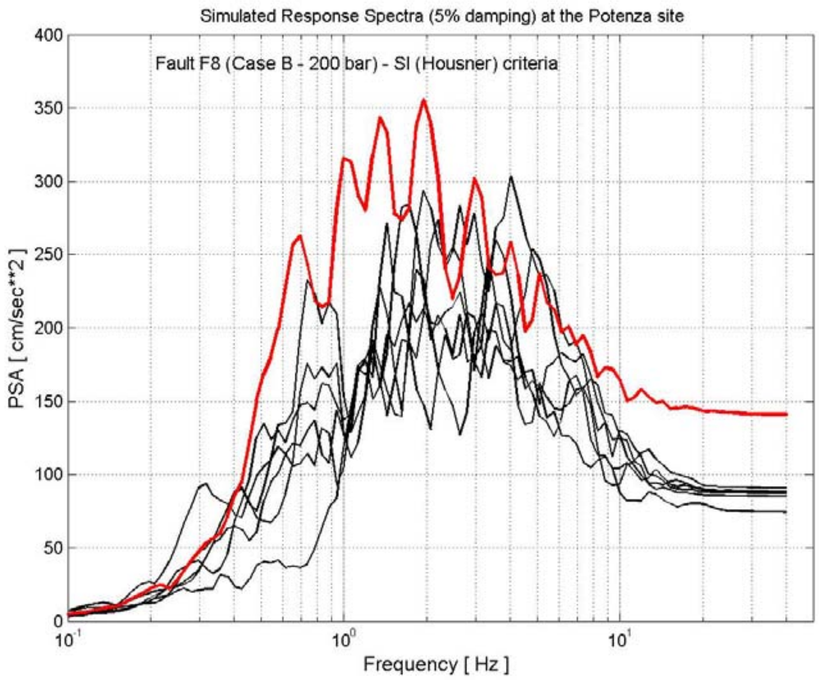

Figure 3.4.5 The bedrock scenarios at the Potenza site, with input selected from the statistical analysis of the shaking SI (Housner) values. The red line shows the response spectra that corresponds to a value of SI (Housner) equal to 95,962 (cm).

Case B --- POTENZA	Stress drop 200 bar

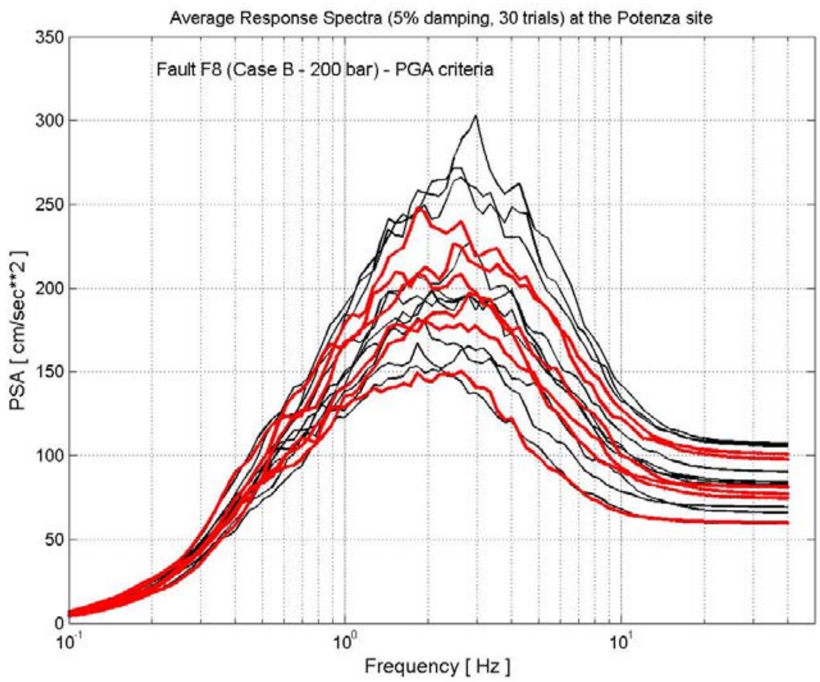

Figure 3.4.6 The EXSIM average response spectra (5% damping, 30 trials) related to all 16 rupture models (black line). The response spectra related to the rupture models (41, 33, 22, 12, 31 and 43) obtained from Fault F8, (Case B - 200 bar) – PGA criteria, are shown (red line).

Case B --- POTENZA	Stress drop 200 bar

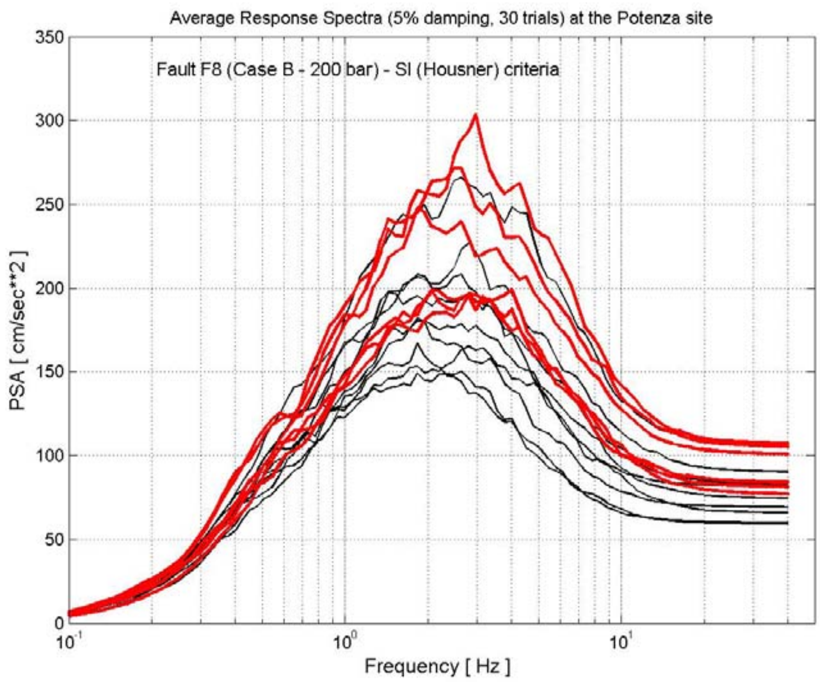

Figure 3.4.7 The EXSIM average response spectra (5% damping, 30 trials) related to all 16 rupture models (black line). The response spectra related to the rupture models (14, 41, 12, 42, 11 and 23) obtained from Fault F8, (Case B - 200 bar) – SI criteria, are shown (red line).

4. INTENSITY SCENARIOS BY A PROBABILISTIC EMPIRICAL APPROACH

A basic information for the assessment of damage scenarios associated to future strong earthquakes is the propagation pattern of the seismic energy radiated at the source to the site of interest (attenuation loosely speaking). Due to structural irregularities in the crustal structure interested by the propagation process, the amount of energy, its spectral distribution and time evolution results quite variable from site to site and from earthquake to earthquake. In principle, the process is entirely deterministic and suitable for a precise quantitative analysis. However, such modelling requires a detailed knowledge of the mechanical structure of the subsoil at least at the scale of the wavelengths of interest. Since this information is generally lacking, an empirical indirect approach becomes mandatory and the purely deterministic problem assumes becomes inherently probabilistic. In fact, the so called attenuation pattern is modelled by using simple empirical models whose parameters are determined by the statistical analysis of data available on past earthquakes. This is true both when instrumental parameters of ground shaking (PGA, Housner, etc.) are of concern and when intensity data are considered.
Of course, such empirical models do not aim at capturing the physical nature of the phenomenon but jut to evaluate some “average pattern” as a function of source parameters (e.g. magnitude, maximum observed intensity, etc.) and simple geometrical constraints (source-site distance, orientation of the source with respect to the site, etc.) and regional structural properties (seismogenic zone, regional tectonic style, etc.). The empirical relationships that allow to compute such average pattern are usually called “attenuation relationships”.
Whatever complex these relationships can be, they cannot represent all the possible situations but just the “average” one. This implies that the simple use of such “empirical” attenuation relationships as an “equivalent” of deterministic attenuation relationship is misleading since the latter are simply unable to capture the possible variability of the phenomenon and may result in dramatic underestimates of actual seismic effects. To take this aspect into account, the attenuation pattern is generally modelled by using a probabilistic form such as

$$P_i(I_s) = prob\left[\geq I_s \middle| T_i\right] \qquad [1]$$

where P is the probability that the ground shaking parameter (or intensity) I at the *s-th* site during the *i*-th earthquake T_i is at least I_s. In general, the probability $P(I_s)$ is conditioned by epicentral ([E]), geometrical ([R]) and structural ([Z])parameters. In this case, the [1] assumes the form

$$P(I_s) = P\left(I_s \middle| [E],[R],[Z]\right) \qquad [2]$$

where, for simplicity, the dependence on the *i-th* event has been considered as implicit. The attenuation relationship in the form [2] makes explicit the empirical

character of the "forecast" provided in this way. In general, by a suitable setting of the empirical parameters involved in the formulation of [2] this kind of equation allows to compute the probability that a specific ground shaking threshold is overcome at the site of interest given a specific configuration of the set of the independent variables ([E],[R],[T]).
As concerns the Italian region, the attenuation relationship relative to macroseismic intensity I_s in the general form [2] has been analysed in detail in the Task 2 of the S1 DPC-INGV project (Albarello et al., 2007). In particular, one of the outcomes described in the deliverable, is an attenuation relationship in the form

$$P(I_s|I_E,D)=\frac{1}{\sigma\sqrt{2\pi}}\int_{I_s-0.5}^{\infty}e^{-\frac{1}{2}\left[\frac{\xi-\mu(I_E,D)}{\sigma}\right]^2}d\xi \qquad [3]$$

where,

$$\mu(I_E,D)=I_E+a(D-h)+b\ln\left(\frac{D}{h}\right) \qquad [4]$$

with

$$D=\sqrt{R^2+h^2} \qquad [5]$$

I_E is the intensity expected at the epicentre, R is the epicentral distance; a,b, h and σ are empirical parameters to be determined empirically (see Albarello et al., 2007 for details).
The analyses described in Albarello et al. (2007), indicate that, when R is in km, the values of the empirical parameters valid for the whole Italian region are

$$a=(0.0086\pm0.0005);\quad b=(1.037\pm0.027);\quad h=(3.91\pm0.27) \qquad [6]$$

By taking these parameters into account, equations [3-5] have been used to compute the probability associated to the overcome of each intensity value at the City of Potenza as a function of different possible hypotheses about the source location and the epicentral intensity of potential damaging earthquakes. Table 5.1 and Figure 5.1 report the results obtained by considering three possible events.

Table 4.1

	Earthquake	Time	Ie	D		I	II	III	IV	V	VI	VII	VIII	IX	X	XI
						1	2	3	4	5	6	7	8	9	10	11
Scenario1_	Andretta-Filano(Mw=6.9)	08/09/1694	11.11	33.22	P	1.00	1.00	1.00	1.00	1.00	1.00	0.99	0.91	0.56	0.16	0.02
					p	0.00	0.00	0.00	0.00	0.00	0.01	0.09	0.34	0.40	0.16	0.02
Scenario2_	Potenza (Mw=5.7)	05/05/1990	8.16	4.31	P	1.00	1.00	1.00	1.00	1.00	1.00	0.96	0.74	0.31	0.05	0.00
					p	0.00	0.00	0.00	0.00	0.00	0.04	0.22	0.43	0.26	0.05	0.00
Scenario3_	Irpinia(Mw=6.8)	23/11/1980	10.87	41.91	P	1.00	1.00	1.00	1.00	1.00	1.00	0.97	0.75	0.31	0.05	0.00
					p	0.00	0.00	0.00	0.00	0.00	0.03	0.22	0.43	0.26	0.05	0.00

For each scenario, are reported: the denomination of the event and the presumed Mw magnitude (earthquake), the time of the considered event (Time), the intensity expected at the epicentre (Ie), the hypocentral distance in km (D). The two rows relative to each scenario respectively report the probability distribution P that the intensity at the site will be not less than the MCS value in the header (I, II, etc.) end the probability density p that the intensity will be exactly equal to the MCS value in the header.

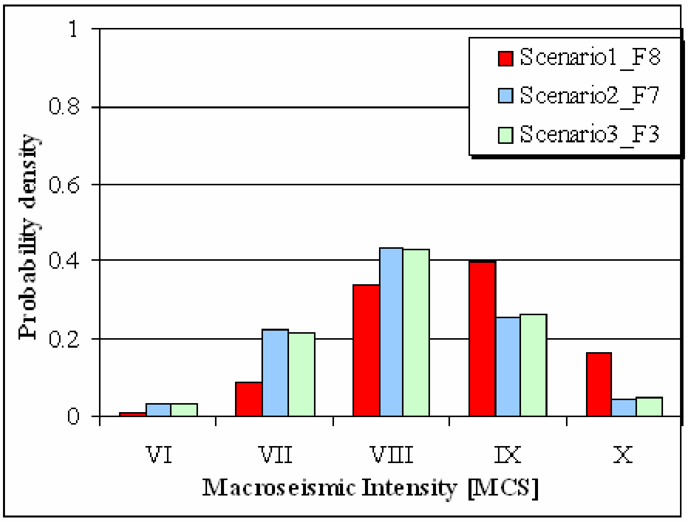

Figure 4.1 Probability associated to each possible value of intensity at the site of Potenza by assuming the different damaging events (scenarios) in table 1.

A visual inspection of the results in figure 5.1, suggests that two of the considered events (scenarios 2 and 3) produces the same results in terms of expected effects. The first scenario, instead appears the most severe with an expected intensity value near IX MCS.

These intensities scenarios have been used to compute the damage scenarios at Potenza, as described in *PS3-Deliverables D18-D19-D24.*

REFERENCES

Albarello D., V. D'Amico, P. Gasperini, F. Pettenati, R. Rotondi e G. Zonno, 2007. Nuova formulazione delle procedure per la stima dell'intensità macrosismica da dati epicentrali o da risentimenti in zone vicine. Progetto DPC-INGV S1, http://esse1.mi.ingv.it/d10.html

Amato, A., Selvaggi, G., 1993. Aftershock location and P-velocity structure in the epicentral region of the 1980 Irpinia earthquake.Ann. Geofis. 36, 3– 15.

Ambraseys, N.N., Douglas, J., Sarma, S.K., Smit, P.M. (2005). Equations for the estimation of strong ground motions from shallow crustal earthquakes using data from Europe and Middle East: Horizontal peak ground acceleration and spectral acceleration, Bull. of Earthquake Engineering, 3, 1-53.

Atkinson, G.M., Beresnev, I.A. [2002] "Ground Motions at Memphis and St. Louis from M 7.5–8.0 Earthquakes in the New Madrid Seismic Zone," Bull. Seismol. Soc. Am, Vol. 92, No. 3, pp. 1015–1024.

Azzara, R., A. Basili, L. Beranzoli, C. Chiarabba, R. Di Giovambattista and G. Selvaggi (1993). The seismic sequence of Potenza (May 1990). Ann. Geofis., 36, 1, 237-243.

Basili, R., G. Valensise, P. Vannoli, P. Burrato, U. Fracassi, S. Mariano, M.M. Tiberti, E. Boschi (2007). The Database of Individual Seismogenic Sources (DISS), version 3: summarizing 20 years of research on Italy's earthquake geology. Tectonophysics (submitted).

Berardi, R., Jiménez, M.J., Zonno, G., García-Fernández, M. [2000] "Calibration of stochastic finite-fault ground motion simulations for the 1997 Umbria-Marche, Central Italy, earthquake sequence," Soil Dynamics and Earthquake Engineering, 20, pp. 315-324.

Beresnev, I.A., Atkinson, G.M. [1998a] "FINSIM - a FORTRAN program for simulating stochastic acceleration time histories from finite fault," Seism. Res. Lett., 69, pp. 27-52.

Boore, D.M. [2003] "Simulation of ground motion using the stochastic method," Pure Appl. Geophys. 160, pp. 635-676.

Burrato, P, and G. Valensise (2007). Rise and fall of a hypothesized seismic gap: source complexity in the 1857, southern Italy earthquake (Mw 7.0). Bull. Seismol. Soc. Am. (submitted).

Carvalho, A., Zonno, G. [2006] "Modeling the 1980 Irpinia Earthquake by stochastic simulation. Comparison of seismic scenarios using finite-fault approaches", Poster, presented to the 1st ECEES - Session "Approaches to Model Seismic Scenarios" in Geneva, Switzerland, 3-8 September, 2006; http://www.ecees.org/

Castro, R.R., Rovelli, A., Cocco, M., Di Bona, M., Pacor, F. [2001] "Stochastic Simulation of Strong-Motion Records from the 26 September 1997 (Mw 6), Umbria-Marche (Central Italy) Earthquake," Bull. Seismol. Soc. Am, Vol. 91, No.1, pp. 27–39.

Chiarabba, C., P. De Gori, L. Chiaraluce, and 21 others (2005). Mainshocks and aftershocks of the 2002 Molise seismic sequence, southern Italy. J. Seismol., 9, 487-494.

CPTI Working Group, 2004. Catalogo Parametrico dei Terremoti Italiani, version 2004 (CPTI04). INGV, Milan, available from http://emidius.mi.ingv.it/CPTI/.

Di Bucci D., Ravaglia A., Seno S., Toscani G., Fracassi U. and Valensise G. (2006). Seismotectonics of the Southern Apennines and Adriatic foreland: insights on active regional E-W shear zones from analogue modeling, Tectonics, 25, TC4015, doi: 10.1029/2005TC001898

DISS Working Group (2006). Database of Individual Seismogenic Sources (DISS), Version 3.0.2: A compilation of potential sources for earthquakes larger than M 5.5 in Italy and surrounding areas. http://www.ingv.it/DISS/, © INGV 2005, 2006 - Istituto Nazionale di Geofisica e Vulcanologia - All rights reserved.

Doglioni, C., Harabaglia, P., Martinelli, G., Mongelli, F., and Zito, G. (1996). A geodynamic model of the Southern Apennines accretionary prism, Terra Nova 8, 540–547.

Fracassi U. and Valensise G. (2007). Unveiling the sources of the catastrophic 1456 multiple earthquake: Hints to an unexplored tectonic mechanism in Southern Italy, Bull. Seismol. Soc. Am., 97, 3, 725-748, doi: 10.1785/0120050250

Gallovic, F., Brokešová, J. (2004). On strong ground motion synthesis with k^-2 slip distributions, J. Seismology 8, 211-224.

Gallovič, F., Brokešová, J. (2007). Hybrid k-squared Source Model for Strong Ground Motion Simulations: Introduction, Phys. Earth Planet. Interiors 160, 34-50.

Herrero, A., and P. Bernard (1994). A kinematic self-similar rupture process for earthquakes, *Bull. Seism. Soc. Am.* **84,** 1216–1228.

Improta L., Bonagura M., Capuano P., Iannaccone G., An integrated geophysical investigation of the upper crust in the epicentral area of the 1980, M_s=6.9, Irpinia earthquake (Southern Italy). Tectonophysics 361 (2003) 139-169.

Mallet R. (1862): *Great Neapolitan earthquake of 1857. The first principles of observational seismology as developed in the report to the Royal society of London*. Chapman and Hall, 2 vols., pp. 431, London

Motazedian D., Atkinson G. M. (2005) "Stochastic Finite-Fault Modeling Based on a Dynamic Corner Frequency", Bull. Seismol. Soc. Am, Vol. 95, No. 3, pp. 995–1010, June 2005.

Pacor, F., Cultrera, G., Mendez, A. , Cocco, M. [2005]. "Finite Fault Modeling of Strong Ground Motion Using a Hybrid Deterministic - Stochastic Method," Bull. Seism. Soc. Am., 95, 225-240.

Pavlides S.B. and Caputo R. (2004): Magnitude *versus* faults' surface parameters: quantitative relationships from the Aegean. *Tectonophys.* **380**, 3-4, 159-188.

Pieri P., Vitale G., Beneduce P., Doglioni C., Gallicchio S., Giano S.I., Loizzo R., Moretti M., Prosser G., Sabato L., Schiattarella M., Tramutoli M. and Tropeano M. (1997)**:** Tettonica Quaternaria nell'area Bradanico-Ionica. *Il Quaternario*, **10(2)**, 535-542.

PS3-Deliverable D0 (2006). TASK 1 – SCENARI DI SCUOTIMENTO - Tecniche di simulazione, Giugno 2006.

PS3-Deliverable D18-D19-D24 (2007). Task5 – Potenza – Deliverable D18. D19, D24 – Effetti di sito e scenari di danno. Task7 – Interfacciamento con l'ingegneria e il DPC – Il caso di Potenza, Luglio 2007

Ruiz Paredes Javier-Antonio (2007). Computing broadband accelerograms using kinematic rupture modeling. PhD thesis Université Paris VII, Géophysique Interne, Directeur de Thèse Pascal Bernard

Valensise, G., D. Pantosti, R. Basili (2004). Seismology and Tectonic Setting of the 2002 Molise, Italy, Earthquake. Earthquake Spectra, 20, 23-37.

ANNEX 1- RESULTS FROM EXSIM SIMULATION

The results for the F3 fault are summarized in Figure 1 and Table 1. The results for the F8 faults are illustred in Figure 2, 3, and 4. In Figure 2, the specific contributions coming from the four different slip distributions are shown: SLIP 1 (blue), SLIP 2 (red), SLIP 3 (green) and SLIP 4 (magenta). In Figure 3, the 16 different rupture models are mapped, which each constitute one slip distribution and one nucleation point (four nucleation points, for four slip distributions). In Figure 4, we can see the different shape of the time series associated with the statistical values of PGA.

In Table 3, Figure 5 and Figure 6, we have analyzed fault F7 (Irpinia). The shaking results from faults F6 and F7 are very close, but we can say that for fault F7 they are a bit higher. The results of fault F7 obtained in Case C (stress drop 100 bar, with a depth of the top of the fault of 7.8 km) are higher, but they are always less that those obtained from faults F3 and F8 (see Table 3.4.4.). In the case of fault F7, we do not have many discrepancies using the different slip distribution models: SLIP 1, SLIP 2, SLIP 3 and SLIP 4. This is due to the small size of the fault and because we have a small number of sub-faults. The trend of the number of the frequency *versus* the PGA classes is very similar for each slip distribution. The time series obtained has a smaller amplitude and a shorter duration in comparison to faults F3 and F8.

In Table 4, Figure 7 and Figure 8, we have analyzed the results from fault F1, with respect to the Tricarico site (TRR).

In Table 5, Figure 9 and Figure 10, we have analyzed the results from fault F1 with respect to the Bagnoli Irpino site (BGI).

The Tricarico station has marked site-effect amplification, while the Bagnoli Irpino station is located on hard rock. Analyzing the forms of the response spectra obtained with fault F1 (Colliano) at the BGI and TRR stations, we can confirm that the use of a 200 bar value appears to be compatible and reasonable. Indeed, the envelope form of the set of simulated response spectra and the PGA values better match those calculated from the recorded data using a 200 bar value.

Table 1. Seismic scenarios using fault F3 (see Table 2.). The shaded rows (grey) are grouping the 120 time series for each slip distribution (i.e. slip distribution 1 with nucleation points 1, 2, 3 and 4 (Random), slip distribution 2 with nucleation points 1, 2, 3 and 4 (Random), and so on …). The time series at the Potenza site were generated using a stress drop value of 100 and 200 bar.

F3 Name Irpinia (0 + 20 sec) - Fault ITGG007

Case A --- POTENZA Stress drop 100 bar

Model --- POT-07-stat.txt

#	median	75%	84%	mean	Mode	Min	Max
11	52.589	62.454	55.577	67.943	52.500	39.221	78.723
12	50.509	61.270	52.884	63.667	47.500	38.052	68.851
13	57.503	65.716	59.485	70.959	57.500	43.275	84.902
14	51.785	57.324	53.823	61.078	47.500	43.833	70.107
21	32.432	35.288	32.911	37.091	32.500	26.169	44.325
22	36.312	40.594	37.717	41.647	32.500	28.323	56.482
23	43.296	48.354	44.656	55.994	42.500	30.631	64.463
24	32.653	35.841	32.888	36.837	37.500	25.613	41.930
31	34.360	38.224	34.865	40.133	32.500	26.859	48.958
32	32.737	35.919	33.700	39.355	32.500	24.181	48.208
33	47.713	51.708	47.319	52.453	47.500	34.052	65.470
34	34.567	38.326	35.404	42.596	32.500	23.140	58.840
41	34.889	39.079	36.280	41.164	32.500	30.428	48.554
42	41.281	43.267	40.907	44.914	42.500	31.486	60.045
43	50.805	60.178	51.864	60.774	62.500	36.822	67.730
44	37.103	40.257	37.266	42.748	37.500	30.492	46.659

	median	75%	84%	mean	Mode	Min	Max
TOT	40.417	49.707	42.972	55.359	32.500	23.140	84.902

1	median	record	172	value	40.399	name	POT-07-01-18-22.acc
2	75%	record	101	value	49.707	name	POT-07-01-25-14.acc
3	84%	record	477	value	42.983	name	POT-07-01-27-44.acc
4	mean	record	110	value	55.359	name	POT-07-01-15-14.acc
5	mode	record	136	value	32.493	name	POT-07-01-19-21.acc
6	min	record	331	value	23.140	name	POT-07-01-21-34.acc
7	max	record	90	value	84.902	name	POT-07-01-26-13.acc

Case B --- POTENZA Stress drop 200 bar

Model --- POT-07-stat.txt

#	median	75%	84%	mean	Mode	Min	Max
11	82.547	95.812	85.790	104.992	77.500	60.676	122.467
12	78.488	94.535	82.229	99.342	72.500	58.555	109.961
13	88.678	101.171	92.117	108.789	77.500	67.957	128.053
14	81.038	86.828	83.031	97.035	72.500	70.120	106.678
21	49.857	53.282	50.524	57.098	47.500	40.587	67.679
22	55.601	62.095	58.205	64.382	52.500	42.550	86.004
23	65.732	73.841	68.469	87.179	72.500	47.578	99.201
24	50.377	55.404	50.931	55.895	47.500	39.151	65.944
31	52.184	58.780	53.410	60.751	57.500	41.932	74.407
32	50.609	55.425	51.979	59.513	47.500	38.664	72.309
33	71.392	79.032	72.451	81.743	72.500	52.148	100.550
34	53.347	58.294	54.245	63.408	57.500	35.060	89.744
41	54.108	59.510	55.868	62.146	52.500	46.461	74.355
42	63.099	66.480	63.104	69.937	67.500	48.257	92.416
43	77.934	92.446	79.855	93.632	77.500	56.943	105.441
44	55.746	62.525	57.669	66.408	52.500	46.107	72.033

	median	75%	84%	mean	Mode	Min	Max
TOT	62.138	76.630	66.242	84.668	52.500	35.060	128.053

1	median	record	190	value	62.129	name	POT-07-01-30-23.acc
2	75%	record	434	value	76.630	name	POT-07-01-16-43.acc
3	84%	record	388	value	66.138	name	POT-07-01-19-41.acc
4	mean	record	72	value	84.668	name	POT-07-01-22-13.acc
5	mode	record	393	value	52.472	name	POT-07-01-24-42.acc
6	min	record	331	value	35.060	name	POT-07-01-21-34.acc
7	max	record	90	value	128.053	name	POT-07-01-26-13.acc

F3 Time series associated to ***median***, ***75%***, ***84%***, ***mean***, ***Mode***, ***Min*** and **Max**

Case A --- POTENZA Stress drop 100 bar

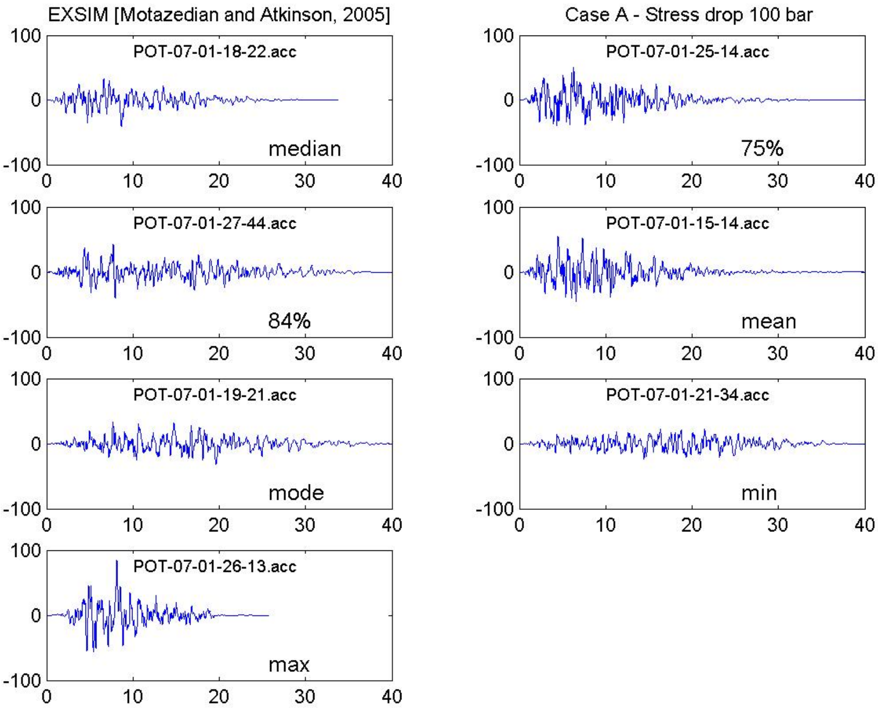

Case B --- POTENZA Stress drop 200 bar

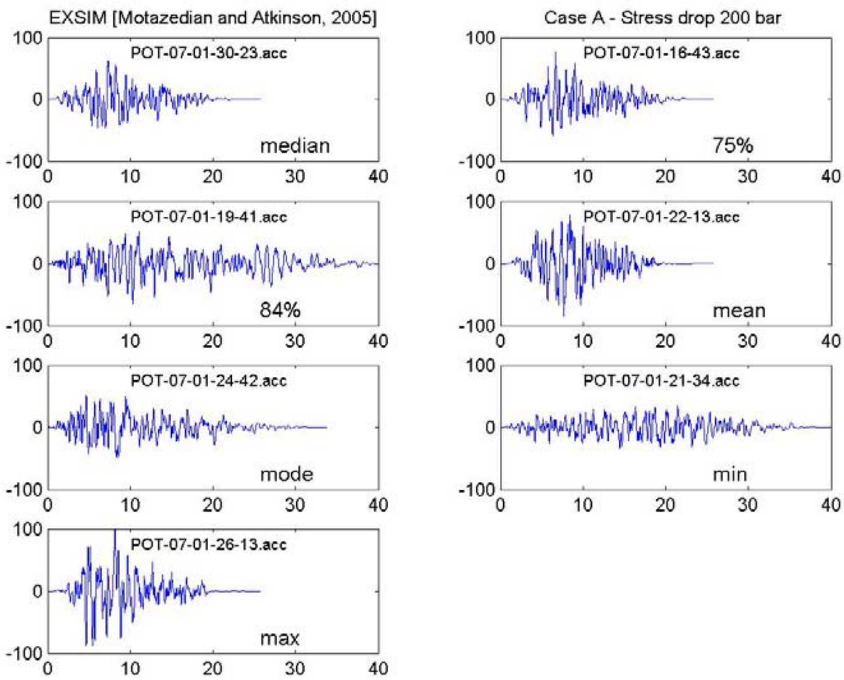

Figure 1. Fault F3 (Irpinia): plots of the simulated time series associated with the statistical values of PGA corresponding to the median, 75% percentile, 84% percentile, mean, mode, minimum and maximum.

Table 2. Seismic scenarios using fault F8 (see Table 2.). Statistical analysis of the time series at the Potenza site using of stress drop values of 100 and 200 bar.

F8 Name Andreatta Filano - Fault ITGG063

Case A --- POTENZA Stress drop 100 bar

Model --- POT-63-stat.txt

#	median	75%	84%	mean	Mode	Min	Max
11	68.846	74.762	68.617	75.292	67.500	53.005	85.559
12	63.480	67.832	64.887	72.286	57.500	51.028	92.205
13	67.841	71.630	67.761	74.832	67.500	51.536	81.877
14	66.713	72.587	67.745	77.243	67.500	51.995	89.572
21	41.636	45.227	42.286	46.938	42.500	31.946	58.082
22	46.896	51.469	47.809	53.403	47.500	36.142	70.281
23	50.140	59.859	52.367	60.990	47.500	36.703	70.978
24	51.444	59.709	53.275	64.080	52.500	38.322	77.281
31	38.268	41.324	38.844	42.623	37.500	28.956	56.113
32	37.741	42.294	38.456	43.575	37.500	32.601	48.703
33	50.997	60.169	52.854	61.848	47.500	34.469	65.261
34	44.718	47.488	45.047	49.254	47.500	34.145	70.657
41	49.704	52.614	49.464	56.675	52.500	38.765	67.367
42	52.815	57.408	53.766	62.657	47.500	40.543	82.817
43	60.835	68.451	62.739	71.556	67.500	47.118	93.558
44	59.233	67.804	58.321	70.476	67.500	38.842	79.079

	median	75%	84%	mean	Mode	Min	Max
TOT	51.667	63.598	54.015	67.832	47.500	28.956	93.558

1	median	record	381	value	51.702	name	POT-63-01-09-41.acc
2	75%	record	46	value	63.598	name	POT-63-01-18-12.acc
3	84%	record	177	value	53.942	name	POT-63-01-17-22.acc
4	mean	record	53	value	67.832	name	POT-63-01-02-12.acc
5	mode	record	353	value	47.488	name	POT-63-01-15-34.acc
6	min	record	241	value	28.956	name	POT-63-01-07-31.acc
7	max	record	450	value	93.558	name	POT-63-01-20-43.acc

Case B --- POTENZA Stress drop 200 bar

Model --- POT-63-stat.txt

#	median	75%	84%	mean	Mode	Min	Max
11	105.536	115.968	106.486	119.335	117.500	83.472	133.906
12	98.226	104.761	100.446	112.446	102.500	79.375	141.375
13	105.561	112.416	105.245	115.616	107.500	82.602	126.188
14	102.978	111.087	104.764	119.005	97.500	80.497	143.170
21	64.904	69.983	65.596	73.806	67.500	48.165	89.915
22	72.465	80.202	74.251	82.255	82.500	56.525	106.320
23	78.909	91.205	81.008	94.618	77.500	57.361	108.368
24	79.842	91.892	82.243	98.286	77.500	57.373	118.852
31	59.494	64.547	59.684	67.505	62.500	43.426	86.722
32	57.206	65.238	59.037	66.684	57.500	49.944	74.951
33	77.594	89.094	81.092	95.707	77.500	52.772	99.802
34	67.816	73.648	69.025	75.610	67.500	54.329	108.018
41	77.077	82.194	76.754	86.752	82.500	61.198	100.982
42	83.829	90.002	83.679	97.005	72.500	63.195	125.519
43	94.544	106.020	97.331	112.430	107.500	73.875	145.796
44	90.613	102.691	89.911	109.033	102.500	61.160	120.830

	median	75%	84%	mean	Mode	Min	Max
TOT	80.575	98.035	83.535	104.761	72.500	43.426	145.796

1	median	record	381	value	80.652	name	POT-63-01-16-41.acc
2	75%	record	328	value	98.035	name	POT-63-01-04-33.acc
3	84%	record	177	value	83.542	name	POT-63-01-30-22.acc
4	mean	record	53	value	104.761	name	POT-63-01-02-12.acc
5	mode	record	305	value	72.485	name	POT-63-01-22-33.acc
6	min	record	241	value	43.426	name	POT-63-01-07-31.acc
7	max	record	450	value	145.796	name	POT-63-01-20-43.acc

F8 Name Andreatta Filano - Fault ITGG063

Case A --- POTENZA Stress drop 100 bar

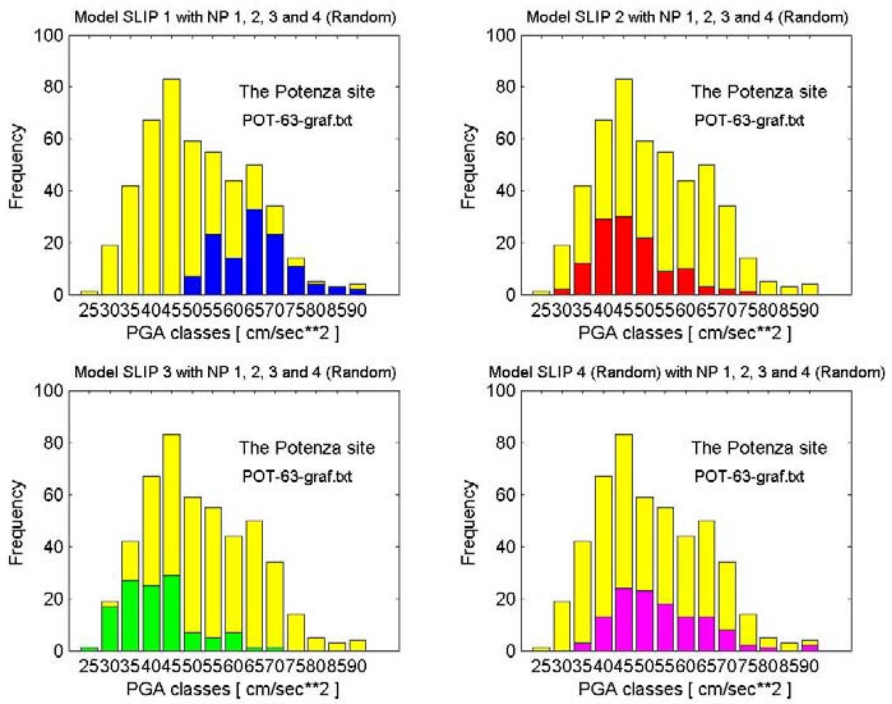

Case B ---POTENZA Stress Drop 200 bar

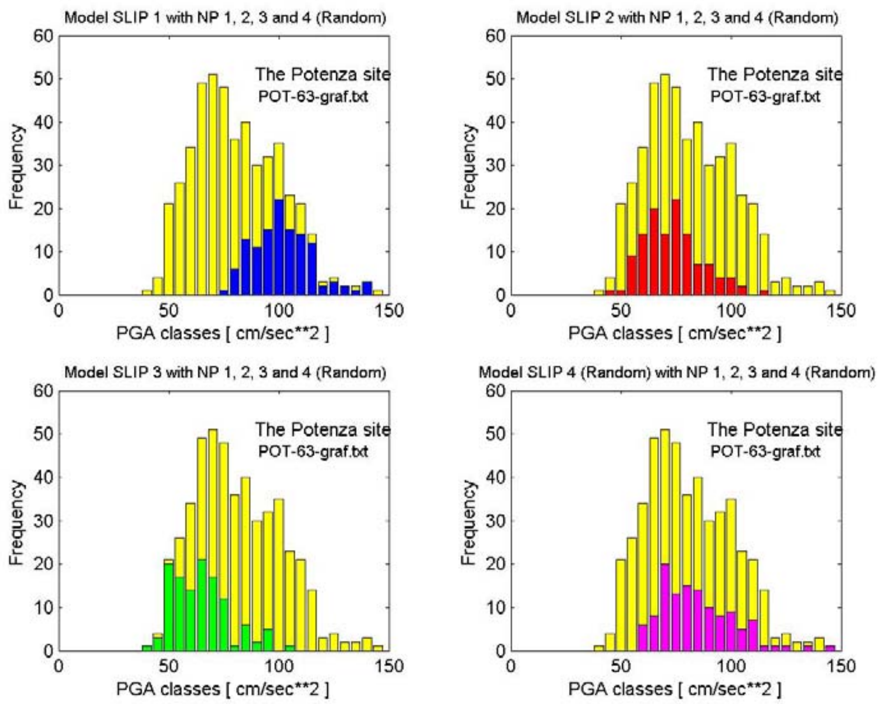

Figure 2. Comparisons of the frequency *versus* PGA class graphs considering the 480 time series produced from fault F8 (yellow bars) and considering the 120 time series from each slip distribution (slips 1, 2, 3 and 4 (Random), respectively, in blue, red, green and magenta.

F8 **Name Andreatta Filano - Fault ITGG063**

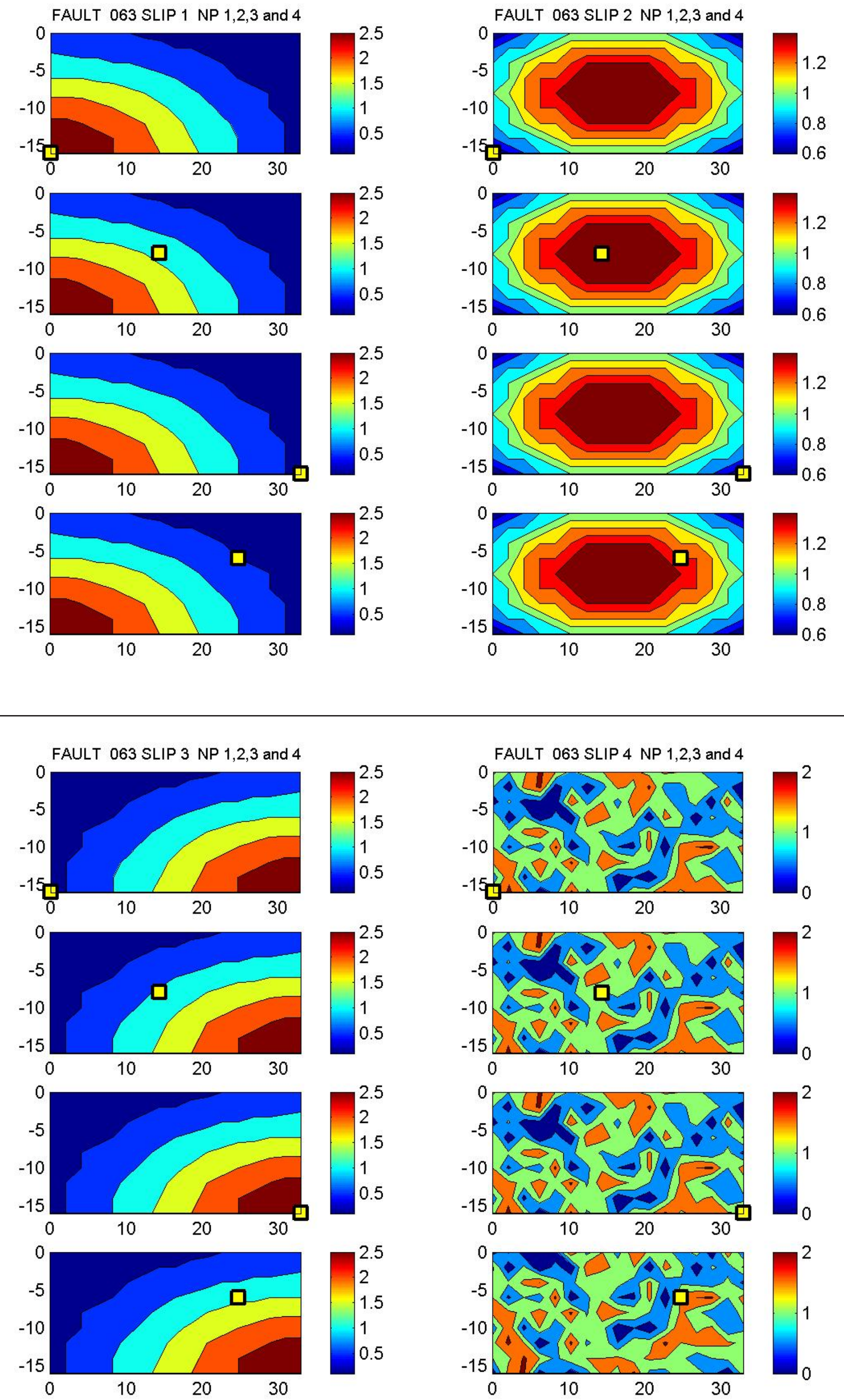

Figure 3. Mapping of the 16 different rupture models, each constituting one slip distribution (meter) and one nucleation point (four slip distributions, and four nucleation points). The case of fault F8 (Andreatta Filano) is shown, but this general scheme has been applied to each of the faults in the Table 2.

F8 Time series associated to ***median, 75%, 84%, mean, Mode, Min*** and ***Max***

Case A --- POTENZA Stress drop 100 bar

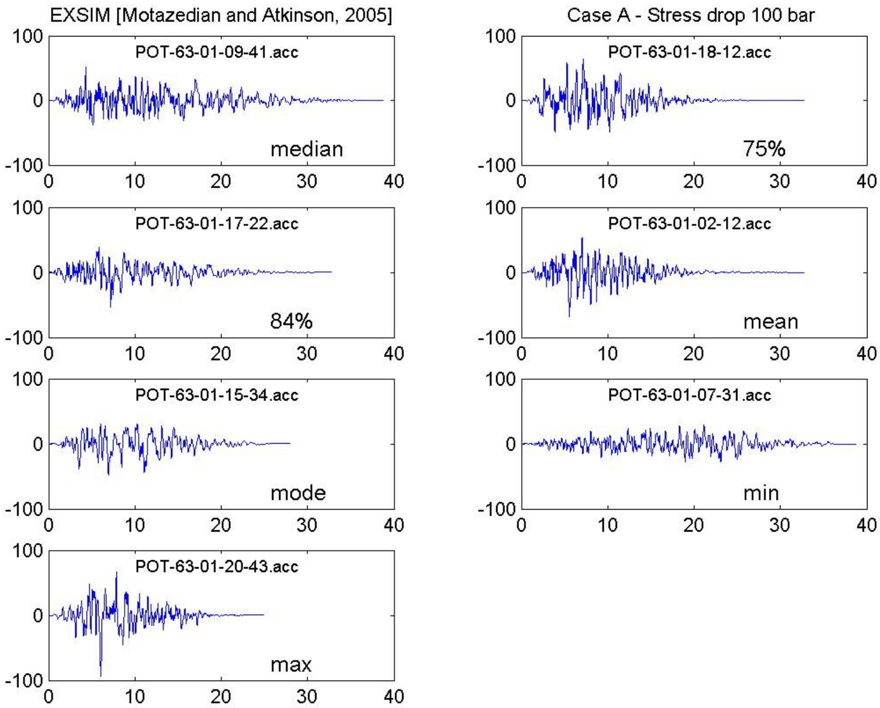

Case B --- POTENZA Stress drop 200 bar

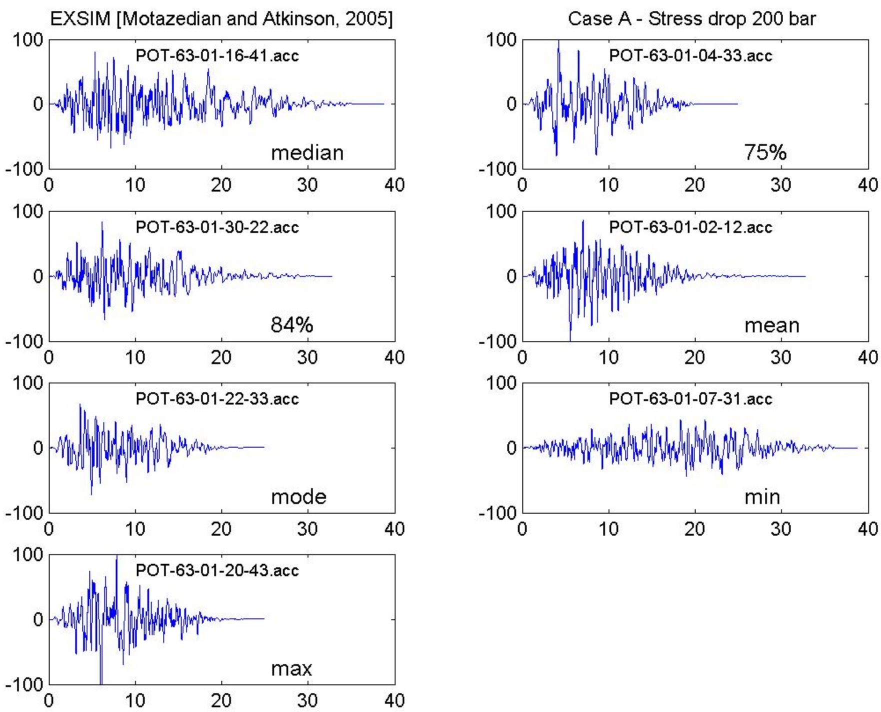

Figure 4. Fault F8 (Andreatta Filano): plots of the simulated time series associated to the statistical values of PGA corresponding to the median, 75% percentile, 84 % percentile, mean, mode, minimum and maximum.

Table 3. Seismic scenarios using fault F7 (Irpinia, ITGGd84) (see Table 2.). Statistical analysis of the 480 time series at the Potenza site for two cases: using a stress drop value of 200 bar (Case A), and using a stress drop value of 100 bars with a depth of 7.8 km (Case B).

F7 Name Potenza - Fault ITGGd84

Case B --- POTENZA Stress drop 200 bar

Model --- POTd84-stat.txt

#	median	75%	84%	mean	Mode	Min	Max
11	40.066	43.007	39.662	44.428	42.500	32.965	50.368
12	35.812	38.375	35.828	39.250	37.500	26.318	52.604
13	36.348	39.534	36.932	42.171	37.500	26.734	47.468
14	34.787	39.659	36.173	42.564	32.500	30.607	43.825
21	32.372	35.991	33.112	36.979	32.500	22.535	47.065
22	32.845	35.425	33.199	38.196	32.500	23.143	46.992
23	33.605	35.157	33.574	38.209	32.500	24.176	46.465
24	35.203	37.760	34.784	38.657	37.500	28.966	42.508
31	33.513	37.255	34.512	40.183	32.500	25.480	54.203
32	35.682	40.415	36.232	44.087	32.500	26.771	49.501
33	36.286	40.734	37.014	42.298	32.500	29.552	46.995
34	34.088	37.676	35.089	41.085	32.500	27.587	46.786
41	32.511	36.713	33.488	37.442	32.500	27.233	48.847
42	32.506	37.469	33.314	39.473	32.500	25.553	43.171
43	34.671	37.463	35.043	40.425	32.500	27.997	51.520
44	35.665	38.126	35.213	40.175	37.500	25.232	44.428
	median	75%	84%	mean	Mode	Min	Max
TOT	34.502	38.262	35.198	40.842	32.500	22.535	54.203

```
   1 median   record   70 value     34.502  name POTd84-01-05-13.acc
   2 75%      record   52 value     38.262  name POTd84-01-04-12.acc
   3 84%      record  203 value     35.157  name POTd84-01-25-23.acc
   4 mean     record   84 value     40.842  name POTd84-01-14-13.acc
   5 mode     record  253 value     32.507  name POTd84-01-06-31.acc
   6 min      record  121 value     22.535  name POTd84-01-09-21.acc
   7 max      record  270 value     54.203  name POTd84-01-08-31.acc
```

Case C --- POTENZA Stress drop 100 bar and depth 7.8 km

Model --- POTd84-stat.txt

#	median	75%	84%	mean	Mode	Min	Max
11	48.785	55.394	50.797	57.411	47.500	40.856	77.876
12	43.507	48.290	45.702	56.694	42.500	34.331	63.265
13	46.803	51.708	49.778	60.413	47.500	36.293	73.298
14	43.804	50.661	46.027	53.868	42.500	36.934	66.833
21	40.257	48.199	42.552	50.905	37.500	35.537	54.729
22	42.251	47.534	42.648	48.975	42.500	32.361	54.905
23	45.543	47.477	45.528	49.072	42.500	34.421	63.546
24	41.513	46.357	42.073	47.686	37.500	35.149	49.671
31	41.000	45.234	42.349	47.316	42.500	32.840	58.109
32	41.195	44.239	41.470	45.577	42.500	32.985	60.463
33	46.089	49.385	47.088	54.413	47.500	36.324	59.670
34	46.176	50.224	45.910	54.136	47.500	33.563	59.206
41	41.868	46.056	42.494	48.264	37.500	35.721	51.938
42	40.929	45.672	42.955	50.399	42.500	33.339	67.082
43	44.573	51.428	46.271	55.115	42.500	36.523	58.583
44	46.811	50.040	47.556	51.694	47.500	34.058	69.883
	median	75%	84%	mean	Mode	Min	Max
TOT	44.045	48.303	45.075	51.428	42.500	32.361	77.876

```
   1 median   record  378 value     44.052  name POTd84-01-26-41.acc
   2 75%      record  439 value     48.303  name POTd84-01-04-43.acc
   3 84%      record  436 value     45.085  name POTd84-01-27-43.acc
   4 mean     record  443 value     51.428  name POTd84-01-09-43.acc
   5 mode     record  228 value     42.488  name POTd84-01-27-24.acc
   6 min      record  151 value     32.361  name POTd84-01-05-22.acc
   7 max      record   30 value     77.876  name POTd84-01-16-11.acc
```

F7 Name Potenza - Fault ITGGd84

Case B --- POTENZA Stress drop 200 bar

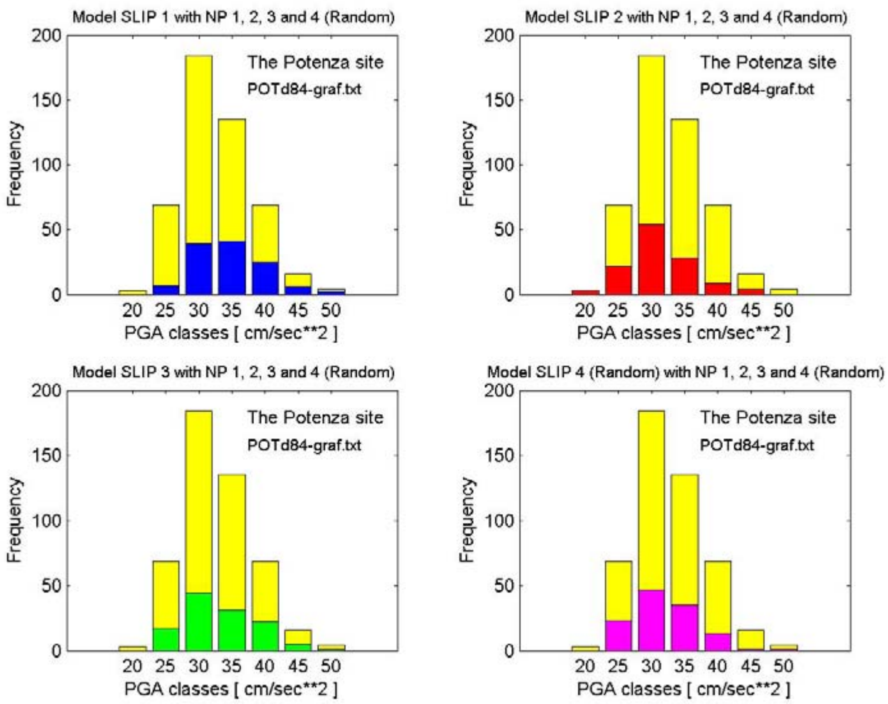

Case C --- POTENZA Stress drop 100 bar & depth 7.8 km

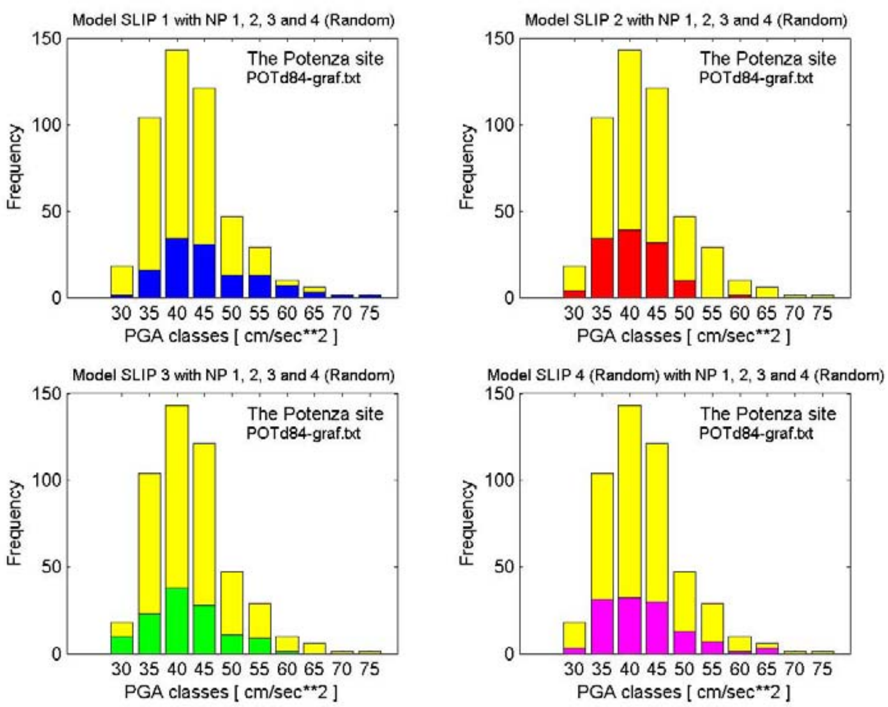

Figure 5. Comparisons of the frequency *versus* PGA class graphs considering the 480 time series produced from fault F7 (yellow bars) and considering the 120 time series from each slip distribution (slips 1, 2, 3 and 4 (Random), respectively, as blue, red, green and magenta. The results of two cases are shown: case A (200 bar) and case B (100 bar and with a depth of 7.8 km).

F7 Time series associated to ***median, 75%, 84%, mean, Mode, Min*** and **Max**

Case B --- POTENZA Stress drop 200 bar

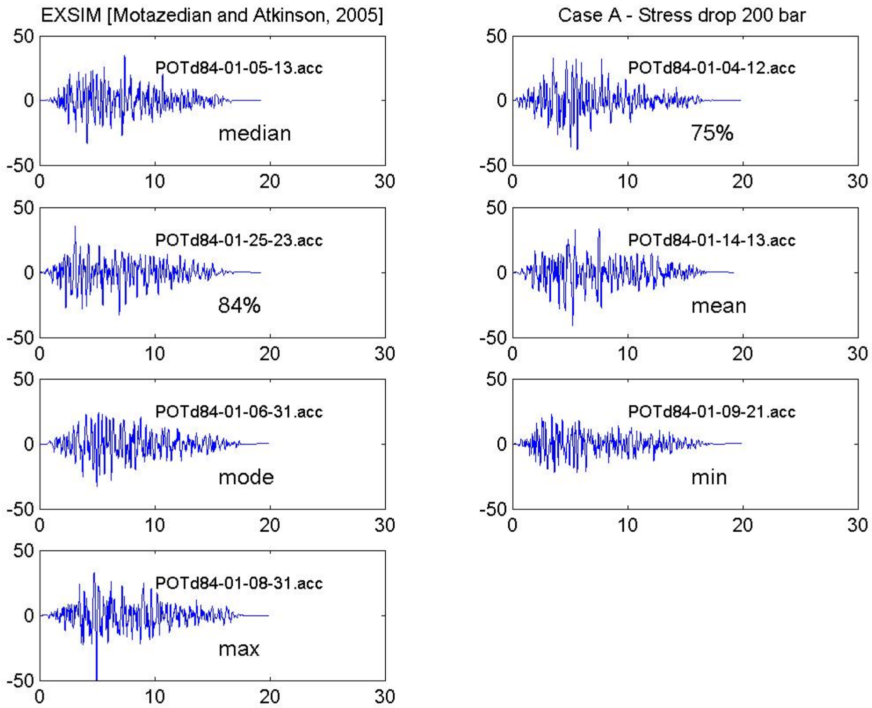

Case C --- POTENZA Stress drop 100 bar and depth 7.8 km

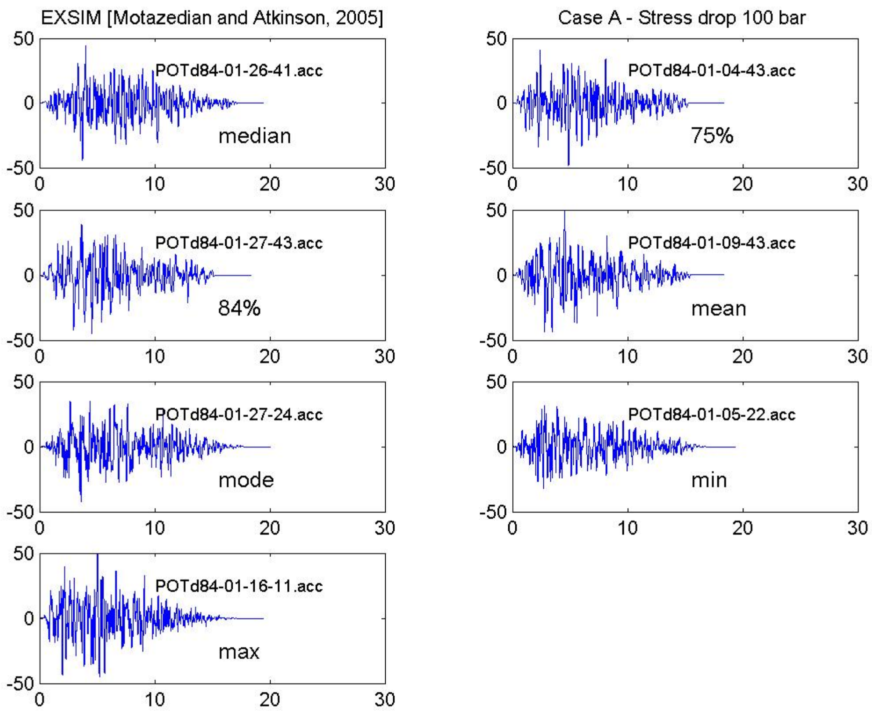

Figure 6. Fault F7 (Irpinia, ITGGd84): plots of the simulated time series associated with the statistical values of PGA corresponding to the median, 75% percentile, 84 % percentile, mean, mode, minimum and maximum.

Table 4. Seismic scenarios using fault F1 (see Table 2.). Statistical analysis of the 480 time series at the Tricarico site using of stress drop values of 100 and 200 bar.

F1 Name Colliano - Fault ITGG077

Case D --- TRICARICO --- Stress drop 100 bar

Model --- TRR077-stat.txt

#	median	75%	84%	mean	Mode	Min	Max
11	27.111	29.281	27.453	30.542	27.500	22.261	36.893
12	26.385	29.628	25.965	30.390	27.500	19.303	34.548
13	28.037	33.321	28.761	33.894	27.500	19.777	39.781
14	26.412	29.001	26.743	30.461	27.500	19.757	44.796
21	18.406	20.198	18.848	21.097	17.500	13.382	25.917
22	19.474	21.551	19.835	23.979	17.500	14.106	25.820
23	21.155	22.986	21.614	24.958	22.500	17.211	27.804
24	19.012	21.152	19.389	23.095	17.500	13.439	25.550
31	22.453	25.247	22.264	25.803	22.500	15.043	27.049
32	20.881	24.735	21.676	25.462	17.500	17.046	29.765
33	26.531	30.030	26.892	30.760	27.500	20.835	33.983
34	21.729	24.560	21.573	25.535	22.500	15.842	27.211
41	23.165	25.578	23.202	26.080	22.500	17.807	28.848
42	25.022	26.780	24.750	29.245	27.500	17.087	35.327
43	26.266	28.740	27.791	35.657	27.500	20.621	42.744
44	22.710	25.230	23.011	27.405	22.500	17.693	30.511

	median	75%	84%	mean	Mode	Min	Max
TOT	23.187	26.641	23.735	28.158	22.500	13.382	44.796

1 median	record	466	value	23.193	name	TRR077-01-04-44.acc
2 75%	record	11	value	26.641	name	TRR077-01-05-11.acc
3 84%	record	429	value	23.758	name	TRR077-01-30-43.acc
4 mean	record	111	value	28.158	name	TRR077-01-11-14.acc
5 mode	record	38	value	22.496	name	TRR077-01-12-12.acc
6 min	record	121	value	13.382	name	TRR077-01-10-21.acc
7 max	record	120	value	44.796	name	TRR077-01-10-14.acc

Case E --- TRICARICO --- Stress drop 200 bar

Model --- TRR077-stat.txt

#	median	75%	84%	mean	Mode	Min	Max
11	40.856	42.950	40.971	46.635	42.500	32.748	52.770
12	40.007	43.696	39.153	45.571	32.500	30.103	53.335
13	42.201	49.996	43.576	51.690	37.500	30.210	63.059
14	39.396	42.979	40.212	45.934	42.500	30.629	67.578
21	28.237	30.493	28.493	32.325	27.500	20.511	40.748
22	28.549	32.218	29.654	35.442	27.500	21.069	38.486
23	31.490	35.686	32.742	37.463	32.500	26.483	44.029
24	27.860	32.203	29.095	35.506	27.500	19.841	38.180
31	33.301	36.746	33.226	39.041	32.500	22.826	41.072
32	31.756	37.584	32.679	39.085	27.500	25.272	43.613
33	39.313	44.263	39.878	45.075	37.500	30.335	49.549
34	32.373	35.519	32.151	37.926	32.500	22.881	41.807
41	34.968	38.684	34.800	39.801	37.500	26.958	42.416
42	38.343	40.292	37.337	43.337	37.500	26.628	52.909
43	39.803	43.571	41.828	52.322	37.500	31.666	62.662
44	34.043	37.971	34.531	40.756	37.500	26.295	47.031

	median	75%	84%	mean	Mode	Min	Max
TOT	35.049	40.090	35.645	42.347	37.500	19.841	67.578

1 median	record	376	value	35.044	name	TRR077-01-16-41.acc
2 75%	record	14	value	40.090	name	TRR077-01-01-11.acc
3 84%	record	203	value	35.686	name	TRR077-01-18-23.acc
4 mean	record	76	value	42.347	name	TRR077-01-13-13.acc
5 mode	record	206	value	37.463	name	TRR077-01-29-23.acc
6 min	record	211	value	19.841	name	TRR077-01-19-24.acc
7 max	record	120	value	67.578	name	TRR077-01-10-14.acc

Case D --- TRICARICO Stress drop 100 bar

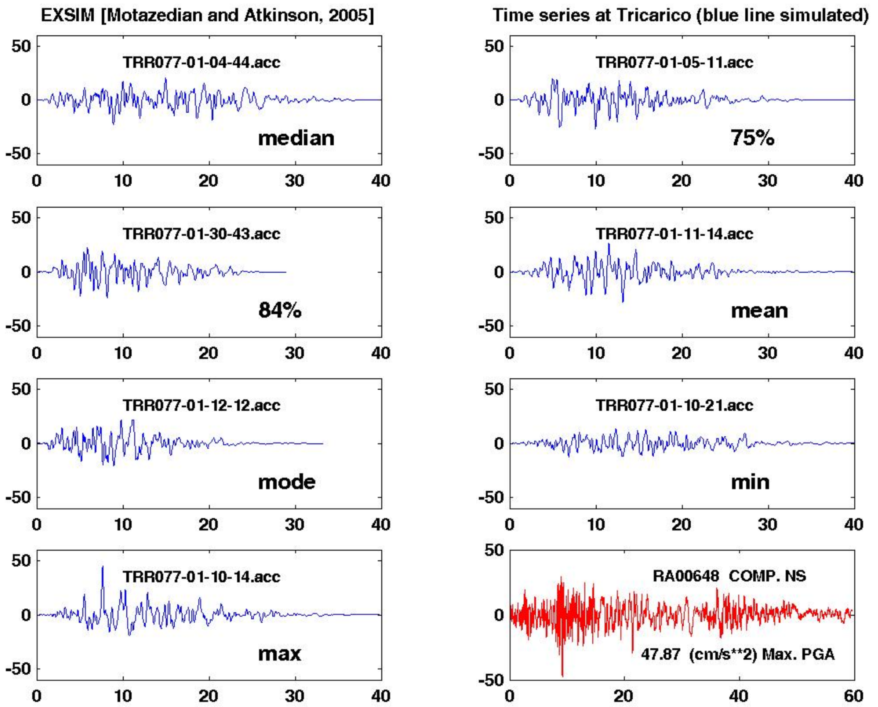

Case E --- TRICARICO Stress drop 200 bar

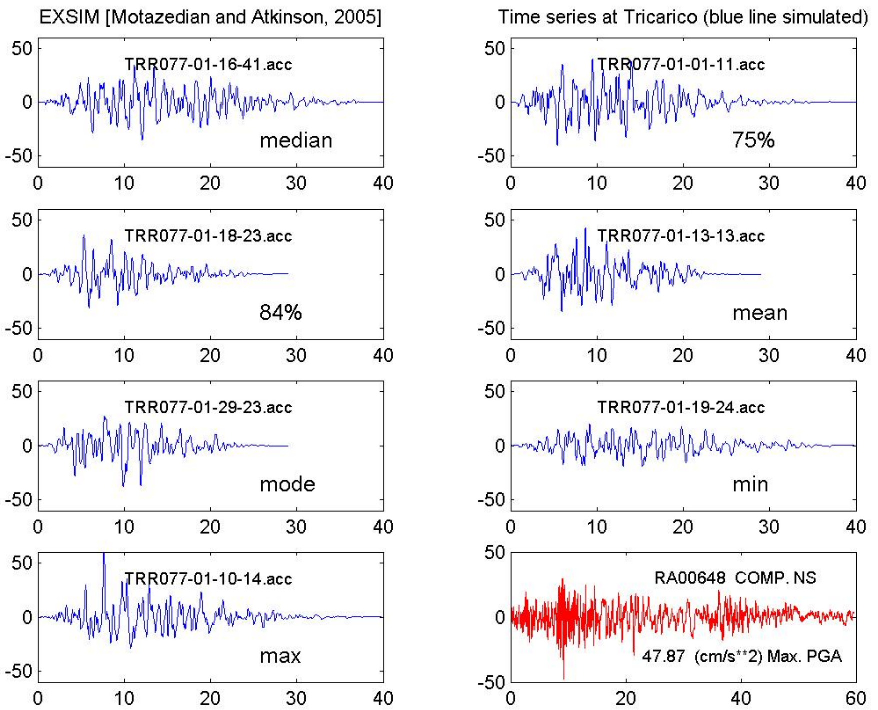

Figure 7. Fault F1 (Colliano): plots of the simulated time series associated with the statistical values of PGA corresponding to the median, 75% percentile, 84 % percentile, mean, mode, minimum and maximum. As a comparison, a plot of the time history of RA00648 COMP. NS (red line) is shown, recorded at the Tricarico station during the1980 Irpinia earthquake for the two cases: Case A (100 bar) and Case B (200 bar).

Case D --- TRICARICO --- Stress drop 100 bar

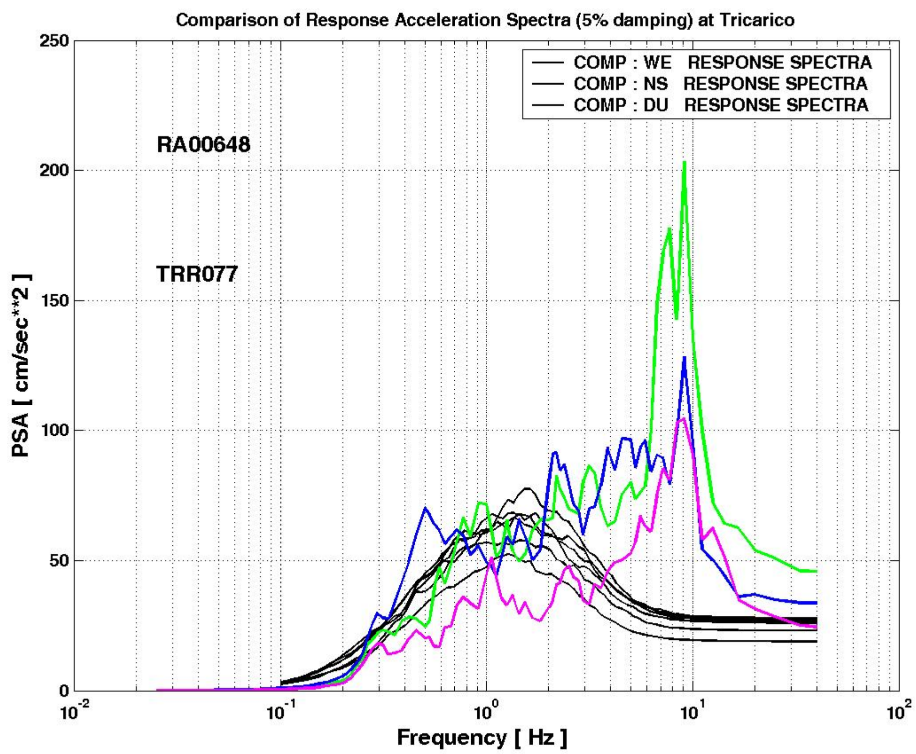

Case E --- TRICARICO --- Stress drop 200 bar

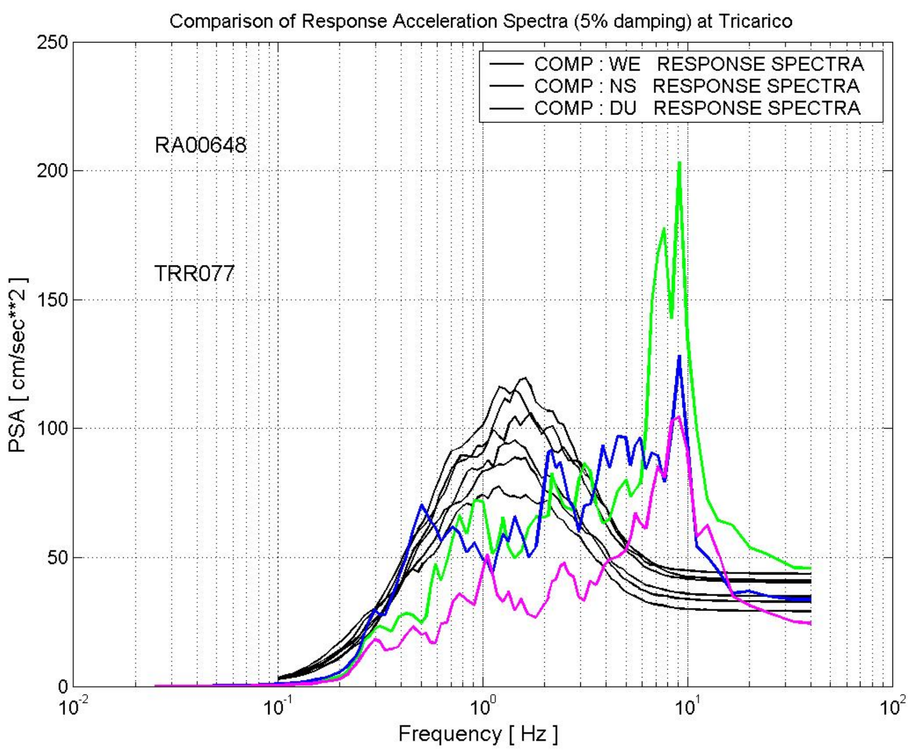

Figure 8. Comparisons of response spectra (5% damping) at the Tricarico site between the simulated response spectra obtained using fault F1 (Colliano), as indicated from the rupture models of the seven time series plotted in Figure 10 (black lines). The computed response spectra of the RA00648 record are shown with COMP. WE (blue line), COMP. NS (green) and vertical COMP. DU (magenta line).

Table 5. Seismic scenarios using fault F1. Statistical analysis of the 480 time series at the Bagnoli Irpino site using of stress drop value of 100 and 200 bar.

F1 Name Colliano - Fault ITGG077

Case D --- BAGNOLI IRPINO Stress drop 100 bar

Model --- BGI077-stat.txt

#	median	75%	84%	mean	Mode	Min	Max
11	72.986	85.399	74.910	87.614	67.500	54.396	98.723
12	61.873	66.787	62.838	71.251	57.500	48.613	86.902
13	55.723	60.850	57.270	70.051	52.500	41.064	77.298
14	69.527	77.016	70.719	78.095	57.500	56.854	110.416
21	98.719	106.158	99.266	108.578	97.500	77.410	139.883
22	94.744	100.266	94.107	106.508	97.500	75.816	118.394
23	84.581	91.985	86.731	94.550	82.500	61.665	121.498
24	100.927	114.294	100.508	117.215	117.500	72.683	124.745
31	125.460	140.814	125.119	146.053	127.500	92.875	158.007
32	111.313	125.896	113.955	132.502	102.500	89.247	159.369
33	127.795	135.968	127.354	141.758	127.500	93.329	182.556
34	118.149	140.462	123.782	143.382	117.500	95.324	181.457
41	111.677	120.334	113.912	137.431	102.500	87.582	145.818
42	94.455	108.573	98.966	113.732	92.500	68.433	134.799
43	96.995	106.759	98.053	108.939	97.500	75.297	145.396
44	108.075	119.457	112.609	132.200	97.500	86.652	182.121

	median	75%	84%	mean	Mode	Min	Max
TOT	97.317	114.761	97.506	122.947	97.500	41.064	182.556

1	median	record	364	value	97.182	name	BGI077-01-05-41.acc
1	median	record	436	value	97.452	name	BGI077-01-27-43.acc
2	75%	record	378	value	114.761	name	BGI077-01-17-41.acc
3	84%	record	437	value	97.504	name	BGI077-01-05-43.acc
4	mean	record	311	value	122.947	name	BGI077-01-27-33.acc
5	mode	record	437	value	97.504	name	BGI077-01-05-43.acc
6	min	record	61	value	41.064	name	BGI077-01-24-13.acc
7	max	record	330	value	182.556	name	BGI077-01-25-33.acc

Case E --- BAGNOLI IRPINO Stress drop 200 bar

Model --- BGI077-stat.txt

#	median	75%	84%	mean	Mode	Min	Max
11	110.861	129.336	115.428	134.448	102.500	86.965	150.672
12	95.022	104.726	97.533	111.778	102.500	74.194	136.454
13	85.816	94.290	88.985	107.897	92.500	64.280	118.560
14	108.457	118.452	109.673	120.321	117.500	87.755	167.671
21	152.249	163.802	153.519	170.756	147.500	116.829	216.604
22	149.053	154.475	146.835	164.622	152.500	117.832	182.185
23	132.210	142.202	135.271	146.208	132.500	94.537	191.383
24	156.551	177.418	156.844	181.750	177.500	114.506	197.272
31	194.937	218.294	195.158	224.981	157.500	145.868	244.760
32	170.935	198.947	177.511	203.041	152.500	136.827	244.403
33	199.475	209.967	198.260	220.389	202.500	142.758	283.031
34	182.970	214.811	192.458	224.489	182.500	151.865	285.293
41	173.283	187.010	177.087	211.225	182.500	136.407	222.949
42	147.014	169.762	154.746	177.521	147.500	107.156	214.131
43	149.637	164.236	152.379	171.050	142.500	116.795	229.364
44	169.462	183.762	175.943	210.092	162.500	135.254	282.102

	median	75%	84%	mean	Mode	Min	Max
TOT	151.193	178.695	151.727	193.091	152.500	64.280	285.293

1	median	record	275	value	151.205	name	BGI077-01-30-32.acc
2	75%	record	341	value	178.695	name	BGI077-01-14-34.acc
3	84%	record	407	value	151.696	name	BGI077-01-13-42.acc
4	mean	record	311	value	193.091	name	BGI077-01-27-33.acc
5	mode	record	170	value	152.485	name	BGI077-01-11-22.acc
6	min	record	61	value	64.280	name	BGI077-01-24-13.acc
7	max	record	360	value	285.293	name	BGI077-01-18-34.acc

Case D --- BAGNOLI IRPINO Stress drop 100 bar

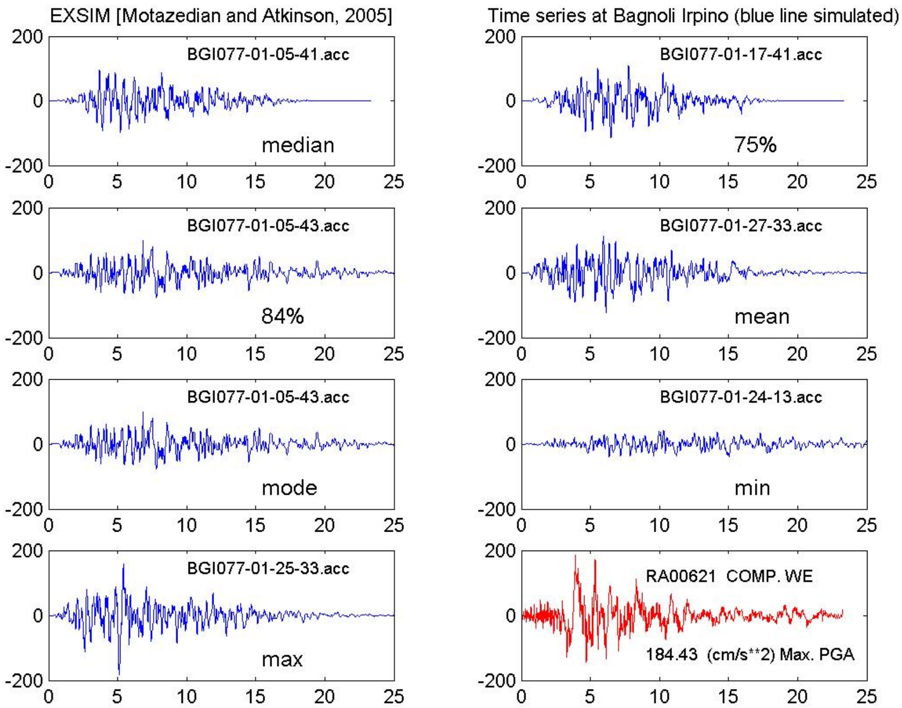

Case E --- BAGNOLI IRPINO Stress dDrop 200 bar

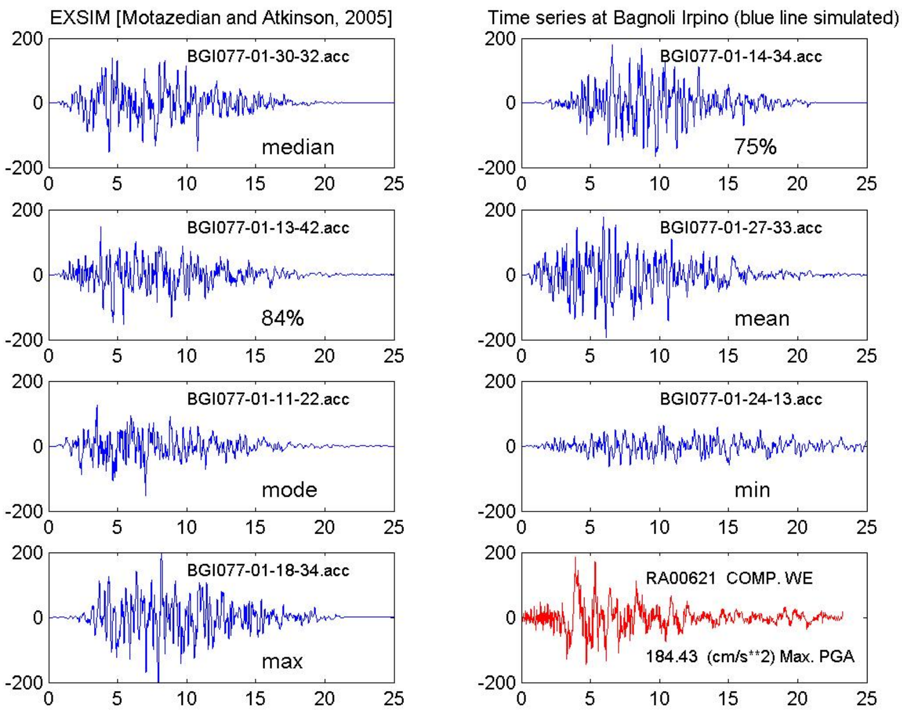

Figure 9. Fault F1 (Colliano): plots of the simulated time series associated with the statistical values of PGA corresponding to median, 75%, 84 %, mean, mode, minimum and maximum. As a comparison, the time history of RA00621 COMP. WE recorded at BGI station of is plotted (red line).

Case D --- BAGNOLI IRPINO --- Stress drop 100 bar

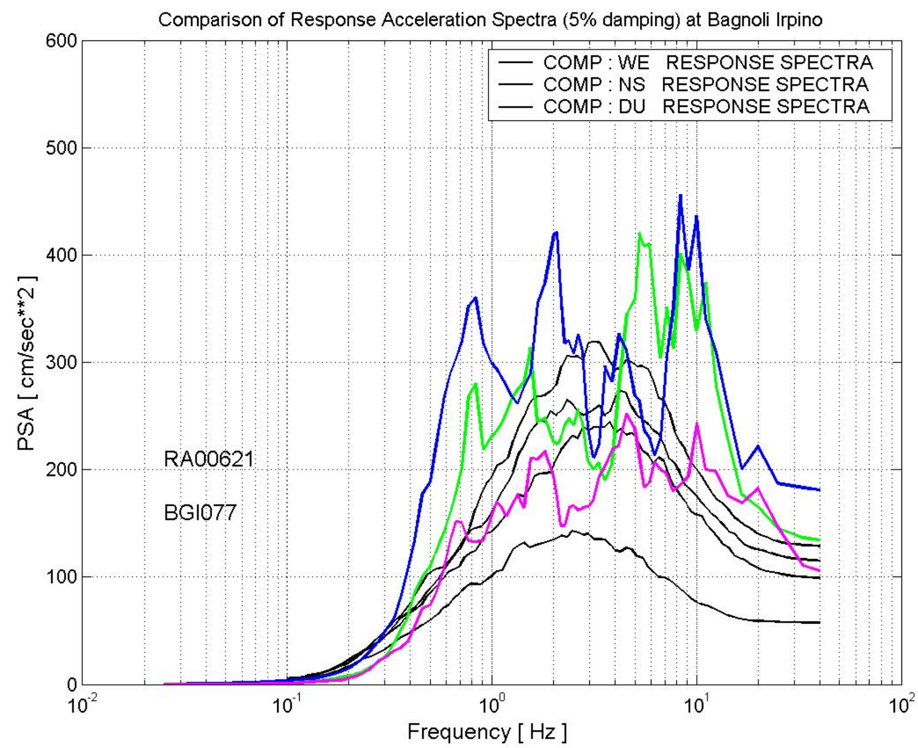

Case E --- BAGNOLI IRPINO --- Stress drop 200 bar

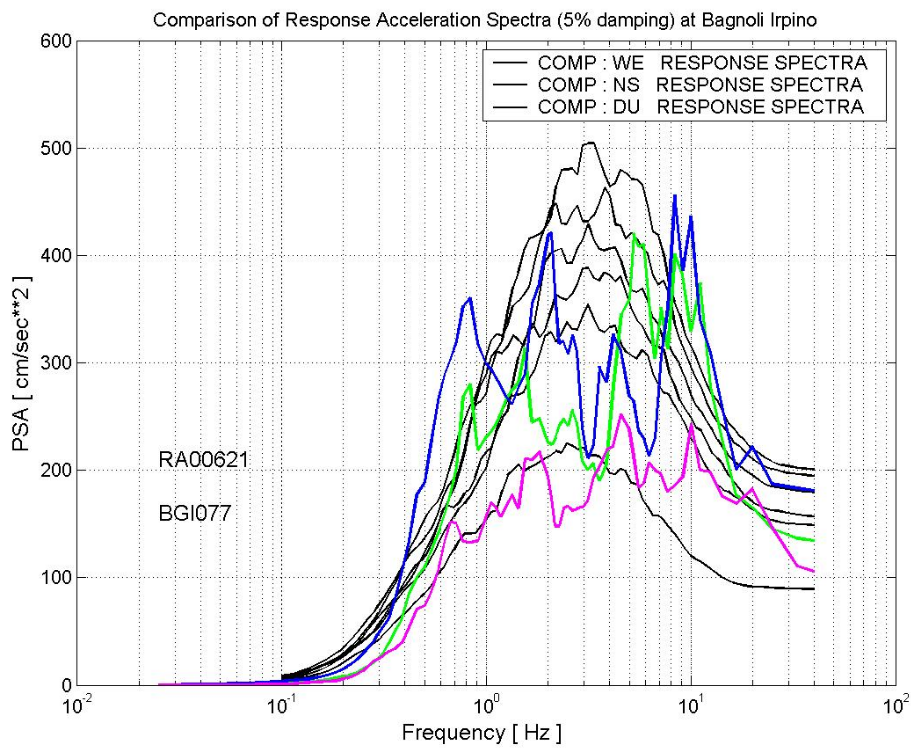

Figure 10. Comparison of response spectra (5% damping) at the Bagnoli Irpino site: the simulated response spectra, using fault F1, are the black lines, while the response spectra of the RA00621 record are shown with COMP: WE (blue line), NS (green line) and vertical DU (magenta line).